# VALIDATION OF AQUEOUS ANGIOGRAPHY IN NORMAL AND ADAMTS10-OPEN ANGLE GLAUCOMA DOGS BEFORE AND AFTER DEVELOPMENT OF GLAUCOMA

By

Jessica Burn

# A THESIS

Submitted to
Michigan State University
in partial fulfillment of the requirements
for the degree of

Comparative Medicine and Integrative Biology – Master of Science

2020

#### **ABSTRACT**

VALIDATION OF AQUEOUS ANGIOGRAPHY IN NORMAL AND *ADAMTS10*-OPEN ANGLE GLAUCOMA DOGS BEFORE AND AFTER DEVELOPMENT OF GLAUCOMA

By

#### Jessica Burn

Glaucoma is a leading cause of blindness in numerous species; however, little is known about the distal conventional aqueous humor outflow pathways in the canine eye. The aim of this work was to develop a diagnostic technique to allow for tailored therapeutic treatment options for canine glaucoma. The studies described herein validate the use of a clinically applicable in vivo imaging technique using intracameral indocyanine green dye in normal and ADAMTS10open angle glaucoma (ADAMTS10-OAG) dogs. These findings were compared to intravenous scleral angiography (SA) to verify outflow of fluorescent dye from the anterior chamber through to the angular aqueous plexus. The initial technique was refined for *in vivo* aqueous angiography (AA) and subsequently performed via a single intracameral injection technique in normal eyes of sedated dogs. After a recovery period, SA of the same eyes was performed for comparative purposes. SA followed by AA was repeated in ADAMTS10-OAG dogs with elevated intraocular pressure. Identical scleral sectors were imaged in all groups using the Heidelberg Spectralis ® Confocal Scanning Laser Ophthalmoscope. Intrascleral vessel depth and lumen diameters were measured in all eyes using optical coherence tomography and computer software. Sectoral and dynamic outflow patterns were observed. The use of AA provides the foundation for improved visualization of post-trabecular conventional aqueous humor outflow pathways in normal and ADAMTS10-OAG dogs, as compared to intravenous SA.

This thesis is dedicated to Mom and Dad.
Thank you for always encouraging me to follow my dreams!

#### **ACKNOWLEDGEMENTS**

I would like to express my appreciation to my supervisor Dr. Chris Pirie for his mentorship and insights throughout this research project and training program. My completion of this project is partly attributed to his encouragement and support through the obstacles we encountered. I would also like to thank my committee members Drs. András Komáromy, Alex Huang, and Art Weber for sharing their knowledge and for guiding me in my scientific training.

I thank Dr. Gillian J. McLellan and her laboratory team at the University of Wisconsin-Madison for their input regarding aqueous angiography techniques in animals. I would also like to recognize Dr. Laurence Occelli, Kristin Koehl, Christine Harman, and Amanda Anderson for their technical assistance with laboratory techniques. I also express the deepest gratitude for the dogs and the Animal Care team at the Vivarium of the MSU College of Veterinary Medicine.

I would like to acknowledge the funding sources that made this research possible:

Michigan State University College of Veterinary Medicine Endowed Research Funds,

Michigan State University startup funds, NIH grants R01-EY025752, K08EY024674, Bright

Focus Foundation, Research to Prevent Blindness Career Development Award, and Research

to Prevent Blindness Unrestricted Grant to UCLA.

Last, but not least, I would like to extend a heartfelt thank you my friends and family for their unwavering support through it all!

# TABLE OF CONTENTS

LIST OF TABLES	vii
LIST OF FIGURES	xiii
KEY TO ABBREVIATIONS	X
CHAPTER 1	1
INTRODUCTION	1
1.1 Aqueous humor dynamics	1
1.1.1 Production of aqueous humor	1
1.1.2 Rate of aqueous humor production	2
1.1.3 Aqueous humor outflow pathways	
1.1.4 Schlemm's canal or angular aqueous plexus	5
1.1.5 Resistance to aqueous humor outflow	
1.1.6 Regulation of intraocular pressure	
1.1.7 Post-trabecular aqueous humor outflow	8
1.2 Canine glaucoma	
1.2.1 Definition of glaucoma	9
1.2.2 Canine primary open angle glaucoma	10
1.2.3 Screening tests for canine glaucoma	10
1.2.4 Current treatment modalities for canine glaucoma	13
1.3 Imaging techniques	17
1.3.1 Corrosion cast studies	17
1.3.2 Angiographic imaging techniques	18
1.3.3 Scleral angiography (SA)	19
1.3.4 Aqueous angiography (AA)	20
1.3.5 Scanning laser ophthalmoscopy and optical coherence tomography (OC	CT)21
1.3.6 Three-dimensional micro-computed tomography	22
1.3.7 Dynamic movement of aqueous humor	
1.3.8 Use of scleral angiography (SA) and aqueous angiography (AA)	
1.4 Study hypotheses and specific aims	24
CHAPTER 2	
MATERIALS AND METHODS FOR PERFORMING AQUEOUS AND SCLER.	AL
ANGIOGRAPHY	
2.1 General experimental outline	26
2.1.1 Normal canine eyes	
2.1.2 ADAMTS10-open angle glaucoma (ADAMTS10-OAG) canine eyes	27
2.2 Validation study for performing aqueous angiography in canine eyes	28
2.2.1 Experiment 1: Ex vivo aqueous angiography (AA) in canine cadaver ey	
2.3 In vivo aqueous angiography (AA) and scleral angiography (SA)	30
2.3.1 General study protocol and pre-medication	
2.3.2 Experiment 2: In vivo aqueous angiography (AA) using a gravity-fed tr	
system in normal canine eyes	32

2.3.3 Experiment 3: <i>In vivo</i> aqueous angiography (AA) via single intracamera injection in normal canine eyes	
2.3.4 Experiment 4: <i>In vivo</i> scleral angiography (SA) in normal canine eyes	32
2.3.5 Experiment 5: <i>In vivo</i> scleral angiography (SA) in <i>ADAMTS10</i> -open ang	
glaucoma (ADAMTS10-OAG) canine eyes	
2.3.6 Experiment 5: In vivo aqueous angiography (AA) via single intracamera	
injection in <i>ADAMTS10</i> -open angle glaucoma ( <i>ADAMTS10</i> -OAG) canine eye	
2.4 Confocal scanning laser ophthalmoscopy aqueous angiography (AA) and sclera	
angiography (SA) imaging and optical coherence tomography (OCT)	
2.5 Measurements and data analysis	
2.5 Measurements and data analysis	90
CHAPTER 3	40
AQUEOUS ANGIOGRAPHY IN NORMAL CANINE EYES	
3.1 Results	
3.1.1 Ex vivo aqueous angiography (AA) in canine eyes	
3.1.2 Experiment 2: <i>In vivo</i> aqueous angiography (AA) using a gravity-fed tro	
system	
3.1.3 Experiment 3: <i>In vivo</i> aqueous angiography (AA) via single intracamera	
injection	
3.1.4 Experiment 4: <i>In vivo</i> intravenous (IV) scleral angiography (SA)	
3.2 Comparison of intracameral (IC) and intravenous (IV) routes of injection	
3.3 Safety	
3.4 Discussion	
CHAPTER 4	
OPEN ANGLE GLAUCOMA STUDY	
4.1 Results	
4.1.1 Intravenous (IV) scleral angiography (SA)	
4.1.2 Intracameral (IC) aqueous angiography (AA)	
4.2 Comparison of intracameral (IC) and intravenous (IV) routes of injection	
4.3 Safety	
4.4 Discussion	
4.5 Conclusion	82
CHAPTER 5	83
CONCLUSIONS AND FUTURE DIRECTIONS	
	_
RIRI IOGRAPHV	91

# LIST OF TABLES

Table 1. Experimental group summary. Experiments 1, 2, 3, 4, 5 and 6 are listed outlining the route of administration, dose and concentration of ICG employed, in addition to, those
performed ex vivo or in vivo27
Table 2. Summary of normal dogs utilized and intraocular pressure measured before and after conducting in vivo aqueous angiography (AA)38
Table 3. Summary of normal dogs utilized and intraocular pressure measured before and after conducting in vivo scleral angiography (SA)39
Table 4. Summary of dog breeds with normal eyes utilized for conducting ex vivo aqueous angiography (AA)
Table 5. Summary of time to fluorescence, vessel location, vessel pattern, and vessel lumen diameters visualized after in vivo aqueous angiography (AA) in normal dog eyes45
Table 6. Summary of normal dogs utilized and intraocular pressure measured before and after conducting conducting in vivo scleral angiography (SA)49
Table 7. Summary of ADAMTS10-open angle glaucoma (ADAMTS10-OAG) dogs utilized for conducting scleral angiography (SA)64
Table 8. Summary of ADAMTS10-open angle glaucoma (ADAMTS10-OAG) dogs utilized for conducting aqueous angiography (AA)

# LIST OF FIGURES

Figure 1. Schematic depicting the conventional and unconventional aqueous humor outflow pathways of the eye
Figure 2. Schematic representation of the gravity-fed fluid delivery and pressure monitoring systems28
Figure 3. Diagram depicting eight sectors of the globe for consistent documentation of location
Figure 4. Representative aqueous angiography (AA) images obtained from 5 dog cadaver eyes using a gravity-fed trocar system and sodium fluorescein (SF)
Figure 5. Schematic demonstrating the sectoral variation in visualization of fluorescent dye administered intracamerally (IC) in 10 ex vivo canine eyes
Figure 6. Representative in-vivo aqueous angiography (AA) image following intracameral (IC) injection of indocyanine green (ICG) into the right eye of a 3-year old intact female beagle dog
Figure 7. Schematic demonstrating the sectoral variation in fluorescent dye outflow after aqueous angiography (AA) in 12 live dogs
Figure 8. Representative in-vivo aqueous angiography (AA) image following intracameral (IC) injection of indocyanine green (ICG) into the left eye of a 1-year old intact female beagle dog
Figure 9. Representative scleral angiography (SA) following intravenous (IV) administration of indocyanine green (ICG) of the left eye from a 1-year old intact female beagle dog (A, B) and 2-year-old male beagle dog (C, D)
Figure 10. Representative standard color (A, E, I), in-vivo intracameral (IC) aqueous angiography (AA) (B, F, J), and intravenous (IV) scleral angiography (SA) (C, G, K) using indocyanine green (ICG) dye from the left eye of a 1-year old intact female beagle dog (A, B, C), the right eye (E, F, G) of a 3-year-old intact female beagle, and the left eye of a 1-year old intact female beagle dog (I, J, K), respectively
Figure 11. Representative standard color (A), IC aqueous angiography (AA) (B), and IV scleral angiography (SA) (C) from the right eye of a 4-year old male Mixed breed dog53
Figure 12. Cross sectional OCT scans from the right eye of a normal 3-year old intact female beagle dog following intracameral (IC) (A) and intravenous (IV) (B) indocyanine

green (ICG) angiography54
Figure 13. Schematic demonstrating the segmental variation in fluorescent dye outflow observed after scleral angiography (SA)
Figure 14. Schematic demonstrating the segmental variation in fluorescent dye outflow observed after performing aqueous angiography (AA)
Figure 15. Standard color image of the temporal sclera of the left eye (A), aqueous angiography (AA) of the same area showing the appearance of 0.25% indocyanine green dye fluorescence 1 minute after intracameral (IC) injection (B), and the same location 20 minutes after initial dye injection (C), demonstrating progression of dye fluorescence and the presence of laminar flow within the scleral vessel over time in a 4-year-old female beagle dog.
Figure 16. OCT imaging was performed in conjunction with intracameral aqueous angiography (A, C) and intravenous scleral angiography (B, D) in the left eye of a 1-year-old pre-glaucomatous female beagle dog
Figure 17. Standard color image of the temporal sclera in a 1-year-old male beagle dog showing branching of conjunctival vessels (arrow) (A). Imaging of the same location after intracameral (IC) injection of 0.25% indocyanine green dye yields fluorescence of a deep scleral vessel (B). Scleral angiography (SA), using 1 mg/kg indocyanine green, of the same region confirms the presence of the same deep scleral vessel (arrowhead), along with numerous thinner, branching conjunctival vessels (arrow) (C)
Figure 18. Standard color images of the temporal sclera of the left eye in 3 different ADAMTS10-open angle glaucoma (ADAMTS10-OAG) beagle dogs with IOP greater than 20 mmHg: a 4-year-old male (A), a 4-year-old male (E), and a 4-year-old female (I) with fluorescence of indocyanine green dye in the deep scleral vessels after aqueous angiography (AA) (B, F, J, respectively) and after scleral angiography (SA) (C, G, K, respectively)75
Figure 19. Cross sectional OCT scans from the left eye of a 1-year old intact female pre- glaucomatous beagle dog following intracameral aqueous angiography (A), and from the right eye of a 3-year old intact female normal beagle dog following intracameral aqueous angiography (B). The orientation of the scan (green arrow) depicts luminal vessels which demonstrated fluorescence

# **KEY TO ABBREVIATIONS**

AAAqueous angiography
ADAMTS10-OAGADAMTS10-open angle glaucoma
CAHO
FFemale
ICIntracameral
ICAIridocorneal angle
ICGIndocyanine green
IOP Intraocular pressure
IVIntravenous
MMale
MIGS
OCTOptical coherence tomography
ODRight eye
OSLeft eye
SA
SFSodium fluorescein
SUNStandardization of uveitis nomenclature
TSCPTransscleral cyclophotocoagulation

#### **CHAPTER 1**

#### INTRODUCTION

# 1.1 Aqueous humor dynamics

# 1.1.1 Production of aqueous humor

To investigate potential avenues to diagnose and treat glaucoma, it is important to understand how aqueous humor is produced as well as its outflow pathways. Aqueous humor is an important component of the globe and its outflow has been described in a variety of species, with studies spanning over the last five decades. <sup>1-7</sup> This fluid is produced by the ciliary body and flows from the posterior chamber, through the pupillary opening and into the anterior chamber. It bathes the anterior aspect of the vitreous, the anterior surface of the lens, the trabecular meshwork, the anterior and posterior iris, and the posterior aspect of the cornea, providing vital nutrients such as electrolytes, amino acids, glutathione, glucose, and ascorbic acid to these intraocular structures. 8–10 Aqueous humor has also been documented to transport ascorbate, an antioxidant, into the anterior segment of the globe. 11 As such, abnormalities in aqueous humor due to uveitis or systemic endocrinopathies, including diabetes mellitus, can lead to insufficient or altered nutrient or electrolyte supply to the intraocular structures, which may result in ocular pathology including cataract formation. 12 Other disease processes including corneal pathology, glaucoma, and certain retinal diseases have also been shown to alter the nitric oxide content and the oxidative stress index of the aqueous humor. 13-15 Additionally, intraocular implants and solutions, such as silicone oxide used for retinal reattachment surgery, have been shown to lead to an increased concentration of sodium ions in the aqueous humor. 16 Identification of

immunoglobulin types G, A, M, and E in the aqueous humor have also been reported with certain systemic disease processes, such as toxoplasmosis.<sup>17</sup>

Aqueous humor is secreted by the epithelium of the ciliary body processes, which is located in the posterior chamber of the globe. The epithelium of the ciliary body processes is composed of two layers: a non-pigmented epithelium overlying a pigmented epithelium, both of which are joined together by gap junctions. <sup>18</sup> Several mechanisms of aqueous humor formation have been described, however, more recently there is consensus regarding movement of water and solute along a unidirectional osmotic gradient from the interstitium of the pigmented epithelial cells of the ciliary body into the posterior chamber. <sup>10,18</sup> This process occurs in 3 stages:

1. Movement of sodium chloride from the stromal interstitium into the pigmented epithelial cells by electroneutral Na+/H+ and Cl-/HCO3- antiport or Na+-K+-2Cl- symport, 2. Movement of solute via gap junctions from the pigmented to the non-pigmented epithelial cells, 3. Release of sodium and chloride ions into the aqueous humor, drawing water with it along its osmotic gradient. <sup>18</sup>

# 1.1.2 Rate of aqueous humor production

An optimal balance between aqueous humor production and drainage from the eye is necessary to maintain IOP within a narrow range. Any disruption to homeostasis of aqueous humor movement may result in either hypertension and glaucoma, or hypotony, both of which could lead to intraocular damage, changes to globe shape, and a loss of vision. A pressure gradient is responsible for driving aqueous humor out of the CAHO pathways, through the scleral venous plexus, and into systemic circulation.<sup>2,19</sup> Thus, the CAHO pathway has been identified as the location of outflow resistance, and subsequently, regulation of physiologic

IOP.<sup>20,21</sup> In contrast, the unconventional aqueous humor outflow route relies on the passive movement of aqueous humor out of the eye in response to osmotic gradients.<sup>22</sup>

The rate of aqueous humor production varies between species. In dogs, the rate has been documented as 2.5µL/min.<sup>23</sup> A constant cycling of aqueous humor occurs where fluid is produced at the same rate that it exits the eye via both the conventional and the unconventional routes of aqueous humor outflow. The balance between these dynamics allows for maintenance of an appropriate hydrostatic pressure, which retains the globe in a spherical shape with a normal intraocular pressure (range 10-20 mmHg).<sup>24–28</sup> This allows for maintenance of proper anatomical positioning of the scleral walls as well as an appropriate refractive index for vision.

# 1.1.3 Aqueous humor outflow pathways

The anterior portion of the ciliary body that forms a recess is known as the cilioscleral cleft. This cleft is proportional in size to the size of the patient. <sup>29</sup> The cilioscleral cleft forms a junction with the base of the iris and the corneoscleral tunic, creating the ICA or filtration angle. Spanning across the cilioscleral cleft, from the corneoscleral junction to the iris root, are strands of tissue known as pectinate ligaments. Within the cilioscleral cleft and caudal to the pectinate ligaments is a matrix of loose, interwoven collagen and cells which forms the trabecular meshwork. The ciliary body muscle also has anterior tendinous extensions which extend into the trabecular meshwork. Once produced by the ciliary body epithelium, aqueous humor moves from the posterior chamber through the opening of the pupil and into the anterior chamber. Once in the anterior chamber, aqueous humor is distributed over the intraocular structures of the anterior globe before flowing to the periphery of the anterior chamber and into the ICA to drain through one of two pathways.

Aqueous humor is filtered through the strands of pectinate ligaments and into the trabecular meshwork, where it exits the eye via the conventional and/or the unconventional routes of aqueous humor outflow. The CAHO pathway involves 85% of the total outflow of aqueous humor in dogs, with fluid egressing through the corneoscleral trabecular meshwork and into the venous plexus. In contrast, the unconventional aqueous humor outflow pathway encompasses uveoscleral, uveovortex, and uveolymphatic absorption of aqueous humor via the uvea, followed by subsequent passage into choroidal circulation. Tormation of intracellular channels, consistent with the scleral plexus, have been identified as early as one week of age in the beagle and do not appear to evolve a great deal with maturation of the dog. 33

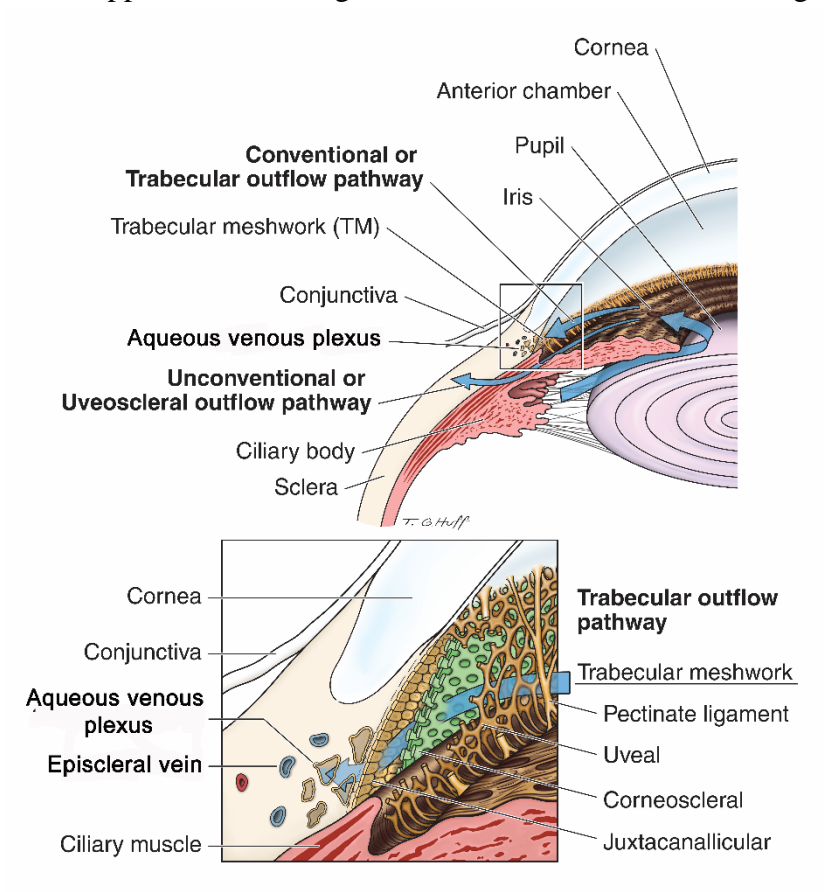


**Figure 1. Schematic depicting the conventional and unconventional outflow pathways of the eye**: 1. The conventional outflow pathway of aqueous humor through the trabecular meshwork and into the aqueous venous plexus back to systemic circulation, and 2. The unconventional outflow pathway of aqueous humor through the uveoscleral vessels and back into systemic circulation.

# 1.1.4 Schlemm's canal or angular aqueous plexus

Aqueous humor that moves out of the eye via the CAHO pathway returns to hematogenous circulation via drainage vessels that are species specific. Both humans and dogs have a juxtacanalicular resistance zone, which surrounds the trabecular meshwork and is comprised of a network of aqueous collecting channels. However, in humans, the trabecular meshwork is located immediately adjacent to a vessel known as Schlemm's canal. Although the trabecular meshwork structure is similar in dogs to that of humans, there is no Schlemm's canal in the dog and aqueous humor leaves the eye via the angular aqueous plexus instead. From either Schlemm's canal or the angular aqueous plexus, these channels coalesce and drain into the intrascleral venous plexus to the vortex veins, followed by the episcleral veins, before returning to the systemic bloodstream. Movement of aqueous humor from the trabecular meshwork to either Schlemm's canal or the angular aqueous plexus can occur via transcellular pores or pinocytotic vesicles located in the inner endothelium, or can be paracellular.

# 1.1.5 Resistance to aqueous humor outflow

Species differences exist with regards to the tissue that is thought to provide the greatest resistance to aqueous humor outflow. It is suspected that Schlemm's canal in humans, and the juxtacanalicular zone in dogs, likely accounts for the main site of resistance within the CAHO pathways. Numerous studies evaluating human eyes have concluded that a substantial degree of aqueous humor outflow resistance is produced by the endothelial lining of Schlemm's canal and the adjacent juxtacanalicular tissue. Adjusted One study identified approximately 75% of total resistance to outflow occurs in the region between the anterior chamber and Schlemm's canal in humans, while 25% of the total resistance was identified within the sclera. A similar study in non-human primate eyes yielded a significantly higher value for total outflow resistance (90%)

occurring between the anterior chamber and Schlemm's canal, with at least 50% of this resistance occurring near the inner wall of Schlemm's canal. The remaining 10% was noted to reside between Schlemm's canal and the episcleral veins. <sup>42</sup> In comparison, in dogs, the extracellular matrix was identified as the main site of aqueous humor resistance in open angle glaucoma. Changes in the extracellular matrix <sup>43</sup>, including loss of hyaluronic acid and decreasing chondroitin-4-sulfate have been linked to increased resistance at this site <sup>44</sup>. In open angle glaucoma beagles with the *ADAMTS10*-OAG mutation, extracellular plaques of unknown origin and fibrillin, a small non-sulfated, elastic microfibril protein, are thought to contribute to outflow resistance of aqueous humor by depositing within the trabecular meshwork. <sup>45</sup>

To date, there is little published information outlining the association and/or importance between the aqueous outflow vessels and episcleral vasculature within the veterinary literature.<sup>33,46</sup> In humans, the importance of this post-trabecular section of the CAHO pathways and its contribution to outflow resistance is well-documented; however, the molecular pathway is still poorly understood.<sup>47,48</sup> Although this mechanism of action is common across a multitude of species, minor anatomic variations in the venous system exist, which appear to dictate outflow of aqueous humor from the anterior chamber.<sup>23,49–51</sup> Several studies in humans, rabbits, and dogs evaluated episcleral venous pressure via direct cannulation, using very fine glass pipettes, as well as via indirect partial-to-complete compression schemes using a torsion-balance system or a pressure chamber.<sup>52–54</sup> Using these techniques, the episcleral venous pressure measured was determined to be between 7-14 mmHg<sup>40,47,55</sup> while the resistance of the tissues involving conventional aqueous humor outflow were measured to be approximately 3-4 mmHg/μL/min.<sup>56</sup> This backpressure from the episcleral tissues is thought to regulate IOP, resulting in approximately 50-75% of the resistance that regulates IOP.<sup>37,57,58</sup>

# 1.1.6 Regulation of intraocular pressure

Glycosaminoglycans have been postulated to play a functional role in the structural organization of the extracellular matrix that form the outflow pathways<sup>44,59</sup> and, subsequently, in the regulation of IOP.<sup>60</sup> Facility of aqueous humor outflow was documented to increase with the addition of an enzyme to degrade glucosaminoglycans.<sup>61</sup> Several types of glucosaminoglycans have been identified in the trabecular meshwork. An increased chondroitin sulfate content and decreased hyaluronic acid level have been documented in glaucomatous human eyes.<sup>44</sup> Other studies in mice documented increased mucopolysaccharide and protein deposition in the trabecular meshwork of glaucomatous eyes<sup>59</sup>, which may contribute to elevations in IOP.

Anatomical structures, including the iris and ciliary body muscle, have also been speculated to increase resistance to the outflow of aqueous humor. In humans, the ciliary muscle tendons attach to the outer aspect of the collagen and elastin fibers that comprise the corneoscleral trabecular meshwork and extend deep into the anterior and posterior walls of Schlemm's canal, allowing for modulation of the width of the trabecular meshwork and aqueous humor outflow. 62,63 Tendons near the juxtacanalicular tissue are more compact and are arranged in parallel formation. 62 The ciliary muscle has tendons that also attach to the sclera and the scleral spur; when the ciliary muscle contracts, the scleral spur is pulled posteriorly leading to inwards movement and subsequent widening of the trabecular meshwork. 64 This action is postulated to decrease outflow resistance, while relaxation of the ciliary muscle increases outflow resistance as the trabecular meshwork decreases in width. In contrast, dogs do not have a scleral spur. Instead, the tendons of the ciliary muscle insert onto the elastic fibers of the trabecular meshwork, the juxtacanalicular tissue, as well as the inner scleral tissue. 35 There is limited scientific data on the role that the ciliary muscle and its tendons play, but it is thought

that they are involved in opening the angular aqueous plexus.<sup>35</sup> Topical cholinergic drugs, prolonged electrical stimulation of ocular sympathetic nerves, and age have all been shown to inhibit movement of the ciliary muscle and decrease outflow resistance in the eye.<sup>65–68</sup> This becomes important as we aim to evaluate eyes affected by conditions that raise IOP. A disruption in the regulation or resistance of aqueous humor outflow via the conventional aqueous outflow pathway leads to an elevation in IOP, known as ocular hypertension, and can progress to glaucoma and progressive loss of vision.

# 1.1.7 Post-trabecular aqueous humor outflow

There is currently no known published data describing the aqueous outflow pathways leading back to systemic circulation and the behavior of aqueous humor in these regions in the canine eye. Recently, the distal component of aqueous outflow has been evaluated in pigs and cows. <sup>69–71</sup> In pig eyes, aqueous humor outflow was shown to be greatest in the superonasal and inferonasal sectors of the globe, which coincided with the location of the largest collector channels. <sup>70</sup> In cow eyes, sectoral increases in aqueous humor outflow were observed distal to the site of ab interno goniotomy, with no change in aqueous humor outflow noted in other segments of the globe. <sup>71</sup> These studies support the presence of communicating regions between aqueous humor outflow and the scleral vasculature, as well as sectoral aqueous humor outflow. However, due to species differences, CAHO pathways in dogs may deviate from what is seen in the previous species studied and direct translation should not be assumed to be the same for dogs. Thus, this is an area of investigation of the project described herein.

# 1.2 Canine glaucoma

# 1.2.1 Definition of glaucoma

Glaucoma comprises a group of optic neuropathies which result in irreversible vision loss. This devastating condition affects approximately 70 million humans worldwide and its prevalence continues to grow, with the number of affected individuals anticipated to reach 111.8 million by 2040.<sup>72,73</sup> This disease also affects a large number of individuals within the canine population.<sup>74,75</sup> Some risk factors for glaucoma include pectinate ligament dysplasia, uveitis, anterior lens luxation, and neoplasia, among others. These all lead to an elevated IOP. In some individuals, elevations in IOP can reach painful levels.

In canines, glaucoma is categorized as primary open angle, primary angle closure, or secondary depending on the underlying etiology. Primary angle closure glaucoma tends to be the predominant type in dogs and certain breeds have been identified as high risk for developing this condition due to their genetic inheritance. These breeds include, but are not limited to, Basset Hounds, Bouviers des Flandres, and English Springer Spaniel dogs. <sup>76–78</sup> Dogs affected by primary angle closure glaucoma have a narrow to closed iridocorneal angle, which results in mechanical obstruction of aqueous humor outflow from the eye. <sup>79</sup> Although primary open angle glaucoma accounts for the majority of human cases, a much smaller subset of the canine population is affected. This form of glaucoma is observed in breeds such as the Beagle, Norwegian Elkhound, Petit Basset Griffon Vendeen, Basset de Fauve, Chinese Shar-pei, Tibetan Terrier, Wire-haired fox Terrier, and Parson Russell Terrier. <sup>80–84</sup> This form of glaucoma arises from resistance to aqueous humor outflow in the trabecular meshwork, despite a normal appearing iridocorneal angle. <sup>85</sup> Further investigation into the genetics involved in canine primary open angle glaucoma led to the identification of a mutation in the *ADAMTS10* gene in Beagle

dogs.<sup>84</sup> This has been an important development for research revolving around the diagnosis, development, and treatment of primary open angle glaucoma. Lastly, secondary causes of glaucoma may also arise from conditions that lead to obstruction of aqueous humor outflow and a subsequent rise in intraocular pressure (IOP). Obstruction of aqueous humor outflow may arise from, but is not limited to uveitis, trauma, posterior synechia, lens instability and vitreal prolapse.<sup>22</sup>

# 1.2.2 Canine primary open angle glaucoma

Primary open angle glaucoma has been linked to both the *ADAMTS10* and *ADAMTS17* genes in dogs. <sup>82,84</sup> Beagle dogs with a mutation in the *ADAMTS10* gene exhibiting *ADAMTS10*-open angle glaucoma (*ADAMTS10*-OAG) have been studied over the past 50 years. Affected beagle dogs have demonstrated a predictable, slow, progressive rise in IOP to a level of 30-40 mmHg over a 2 to 3 year time period. <sup>86,87</sup> Dogs with elevated IOP tended to respond more readily to topical therapies, including pilocarpine and carbonic anhydrase inhibitors, compared to dogs affected by primary angle closure glaucoma. <sup>86–88</sup> These properties make for an ideal canine population to study the characteristics of aqueous humor outflow at various stages of progression in a glaucomatous eye. Dogs affected with primary open angle glaucoma exhibit a naturally occurring and well-documented disease process with similar ocular biomechanics as humans with normotensive glaucoma. As such, this breed currently serves as a model for normotensive glaucoma in humans. <sup>86</sup>

#### 1.2.3 Screening tests for canine glaucoma

At this time, current techniques used to assess the conventional aqueous humor outflow (CAHO) pathways are limited in providing prognostic information for this disease process.

Screening tools do not allow for direct visualization of all the components of the iridocorneal angle (ICA), thus limiting the ability of observers to truly predict those patients who are at risk and their potential response to glaucoma treatments. These tools include gonioscopy, administration of topical ophthalmic mydriatic agents, and imaging using ultrasound biomicroscopy. More advanced imaging of the posterior segment is possible using optical coherence tomography, but is currently limited to research purposes due to the cost of the equipment required and the need for a refined technique that is clinically applicable.<sup>89</sup>

Direct observation of the ICA is possible using gonioscopy, however, this tool limits visualization to the superficial layer of tissue comprising the ICA. Even though clinical grading schemes to assess the status of the canine ICA have been established<sup>90</sup>, this does not provide information regarding aqueous humor outflow or if the abnormalities visualized, such as pectinate ligament dysplasia or synechiae, impair outflow. (Figure 1) These grading schemes rely on subjective assessment of the width of the iridocorneal angle and the presence of individual pectinate ligaments versus sheets of tissue. Due to poor visibility into the ICA, the deeper layers of the trabecular meshwork cannot be assessed using gonioscopy. The lack of ability to assess the deeper structures of the ICA means that the grading schemes employed do not always correlate well with clinical observation of a reduction in outflow facility.<sup>91</sup>

A second screening tool that has been used as a crude assessment of pectinate ligament dysplasia is the use of direct and indirect acting muscarinic cholinergic antagonists. In eyes affected by pectinate ligament dysplasia, these agents can induce abrupt elevations in IOP within one hour after administration. Several muscarinic receptor subtypes have been identified in the ciliary muscle in dogs, including M<sub>3</sub> and M<sub>5</sub> in brown eyes and M<sub>5</sub> muscarinic receptors only in blue eyes. 92,93 Administration of topical 1% tropicamide and 1% atropine were documented to

result in significant increases in IOP up to 35% and 50%, respectively, in a colony of Basset Hounds affected by inherited primary angle-closure glaucoma. <sup>94</sup> By applying stress to the ICA, cholinergic antagonists can be used to assess the potential for elevated IOP in primary angle-closure glaucoma dogs in the field.

In contrast, latanoprost 0.005% ophthalmic solution has an opposing effect on the ciliary muscle as compared to cholinergic antagonists, which is likely a result of centripetal traction of the iris root.  $^{95}$  Topical prostaglandin  $F2\alpha$ 's have also been shown to result in contraction of the iris sphincter muscle, resulting in a narrowed iridocorneal angle.  $^{96,97}$  In contrast, other miotic agents, such as topical 2% pilocarpine have also been shown to result in ciliary muscle contraction in dogs with closed-angle glaucoma, however, these medications increase the width of the cilioscleral cleft, thereby increasing outflow of aqueous humor. Other miotic ophthalmic drugs have also demonstrated similar responses in cilioscleral cleft expansion.

Ultrasound biomicroscopy has also been used as a screening tool to assess the ICA and its potential to drain aqueous humor. <sup>91</sup> This imaging modality allows for a detailed cross-sectional view of the ICA. This allows the user to evaluate the ICA for any abnormalities in width, number or size of pectinate ligaments (i.e. strands or sheets), or other structural abnormalities and/or their severity. The information provided by this may help to identify patients that are predisposed to developing elevated IOP, however, findings from ultrasound biomicroscopy do not correlate to reductions in aqueous humor outflow and subsequent elevations in IOP. <sup>91</sup>

# 1.2.4 Current treatment modalities for canine glaucoma

The challenge of identifying at-risk breeds and predicting the progression of disease is not the only obstacle to glaucoma. Treatment interventions include medical therapy and surgery, both of which have poor or undetermined long-term success rates. 98–100 Topical medical therapy most often includes the use of carbonic anhydrase inhibitors, beta blockers, and/or prostaglandin analogues. 101,102 Carbonic anhydrase inhibitors, such as dorzolamide, decrease aqueous humor production by inhibiting carbonic anhydrase in the ciliary processes of the eye; this slows the formation of bicarbonate ions and reduces sodium and fluid transport. <sup>18</sup> Beta blockers, such as timolol, reduce intraocular pressure by binding to beta-adrenergic receptors located on the nonpigmented ciliary epithelium and inhibiting the action of sympathetic nerves. 103 Latanoprost is a prostaglandin analogue which decreases intraocular pressure by increasing outflow of aqueous humor through the ciliary muscle region to the suprachoroidal space and episcleral veins, via the unconventional outflow pathway. 104 Newer medications are slowly being developed, including the more recent latanoprostene bunod (Vyzulta<sup>TM</sup>; Bausch & Lomb Incorporated) and netarsudil (Rhopressa<sup>TM</sup>; Aerie Pharmaceuticals). Latanoprostene bunod is a prostaglandin F2α agonist that donates nitric oxide; this drug has been shown to be more efficacious in lower IOP in ADAMTS10-OAG beagle dogs 105,106 as compared to the well-known prostaglandin analogue, latanoprost. 107 Frequent administration of this medication may initially help to lower and control IOP for an indeterminate period of time. However, netarsudil 0.02% ophthalmic solution, a rho kinase inhibitor, did not have a clinically significant effect on IOP reduction in normal or open angle glaucoma-affected dogs. 108 Most dogs experiencing glaucoma in clinical situations will ultimately become refractory to topical therapy over time resulting in an uncontrolled rise in

IOP, resulting in damage to the retinal ganglion cells and to the optic nerve. Thus, the search for more effective long-term medications continues.

Several vision-sparing surgical interventions to treat glaucoma in dogs have been employed, including the use of laser and gonioimplants. 100,109,110 These treatments are most effective in early stages of glaucoma when eyes are still visual and have only mildly elevated IOP. Laser therapy includes transscleral cyclophotocoagulation (TSCP) or endolaser cyclophotocoagulation. TSCP involves the use of an external diode laser that is placed on the sclera of the affected eye with the laser beam aimed at the ciliary body processes within the globe. Laser energy of 1000-1500 mW is administered to the ciliary body processes for a duration of 1500-4000 ms at 35-40 different sites, with the goal of destroying the ciliary body epithelium in an effort to slow or stop the production of aqueous humor within the eye. 111 Variable results in the management of canine glaucoma have been documented for TSCP. One study showed that IOP was reduced to less than 25 mmHg in 92% of eyes treated with TSCP with only 50% of these eyes remaining visual over a period of one year. 112 Another study demonstrated an 81.5% success rate with TSCP maintaining IOP below 20 mmHg and maintenance of vision throughout the 6 month postoperative period in 42.6% of eyes. 100 A newer form of TSCP has been described using MicroPulse<sup>TM</sup> technology. This modality delivers laser energy at a power of 2000-2800 mW in a pulsatile manner for a duration of 90-180 seconds per hemisphere. 113 In a preliminary study, at 315 days post-operative, Micro-Pulse TM TSCP has been shown to keep IOP below 25 mmHg in 42% of eyes and to retain vision in 50% of dogs. 113

Endolaser cyclophotocoagulation works along a similar concept, with the added advantage of direct visualization of the ciliary body processes. Endolaser cyclophotocoagulation often requires removal of the lens, typically via phacoemulsification surgery, to access the

posterior chamber of the globe. The endolaser probe is then inserted intraocularly through the pupillary opening and into the posterior chamber to directly visualize the ciliary body processes. The ciliary body processes are then "painted" with laser energy set at 250 mW on a continuous mode or at 250 mW at a duration of 9000 ms to cover 270-320° of the ciliary bodies until they become white and shrink down slightly. The success rate of endolaser cyclophotocoagulation was documented to be between 85.0% after 1 year and 71.8% after 3 years for control of IOP and 71.8% after 1 year and 53.3% after 3 years for retention of vision following surgery. 114

Gonioimplant devices in dogs lags behind that of humans with regards to available options and their long-term success rates. These devices are designed to be implanted with minimal trauma and to provide a means for aqueous humor to passively leave the eye once a threshold intraocular pressure is reached. While microinvasive glaucoma surgery (MIGS) is not yet commonly available in the canine population, preliminary studies have been performed to investigate the use MIGS implants, including the Ex-Press and SalVO/Brown Glaucoma Implant (MicroOptx) in glaucomatous dogs. 115–117 The aim of these studies was to find a smaller, more cost-effective implant that provides a higher level of efficacy in maintaining a normal IOP than the current gonioimplants being utilized. Although initial results have been promising, studies with greater long term follow-up have demonstrated a high incidences of device failure by extrusion, endophthalmitis, and/or uveitis within 4 months of implantation. 116

Currently, the most common glaucoma shunts available for use in dogs are much larger than the MIGS implants. Glaucoma shunts include the Ahmed valve and the Baerveldt implant devices. Variable success rates have been documented using these glaucoma implants. The Ahmed valve shunts were shown to be successful in maintaining IOP below 20 mmHg for a group of 9 dogs over a median time interval of 326 days with 88.9% vision retention over a 1

year post-operative period.<sup>110</sup> Evaluation of Baerveldt shunts demonstrated maintenance of IOP below 20 mmHg in 71.4% of eyes and retention of vision in 69.9% of eyes over a period of 3 months post-shunt implantation.<sup>100</sup> Combinations of laser treatment coupled with Ahmed valve glaucoma implants have also been investigated. One report yielded a 76% success rate in controlling IOP below 25 mmHg with vision retained in 41% of eyes over a period of 12 months post-operative.<sup>118</sup>

The most common long-term complication associated with gonioimplant procedures was cataract formation (up to 28.6% of eyes). 100,118 Short-term complications included persistence of intraocular hypotony or hypertension, development of post-operative fibrosis surrounding the implant valve, conjunctival dehiscence or necrosis, and fibrinous anterior uveitis. 110,118 To prevent capsular fibrosis and to decrease the thickness of the overlying conjunctival tissue, topical chemotherapy agents such as 5-fluoruracil and mitomycin-C have been successfully administered to the pocket prior to implantation of the glaucoma drainage device. 119,120 Mitomycin-C is a hundred times more potent than 5-fluorouracil<sup>121</sup>, and has a greater potential to lead to conjunctival necrosis and dehiscence. 110 These complications typically require a second surgery to repair the area and/or to place a new valve in a different location. Fibrinous anterior uveitis and subsequent obstruction of the shunt tubing system has led to complications of aqueous humor drainage and failure of the apparatus. In some studies, tPA injection, in an effort to breakdown fibrin formation and permit outflow via the shunt, has been reported in over half of operated eyes within one month of surgery. 100,110 If aqueous humor is unable to properly drain, then there is a recorded rise in IOP and recurrence of glaucoma symptoms. In addition to this, the use of gonioimplants in dogs typically requires an intensive level of post-operative care, with frequent rechecks. Given a substantial initial cost of gonioimplant surgery, the need for frequent

post-operative rechecks, this form of surgical intervention can be a financially prohibitive investment for many dog owners.

# 1.3 Imaging techniques

#### 1.3.1 Corrosion cast studies

Investigation of the post-trabecular distal aqueous humor outflow tract as a source of increased resistance has been described within the physician based literature. <sup>69,122</sup> Although little has been published on this topic in dogs, several studies have identified the vascular and microvascular structures associated with the CAHO pathways of dogs via corrosion casting techniques. <sup>1,3</sup> Casting dyes injected via an intracameral (IC) route readily moved from the anterior chamber into the intrascleral venous plexus of Hovius. The CAHO pathways have been shown to be comprised of complex networks, with intraspecies variations. Buskirk et al. (1979) noted redundancy of CAHO pathways with anastomosis among the aqueous collector channels and the intrascleral venous plexus of Hovius in some dogs, while in others very little branching or deviation was observed. Multiple redundancies have also been noted between vessel pathways, resulting in communication between aqueous humor outflow pathways and uveal vessels, consistent with previous corrosion cast studies.<sup>3</sup> Histopathologic analysis of the angular aqueous plexus confirmed that development of the complex anastomoses were developed by 4 weeks of age in dogs, with vessel lumen diameters measuring up to 1.5 μm. <sup>33</sup> Overall, these casting techniques, while highlighting the complexity of the CAHO pathways, fail to provide insight into their true role and functionality at regulating IOP in-vivo.

# 1.3.2 Angiographic imaging techniques

As a result of the challenges incurred with diagnosing and treating glaucomatous eyes in dogs, methods to evaluate and identify eyes at-risk and to treat them in the most effective manner are required to help preserve vision and comfort long-term. A number of different angiographic imaging techniques have been described in humans and in animals that allow for direct visualization of aqueous humor outflow and/or the vasculature of the eye. 123–126 The majority of these imaging modalities have been described using IV fluorescent dyes, however, several have documented IC delivery of dye to allow for imaging of specific regions of the aqueous outflow pathways. 7,123,124,127–132 Different fluorescent dyes have been used, each with a unique set of spectral characteristics, to highlight different vascular components within the globe. 7,123,131,132 Common dyes described include sodium fluorescein (SF) and indocyanine green (ICG).

SF is a smaller molecule (375 Da), which allows it leak readily from vessels into the interstitial space. <sup>133</sup> This dye penetrates poorly into tissue and does not completely bind to blood proteins. It fluoresces at a wavelength within the visible spectrum of light (525nm). <sup>134</sup> In contrast, ICG is a much larger molecule (751 Da), exhibiting high protein binding, which reduces its ability to leak from vessels as readily. <sup>135</sup> The spectral properties of ICG allow for fluorescence at a wavelength of light in the near infrared spectrum (835nm). These spectral characteristics allow for greater detection/visualization of structures deeper within tissues. <sup>135</sup> Overall, SF lends itself well to viewing superficial structures present within the eye (retinal vasculature), however, due to its rapid extravasation, it is likely a less effective dye for studying aqueous humor outflow pathways. On the other hand, ICG would be considered an ideal dye for viewing aqueous humor outflow pathways, as it does not tend to extravasate as readily into the interstitial space. <sup>136</sup> Despite their different spectral properties, IV and IC delivery of SF and ICG

dyes each allow for evaluation of different vascular components within the eye when used either together or independently. 136

# 1.3.3 Scleral angiography (SA)

Anterior segment angiography has been reported *in vivo* in humans over the past three decades. <sup>137,138</sup> This technique has been used to evaluate inflammatory conditions of the sclera, which revealed increased leakage of fluorescent dye from the vasculature with increasing severity of scleritis. <sup>137</sup>

SF was the most common fluorescent dye used, at a concentration of 2.5%.<sup>137</sup> The second most common fluorescent dye used was indocyanine green, which was injected at a dose of 25 mg IV.<sup>137</sup> In cases where both dyes were used under the same imaging session, a single bolus of ICG was administered first.<sup>7,137</sup> Once the ICG diffused out of the vasculature, a single bolus of SF was then injected as quickly as possible IV. In both instances, recording of the scleral segment started up to 5 seconds after injection.<sup>137</sup> The use of both of these fluorescent tracers was valuable to demonstrate outflow pathways, however, ICG was a superior dye to SF to observe vessel patterns as this dye stayed intraluminal longer than SF.<sup>137</sup>

The time to first appearance of sodium fluorescein within scleral vessels occurred rapidly, in as little as 4 seconds post injection, while indocyanine green dye took longer to visualize and was first observed 29.7 seconds post blous. Features such as delayed perfusion of vessels, leakage of fluorescent dye from vessels, and new vessel were identified and recorded as potential pathologic features in human eyes with scleritis; SF was observed to leak readily from scleral vasculature, while ICG was only noted to leak in intermediate and late phases around hypoperfused areas. Indocyanine green proved to be a superior dye to visualize new

vessel formation as ICG bound rapidly to vessel walls allowing for improved visibility of the vascularization even through leakage of overlying SF.<sup>137</sup>

Based on the observations of SA in humans described above, this technique may help to validate the structures observed during AA imaging are indeed congruent with the angular aqueous plexus and the conventional outflow pathways in dogs. SA allows for observation of both superficial conjunctival vessels as well as the location and depth of episcleral veins within the scleral tissue via both SF and ICG angiography. Laminar flow patterns have also been visualized with SA and this feature has been used to help identify return of aqueous humor into hematogenous circulation.

# 1.3.4 Aqueous angiography (AA)

In contrast to the more commonly performed SA, injection of dye IC is a newer technique known as AA. This imaging modality permits direct evaluation of fluorescent dye movement through the major outflow pathways present within the eye, the CAHO pathways. AA relies on administration of a fluorescent dye directly into the anterior chamber, as opposed to IV administration Although this technique has been successfully applied in live humans and non-human primates<sup>7,127</sup>, and *ex vivo* in felines and canines<sup>126,140</sup>, the movement of dye through these structures and the fluid dynamics observed have yet to be characterized in an *in vivo* canine experimental model.

Similar to SA, AA can also be performed with SF or ICG dyes. <sup>127,132,137</sup> ICG has been used in recent years to improve visualization of dye within scleral vasculature, and has been shown to be a useful dye to evaluate aqueous humor outflow pathways due to its higher molecular weight and tendency to remain intraluminal compared to SF. <sup>132</sup> In studies across

multiple species, a standard concentration of 0.4% indocyanine green was injected as a gravity-fed system to replace aqueous humor volume while maintaining an IOP of up to 18.7 mmHg.<sup>126,127</sup> Currently, no single bolus injection techniques for delivery of IC dye have been described in any species.

At the present time, there is little published data regarding AA in live dogs. Most prior works have focused on utilizing *ex vivo* models. <sup>132,141,142</sup> However, recent publications conducted on human patients demonstrated the *in vivo* diagnostic potential of this imaging technique. <sup>127–129</sup> A similar approach was performed *ex vivo* with dogs and cats. <sup>126,143</sup>, and *in vivo* in cats <sup>140</sup>, rabbits <sup>144</sup>, and non-human primates to provide baseline descriptions in normal animals <sup>7</sup>; however, the diagnostic utility of this technique has yet to be established in animal models with ocular conditions resulting in abnormal aqueous humor outflow. AA is believed to have a strong clinical application in the future management of diseases causing mechanical obstructions of aqueous humor outflow, such as glaucoma. Preliminary studies have been identified changes in sectoral outflow of aqueous humor in humans treated with minimally invasive glaucoma surgery, and we hope to be able to develop this technique in veterinary species. <sup>145</sup> Thus, this study aims to outline a clinical approach for conducting *in vivo* AA in dogs, which will directly assess the CAHO pathways and determine its clinical application.

# 1.3.5 Scanning laser ophthalmoscopy and optical coherence tomography (OCT)

Imaging of both SA and AA has most commonly been performed using a Heidelberg® Spectralis OCT machine (Heidelberg Engineering Inc.; Heidelberg, Germany)<sup>132</sup>, although modified retinal cameras with filter systems specifically for anterior segment angiography have also been successfully used.<sup>137</sup> As these camera systems are rather costly, they are not readily available in most clinical settings. Therefore, this currently limits this angiographic technique to

a research setting. As the technique is further refined and its utility in diagnosing obstructive aqueous humor outflow pathways becomes more widespread, it is hoped that this imaging modality will eventually be commonplace in everyday clinical practice. With constant advancements in imaging technologies, it is possible that camera adaptors may become more routinely available for use with less expensive alternatives than the Heidelberg Spectralis. The downside to using a camera adaptor would be losing the capabilities of measuring vessel lumen depth and diameters within the scleral tissue. However, when used as a screening tool, this may not be a necessary function.

# 1.3.6 Three-dimensional micro-computed tomography

There are currently only a handful of reports using three-dimensional micro-computed tomography in human cadaver eyes. 146,147 This is another imaging tool that allows for detailed non-invasive imaging of the anatomic structures of the human eye, including examination of the trabecular meshwork, Schlemm's canal, aqueous humor collecting ducts, and the intrascleral venous plexus. 146 Although this modality has been used to evaluate anatomical structures of the eye with and without contrast stains, it has not yet been utilized to evaluate aqueous humor outflow in veterinary species. 148 As such, future works could be conducted to evaluate and to establish baseline measurements of the CAHO pathways and their intrascleral location. This could also be a useful tool to identify effective treatment modalities based on increased post-treatment diameter of aqueous outflow channels in veterinary species. 147

#### 1.3.7 Dynamic movement of aqueous humor

Aqueous humor movement through trabecular meshwork and into the scleral venous plexus can be described as having one of three distinct characteristics: laminar flow, bi-

directional turbulence, or pulsatility. It is possible to see one or more of these characteristics, concurrently, within the same eye. It is also possible that none of these characteristics may be observed. Laminar flow has been described as discrete movement of aqueous humor along the vessel wall as it moves from the trabecular meshwork and into venous circulation. The appearance is likened to that of the aqueous hugging the vessel wall to create a multipartite pattern within the vessel lumen. This is highlighted with the use of angiographic imaging techniques. Laminar flow appears to be a characteristic of blood displacement by aqueous humor, but may have little to do with the properties of different fluids themselves. 149

Bi-directional turbulence arises as aqueous humor mixes with blood upon initial entry into the venous scleral plexus. The disorder caused by this mixing action appears as swirls of movement, which is highlighted using fluorescent dyes and angiographic imaging modalities. The majority of aqueous humor containing fluorescent dye is continually pushed into venous circulation via a pressure gradient from the CAHO pathway, while a smaller percentage of aqueous humor leaves the anterior chamber via an osmotic gradient through the unconventional aqueous humor outflow pathway; as blood is pumped through the venous scleral plexus slight backflow is seen upon relaxation of the vessel wall, leading to bi-directional movement of aqueous humor and blood. This turbulent movement of blood has been similarly visualized using retinal angiography.<sup>139</sup>

Pulsatile movement of aqueous humor is intermittent visualization of aqueous humor after the fluorescent marker in the aqueous humor mixes with venous blood. The rhythmic pulsation has been shown to be congruent with the rate of the patient's cardiac cycle. A suggested mechanism for this characteristic movement of fluid is that the choroid pumps blood, acting as a piston, to move fluid out of the anterior chamber and into the scleral venous plexus. 150

That, coupled with movement of blood from the cardiac cycle leads to a forward and backward motion of fluid. It has also been observed that decreases in or cessation of pulsatile flow into the aqueous veins occur at the same time or immediately after changes in diurnal rises in IOP. <sup>151</sup>

# 1.3.8 Use of scleral angiography (SA) and aqueous angiography (AA)

The use of SA and AA are complementary to each other. As mentioned above, SA highlights scleral vasculature, while AA allows for visualization of aqueous humor outflow pathways and dynamic movement of aqueous humor as it leaves the eye. The use of both these techniques together allows for validation of anatomic structures, such as the venous circle of Hovius and the intrascleral venous plexus that is seen in the latter stages of AA when aqueous humor rejoins the systemic hematogenous circulation. This is important as numerous lymphatic and arterial blood vessels reside within the sclera. These imaging modalities in combination could identify vessels transporting aqueous humor as opposed to those carrying and returning blood to the systemic circulation.

Although these imaging modalities can and have been used independently of each other in the past, it would be beneficial in the preliminary stages of identifying these outflow pathways in dogs to show the consistency in location and size of these vessel lumens using both techniques.

# 1.4 Study hypotheses and specific aims

As primary glaucoma is a bilateral disease that can affect one eye at a time, the findings of the following studies may help to identify changes in CAHO dynamics and predominant locations of outflow, if any, and help to guide early medical and/or surgical treatment for affected animals with the goal of preserving vision and comfort long-term. It is anticipated that

AA may aid in the prediction of clinically normal canine patients of predisposed breeds in developing glaucoma by demonstrating variations in the CAHO pathways, such as alterations in laminar flow, turbulence, or pulsatility of aqueous humor. We hypothesize that AA will demonstrate delayed filling of CAHO pathways and/or altered outflow patterns (reduced number and caliber of vessels) in *ADAMTS10*-OAG dog eyes, as compared to observations noted in normal dog eyes. Although aqueous humor outflow dynamics in dogs is not yet completely understood, we hope to provide the foundation for this technique with the eventual goal of being able to identify dogs of "at-risk" breeds prior to the onset of glaucoma.

A secondary objective of this study is to explore the potential utility of SA in live dogs. Firstly, it would be used to verify CAHO pathways and the overlap of regions where aqueous humor returns to hematogenous circulation. SA would also be evaluated for any observation of dynamic flow of fluid within the venous circle of Hovius and the adjacent intrascleral venous plexus. This may help to elucidate if AA is an adequate tool to visualize aqueous humor dynamics and distal outflow at the point where aqueous humor mixes with blood to return to systemic circulation.

#### **CHAPTER 2**

# MATERIALS AND METHODS FOR PERFORMING AQUEOUS AND SCLERAL ANGIOGRAPHY

# 2.1 General experimental outline

# 2.1.1 Normal canine eyes

Following validation of aqueous angiography in cadaver eyes (see section 2.2.1), AA was subsequently conducted ex vivo and in vivo on normal canine eyes (Table 1). One day prior to conducting angiography in live dogs, all animals received a complete physical and ophthalmic examination, which included a Schirmer tear test I (Merck Animal Health: Madison, NJ, USA), topical fluorescein staining (Ful-Glo: Akorn, Decatur, IL), slit lamp biomicroscopy (Kowa SL-17; Kowa Company, Tokyo, Japan), rebound tonometry (Tonovet, icare USA, Raleigh, NC), and indirect ophthalmoscopy (Keeler All Pupil II: Keeler Instruments, Broomall, PA, USA). Imaging of either the left or right eye was selected based on their normality, with efforts made to achieve an equal distribution between left and right. In cases where the same dog was imaged more than once, the same eye was imaged for comparative purposes with a recovery period of at least 7 days. Data collected included history, breed, gender, age, and relevant ophthalmic diagnostics (i.e. IOP, tear test values). Following examination of the 10 dogs, two experiments were performed. One eye from each dog was evaluated following IC administration and subsequent IV administration of ICG after a recovery period of at least 10 days. The same eye was imaged for each experiment to allow for comparison. Complete ophthalmic examinations were performed immediately following the completion of angiography and daily thereafter for up to 1 week to monitor for any potential post-procedure changes/complications. All studies were carried out in

compliance with the ARVO Statement for the Use of Animals in Ophthalmic and Vision

Research and were approved by Michigan State University Institutional Animal Care and Use

Committee.

**Table 1.** Experimental group summary. Experiments 1, 2, 3, 4, 5 and 6 are listed outlining the route of administration, dose and concentration of ICG employed, in addition to, those performed ex vivo or in vivo

Experiment	Route of	ICG Dose	ICG	In vivo or ex vivo
	administration		Concentration	
1, 2	Gravity-fed trocar	Constant	Exact	Ex vivo (1) and in vivo
	system	gravity-fed	concentration	(2), imaged within 1 hour
		flow	unknown	of euthanasia
3	Single IC injection	0.1 mL	0.25%	<i>In vivo</i> normal
4	Single IV injection	1 mg/kg	0.25%	<i>In vivo</i> normal
5	Single IV injection	1 mg/kg	0.25%	In vivo ADAMTS10-OAG
6	Single IC injection	0.1 mL	0.25%	In vivo ADAMTS10-OAG

<sup>\*</sup>Abbreviations: IC, intracameral; IV, intravenous

## 2.1.2. ADAMTS10-open angle glaucoma (ADAMTS10-OAG) canine eyes

Two experiments (experiments 5 and 6) were performed on a group of 10 purpose-bred *ADAMTS10*-OAG beagle dogs. Dogs were categorized as glaucomatous based on average diurnal IOP readings (≥20 mmHg) and observation of optic nerve head changes by indirect ophthalmoscopy and OCT over the previous 6 months, prior to conducting angiography.

One eye from each dog was evaluated following the IV administration and subsequent IC administration of ICG after a recovery period of at least 24 hours. The half-life of ICG is 3-4 minutes, permitting repeated dye administration within the same dog following a short time period. The same eye was imaged in each experiment for comparative purposes.

### 2.2 Validation study for performing Aqueous Angiography in canine eyes

## 2.2.1 Experiment 1: Ex vivo aqueous angiography (AA) in canine cadaver eyes

The experimental set up for conducting AA in 10 canine cadaver eyes was designed based on recent published works performed in human subjects and is depicted in Figure 2.7,126,127 (Telle MR, et al. Vet Ophthalmol 2019:22: ACVO E-Abstract E32) Eyes were from dogs euthanized for reasons unrelated to this study. Owner consent was obtained for all dogs. The experimental set up was modified to include direct manometry to ensure IOP was consistently maintained at 20 mmHg. 126 (McLellan GJ, et al. IOVS 2019:60: ARVO E-Abstract 3184) The setup was comprised of two separate systems; a gravity-fed fluid delivery trocar system and a pressure monitoring trocar system.

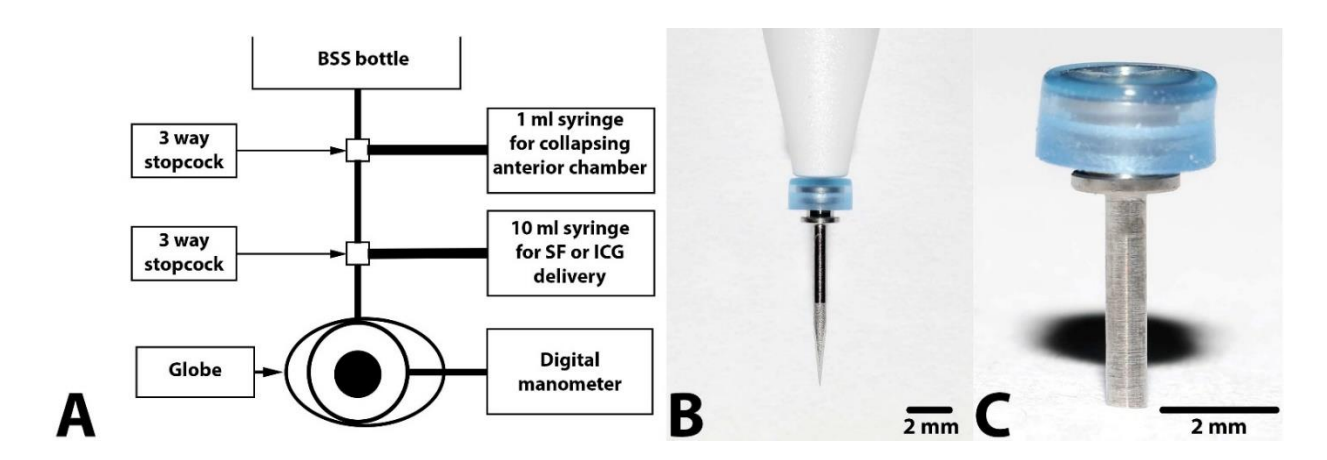
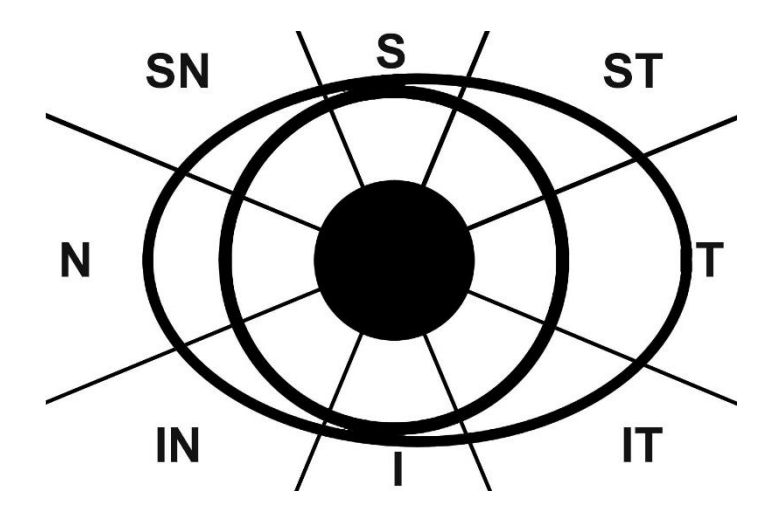


Figure 2. Schematic representation of the gravity-fed fluid delivery and pressure monitoring systems (A). Balanced salt solution and adjustment of the bottle height were employed to maintain IOP as determined via a digital manometer. The 1 mL syringe was utilized to collapse the anterior chamber and the 10-mL syringe contained 2% sodium fluorescein (SF) or 0.25% indocyanine green (ICG), permitting entry into the anterior chamber. Photographs of the trocar delivery system, insertion cannula and trocar (B); close up of valved trocar employed for conducting aqueous angiography (AA) in the ex-vivo (cadaver) experimental set-up (C).

The 10 cadaver globes utilized for AA were placed in an anatomically correct orientation, ensuring that the optic nerve was directed inferonasally to match that of a dog in sternal recumbency. A 23-G trocar system (Disposable One Step Cannula System, Dorc: Exeter, NH), attached to a BSS fluid reservoir, was inserted through the superior limbus into the anterior chamber to maintain a normal physiologic IOP value (20 mmHg). The eye was perfused with balanced salt solution (BSS) for a total of 1 hour. 132,141,142,155. (Figure 2) A second 23-G trocar system connected to a digital manometer (Traceable® Manometer, Webster, TX) was inserted through the inferior limbus of the globe, permitting direct IOP measurements. The manometer was calibrated by the manufacturer and consistency was shown between this device and rebound tonometry (Tonovet). The Tonovet was calibrated by the manufacturer within less than 1 year before and after the study.

The height of the BSS reservoir was adjusted until the IOP was stabilized at 20 mmHg prior to introduction of the angiographic dye into the anterior chamber. As the delivery system was gravity-fed, no quantification of dye volume or concentration entering the anterior chamber was performed. For conducting SF AA, 2% sodium fluorescein (Akorn, AK-Fluor 10%: Decatur, IL) was used. For ICG AA, 0.25% ICG (Diagnostic Green, Farmington Hills, MI) was administered. Imaging of all limbal scleral sectors was performed using an en face view, to include the superior, inferior, nasal, and temporal aspects, and all possible scleral regions in between. (Figure 3) These sectors were observed for visualization of fluorescent dye using the Heidelberg Spectralis® Confocal Scanning Ophthalmoscope as described below. Different sectors were imaged based on where fluorescence was observed.



**Figure 3. Diagram depicting eight sectors of the globe for consistent documentation of location**. S=superior, T=temporal, I=inferior, N=nasal, ST = superotemporal, IT=inferotemporal, IN=inferonasal, SN= superonasal

### 2.3 In vivo aqueous angiography (AA) and scleral angiography (SA)

## 2.3.1 General study protocol and pre-medication

All live dogs received a single subcutaneous injection of a non-steroidal antiinflammatory medication, carprofen, at 4.4 mg/kg (Rimadyl, Zoetis: Parsippany, NJ) 1 hour prior
to performing angiography. All dogs received maropitant citrate (1.0mg/kg subcutaneous (SQ);
Cerenia, Zoetis: Parsippany, NJ) and diphenhydramine hydrochloride (2.0mg/kg SQ;
BionichePharma; Lake Forest, IL) 20 minutes prior to injection of dye; these medications were
used as a prophylactic measure to counteract potential emesis and anaphylaxis, respectively,
associated with dye administration. <sup>156</sup> All live dogs had a sterile 20-gauge IV catheter (BD
Insyte<sup>TM</sup>, Franklin Lakes, NJ, USA) placed in the right or left cephalic vein for Experiments 3, 4, 5
and 6. Blood pressure was not recorded for Experiments 3, 4, 5 and 6 due to the use of heavy
sedation. A pulse oximeter was used to monitor vital statistics (heart rate, oxygen saturation
level) in sedated dogs.

All 4 dogs in Experiment 2 were pre-medicated with butorphanol tartrate (0.2 mg/kg IM; Torbugesic; Zoetis: Parsippany, NJ, USA). All dogs were subsequently anesthetized with propofol (4 mg/kg IV; Propoflo 29, Zoetis: Parsippany, NJ, USA). Once anesthetized, all dogs were intubated and maintained with supplemental oxygen and isoflurane gas (0.5-2.5%; Isothesia, Henry Schein, Melville, NY, USA). The percentage of isoflurane was adjusted throughout the procedure to achieve a safe and constant plane of anesthesia. The dogs were continuously monitored during the procedure, and parameters including heart rate, respiratory rate, temperature, pulse oximetry and blood pressure were recorded using a portable multiparameter veterinary monitor (model PM-9000Vet; Shenzhen Mindray; Bio-Medical Electronics, Co., Ltd., Nanshan, Shenzhen, PR, China).

All normal dogs in Experiments 3 and 4 and all *ADAMTS10*-OAG dogs in Experiments 5 and 6 underwent a standard sedation protocol for both angiographic techniques. Butorphanol tartrate 0.3 mg/kg IM (Torbugesic; Zoetis: Parsippany, NJ) and dexmedetomidine 6mcg/kg IV (Dexdomitor, Zoetis: Parsippany, NJ) were administered. Upon completion of angiographic imaging, a dose of 5mg/mL atipamezole (Antisedan, Zoetis: Parsippany, NJ) equivalent in volume to the dose of dexmedetomidine administered was injected intramuscularly in each dog.

All dogs were positioned in sternal recumbency with a towel under their chin, elevating their head. Topical proparacaine hydrochloride 0.5% ophthalmic solution, USP (Akorn, Decatur, IL) was applied to the eye to be imaged and the periocular skin and ocular surface were aseptically treated with dilute 2% povidone-iodine solution. In Experiment 2, a wire eyelid speculum was used to provide exposure to the globe. In Experiments 3, 4, 5, and 6 two stay sutures (4-0 silk; Ethicon, Somerville, NJ) were placed in the superior and inferior bulbar conjunctiva to allow for adequate globe positioning during imaging. The eyelids were then manually retracted in these latter experiments, with careful attention to avoid compression of the globe or placement of excess tension on the eyelids, to allow for adequate exposure of the sclera

while imaging. Once the dogs were positioned, IOP was measured prior to and post-administration of ICG using rebound tonometry. Post-procedural rebound tonometry was performed within a timeframe of approximately 15 minutes post-injection of dye, allowing angiographic imaging to be completed without disruption. Neomycin-polymyxin-B-dexamethasone ophthalmic ointment (Sandoz; Princeton, NJ) was applied to the eye that was imaged on recovery, and every 12 hours until resolution of any observed intraocular inflammation and/or fibrin post-imaging.

## 2.3.2 Experiment 2: *In vivo* aqueous angiography (AA) using a gravity-fed trocar system in normal canine eyes

A pilot study was performed on 4 purpose-bred dogs to evaluate the feasibility of conducting AA *in vivo*, using the gravity fed trocar system. All dogs underwent general anesthesia, as described above, and were continuously monitored during the procedure. Preprocedure and post-procedure IOPs were measured using rebound tonometry.

## 2.3.3 Experiment 3: *In vivo* aqueous angiography (AA) via single intracameral (IC) injection in normal canine eyes

Twelve normal, purpose-bred dogs were heavily sedated and AA was performed through IC dye administration. Four of these dogs underwent AA utilizing trocars, 2 weeks prior. A sterile 20-G IV catheter was placed in either the right or left cephalic vein. All dogs received a standard sedation protocol consisting of butorphanol 0.3 mg/kg IV and dexmedetomidine 6 µg/kg IV (Dexdomitor, Zoetis: Parsippany, NJ).

The right eye was selected for the first 6 dogs and the left for the remaining 6 dogs; however, in the case of the 4 dogs which recently underwent AA, the same eye was imaged for

comparative purposes. AA was subsequently performed via IC injection of 0.1 mL of 0.25% ICG under steady pressure using a 25-G needle and 1 mL syringe. The needle was placed within the superonasal limbal sector and tunneled to achieve a tight seal and help minimize extrusion of ICG and subconjunctival bleb formation. Imaging of all visible scleral sectors was performed as described below.

## 2.3.4. Experiment 4: In vivo scleral angiography (SA) in normal canine eyes

The same eye of each of the 12 dogs that underwent *in vivo* AA by a single IC injection were subsequently imaged using 0.25% ICG IV using the same sedation protocol as Experiment 3. Imaging was performed following a recovery period of 10.7±3.3 days. Rebound tonometry was performed pre- and post-administration of ICG dye. For conducting SA a total of 1 mg/kg ICG was injected IV under steady pressure via the catheterized cephalic vein. Standard color images were taken of the superior, superotemporal, temporal, inferotemporal, and inferior scleral sectors of each eye being imaged immediately prior to angiography (Canon EOS 5D Mark IV with Canon EF 100mm f/2.8L Macro IS USM Lens, Canon, Tokyo, Japan). SA imaging was performed as described below.

# 2.3.5 Experiment 5: *In vivo* scleral angiography (SA) in *ADAMTS10*-open angle glaucoma (*ADAMTS10*-OAG) canine eyes

As the technique for AA was further refined, it was possible for 10 eyes from *ADAMTS10*-OAG beagle dogs to undergo SA prior to AA under the same anesthetic event. Performing SA prior to AA permitted a shorter recovery period as SA is less invasive and ICG has a short half-life. SA was used to verify structures identified on AA as the intrascleral venous plexus. Standard color images were taken of the superior, superotemporal, temporal,

inferotemporal, and inferior scleral sectors of each eye being imaged immediately prior to angiography (Canon EOS 5D Mark IV with Canon EF 100mm f/2.8L Macro IS USM Lens, Canon, Tokyo, Japan). Once the dogs were adequately sedated and positioned, 1 mg/kg ICG was administered IV through the catheter to facilitate SA. Angiography images were obtained immediately following dye administration, as described below.

## 2.3.6 Experiment 6: *In vivo* aqueous angiography (AA) via single intracameral (IC) injection in *ADAMTS10*-open angle glaucoma (*ADAMTS10*-OAG) canine eyes

The same eye in each of the 10 dogs that previously underwent SA was imaged, for comparative purposes. A recovery period of at least 24 hours was allowed between SA and AA. Once the dogs were adequately sedated and positioned, a 27-gauge needle and 1 mL syringe were used to inject 0.1 mL of 0.25% ICG into the anterior chamber through the superonasal limbus. The needle was tunneled through the superonasal bulbar conjunctiva and sclera to minimize leakage of ICG post-injection and subsequent subconjunctival bleb formation. Imaging of identical scleral sectors, as performed during SA, was performed immediately following dye injection.

## 2.4 Confocal scanning laser ophthalmoscopy aqueous angiography (AA) and scleral angiography (SA) imaging and optical coherence tomography (OCT)

All angiographic imaging was performed using a Heidelberg Spectralis® Confocal Scanning Ophthalmoscope fitted with a 55° lens. Automatic Real-time Tracking was employed to maximize still image quality. In Experiments 3 and 4, AA was performed prior to SA. With further refinement of the technique for AA it was possible to perform SA immediately followed by AA under the same sedation for Experiments 5 and 6.

The imaging sequence for AA was initiated upon entrance of angiographic dye into the anterior chamber, using the appropriate settings (i.e. 488 nm excitation laser and 500 nm barrier filter for SF, and 790 nm excitation laser and 830 nm barrier filter for ICG). A video sequence of the temporal region of the sclera was recorded for an initial 40 seconds immediately following injection of ICG (IV or IC). Time stamps were started post-dye injection. Imaging was performed every 5 seconds for a total duration of 20 minutes; this timeline allowed at least 5 minutes of imaging without any further changes seen in dye movement. Video recordings with a frame rate of 30 frames per second were obtained and were time stamped to permit accurate temporal documentation. En face views allowed for the entire sclera to be imaged in the cadaver eyes. Because of the nictitating membrane covering the superonasal, nasal, and inferonasal aspects of the globe, only the superior, superotemporal, temporal, and inferotemporal sectors of the sclera were consistently imaged *in vivo*.

Once dogs were adequately sedated and positioned, and immediately prior to SA, standard color images (Canon EOS 5D Mark IV with Canon EF 100mm f/2.8L Macro IS USM Lens, Canon, Tokyo, Japan) were obtained of each visible scleral sector by rotating from the superior sclera through the superotemporal, temporal, and inferotemporal scleral sectors, for comparative purposes. For IV SA, the imaging sequence was initiated immediately following the rapid bolus of dye administration and the superior, superotemporal, temporal, and inferotemporal scleral sectors were imaged for each eye. Video footage was recorded for 40 seconds post bolus, followed by a combination of still images and video sequences thereafter for a total time period of 10 minutes post dye administration; this approach allowed at least 5 minutes of imaging without any further observable changes in dye movement.

OCT using a Heidelberg Spectralis® and an anterior segment lens provided crosssectional information of the sclera and observation of luminal vessels in sectors where fluorescence was observed.

#### 2.5 Measurements and data analysis

Angiograms were reviewed by 2 separate individuals independently (JB/CP) upon completion of each study. A subjective qualitative analysis was provided for each angiogram. Descriptive statistics were employed for each study group (means, standard deviations) for evaluating time at which angiographic dye was injected IC or IV (time zero) to time of visualization of dye within the CAHO pathways. Values recorded by each observer were averaged, however, no statistical analysis (i.e. interclass correlation) comparing graders was performed due to the small sample size. Absolute differences and individual standard deviations between individuals imaged were calculated based on each grader's recorded values. The ability to clearly visualize CAHO pathways was subjectively analyzed for both AA and SA. Characteristics of outflow pathways were recorded, including the location of outflow pathways, the presence or absence of circumferential vessels and their approximate distance from the limbus, the number and caliber of outflow pathways, and the presence of any anastomoses or complex branching pathways. Angiographic techniques (IC vs. IV) were compared through subjective characterization of each route's capacity to provide clear visibility of the CAHO pathways. Absolute differences, individual standard deviations, and relative absolute differences were also calculated for pre- and post-procedure IOPs between Experiments 3, 4, 5 and 6 (Tables 2, 3, 7 and 8). Statistical analysis was performed using a paired t-test to compare baseline- and post-procedure IOP results. In eyes where visualization of the CAHO pathways was detected after IC and IV administration of ICG dye, cross-sectional scans using OCT were obtained to verify the presence of scleral vessels. Intrascleral vessel lumen diameters were also measured along their vertical axis using OCT images and the ruler function in Adobe Photoshop computer software (Table 5). A custom measurement scale was created using the scale bar generated by the Heidelberg Spectralis ® device. Additionally, digital overlays of identical scleral sectors comparing angiographic techniques (AA and SA) were generated using Adobe Photoshop (Adobe, San Jose, CA) via the color render command. All eyes pre- and post-experimentation were evaluated using the Standardization of Uveitis Nomenclature (SUN) scale.<sup>157</sup>

As in previous studies, aqueous humor movements were qualified as pulsatile, turbulent, or demonstrating laminar flow. 149 Pulsatile aqueous humor was observed to move in a cyclic pattern in unison with the dog's heartbeat. Turbulent flow was visualized as irregular flow of fluorescent dye as it mixed with blood upon entering the vascular channels. Laminar flow was used to describe a higher signal strength of fluorescent dye hugging the vessel wall upon entry into the blood stream.

 Table 2. Summary of normal dogs utilized and intraocular pressure measured before and after

conducting in vivo aqueous angiography (AA)

ID	Sex*	Age (years)	Eye †	Pre IOP (A) (mmHg)	Post IOP (B) (mmHg)	Absolute difference [A-B]	Individual SD √[(A−B)2)/2]	Change [B-A]/A
1	F	3.87	OD	16	8	8	5.66	-0.50
2	F	3.89	OD	11	18	7	4.95	0.64
3	M	5.87	OD	11	4	7	4.95	-0.64
4	F	3.90	OD	11	9	2	1.41	-0.18
5	M	2.17	OD	12	5	7	4.95	-0.58
6	F	2.38	OS	22	5	17	12.02	-0.78
7	F	1.55	OS	14	19	5	3.54	0.36
8	F	1.57	OS	10	20	10	7.07	1.00
9	M	2.61	OS	14	20	6	4.24	0.43
10	F	2.61	OS	9	22	13	9.19	1.44
11	M	1.60	OS	12	25	13	9.19	1.08
12	F	1.60	OD	21	9	12	8.48	-0.57
Mea	ın	2.80		13.58	13.67	8.92	6.31	0.14
SD		1.33		4.17	7.66	4.19		0.78

<sup>\*</sup>Gender defined as male (M) or female (F)

<sup>†</sup>Eye imaged was either right (OD) or left (OS)

**Table 3.** Summary of normal dogs utilized and intraocular pressure measured before and after conducting in vivo scleral angiography (SA)

ID	Eye*	Pre IOP (A)(mmHg)	Post IOP (B)(mmHg)	Absolute difference [A-B]	Individual SD √[(A−B)2)/2]	Relative Change [B-A]/A
1	OD	14	18	4	2.83	0.29
2	OD	9	7	2	1.41	-0.22
3	OD	13	8	5	3.54	-0.38
4	OD	10	7	3	2.12	-0.30
5	OS	15	11	4	2.83	-0.27
6	OS	16	9	7	4.95	-0.44
7	OD	19	12	7	4.95	-0.37
8	OS	23	20	3	2.12	-0.13
9	OS	7	4	3	2.12	-0.43
10	OS	16	13	3	2.12	-0.19
11	OS	14	12	2	1.41	-0.14
12	OD	17	11	6	4.24	-0.35
Mean		14.42	11.00	4.08	2.89	-0.24
SD		4.40	4.57	1.78		0.20

<sup>\*</sup> Eye imaged was either right (OD) or left (OS)

#### **CHAPTER 3**

## AQUEOUS ANGIOGRAPHY IN NORMAL CANINE EYES

#### 3.1 Results

## 3.1.1 Experiment 1: Ex vivo aqueous angiography (AA) in canine cadaver eyes

The 10 eyes used in this experiment were obtained from 8 mixed breed dogs, 1 Chihuahua, and 1 Havanese (Table 4).

**Table 4.** Summary of dog breeds with normal eyes utilized for conducting ex vivo aqueous angiography (AA)

ID	Gender*	Age (months)	Breed	Eye†
1	F	2	Mixed	OD
2	F	2	Mixed	OS
3	F	5	Mixed	OD
4	F	5	Mixed	OS
5	F	96	Chihuahua	OD
6	F	96	Chihuahua	OS
7	M	2	Mixed	OD
8	M	144	Havanese	OD
9	M	144	Havanese	OS
10	M	2	Mixed	OS

<sup>\*</sup>Gender defined as male (M) or female (F)

†Eye imaged was either right (OD) or left (OS)

The gravity-fed trocar system employed was found to be relatively easy to use and permitted adequate control/regulation of IOP to maintain a pressure of 20 mmHg. Use of the valved trocar system allowed easy entry within the anterior chamber, and no detectable leakage

surrounding the trocars was noted. Dye fluorescence within the CAHO pathways was visualized in a total of 8 of 10 (80%) of the dog eyes imaged. Time to fluorescence within the CAHO pathways, regardless of the dye employed was  $24 \pm 3.6$  seconds following entry into the anterior chamber. Noted outflow patterns were highly variable in their presentation ranging from solitary vessels within a single quadrant, exhibiting minimal branching patterns, to extensive and complex vascular networks (Figure 4). Sectoral variation was also noted amongst the eyes imaged (Figure 5). No notable difference in the observed intensity of fluorescence was observed between locations. Diffusion of SF was observed over time, hindering visualization. No cross-sectional OCT scans were obtained.

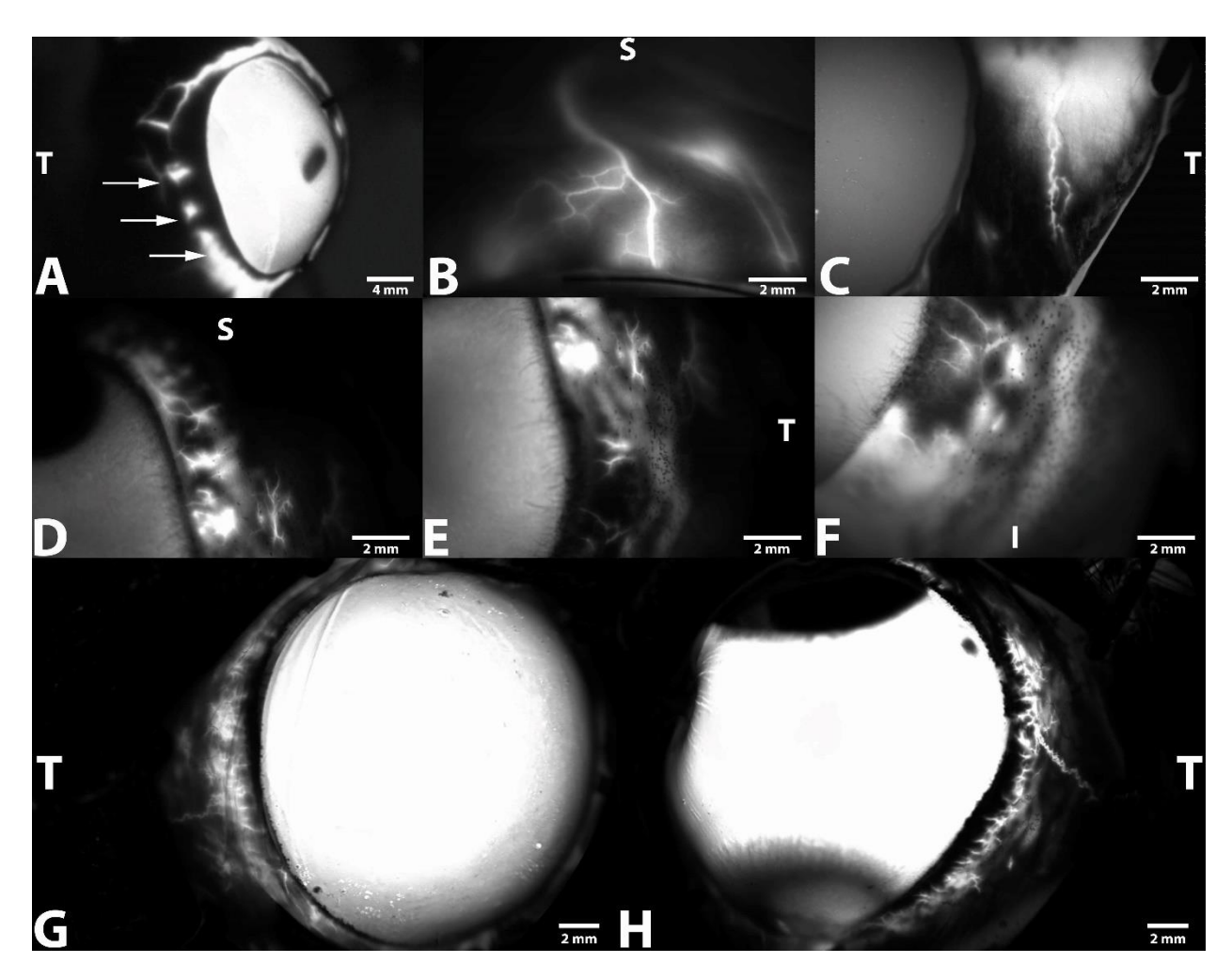


Figure 4. Representative aqueous angiography (AA) images obtained from 5 dog cadaver eyes using a gravity-fed trocar system and sodium fluorescein (SF). Images depict intraspecies and regional differences associated with the conventional aqueous humor outflow (CAHO) pathways observed. A - The right globe from a 5-month-old spayed female mixed breed dog depicts large circumferential vessels with minimal bifurcation within the superior, temporal, and inferior scleral sectors 10 minutes after dye entry into the anterior chamber. Note marked extravasation of SF (arrows). B - Fluorescence and visualization of a solitary CAHO pathway within the superior scleral sector (10 minutes) within the right globe from a 5-month-old spayed female mixed breed dog. C - Extensive circumferential vessels, demonstrating numerous complex and intricate collateral channels are noted (10 minutes) within the temporal scleral sector in the left eye from an 8-year-old mixed breed dog. Images (D, E and F) depict regional differences associated with the CAHO pathways at 3 minutes following dye entry into the anterior chamber within the superior (D), temporal (E), and inferior (F) scleral sectors of the same eye from a 6-month old mixed breed. Images (G; right eye and H; left eye) depict variations associated with the CAHO pathways between eyes noted at 5 minutes from the same 8-year old mixed breed dog. S=superior, T= temporal, I= inferior

## SEGMENTAL VARIATION OF AA IN CADAVER EYES

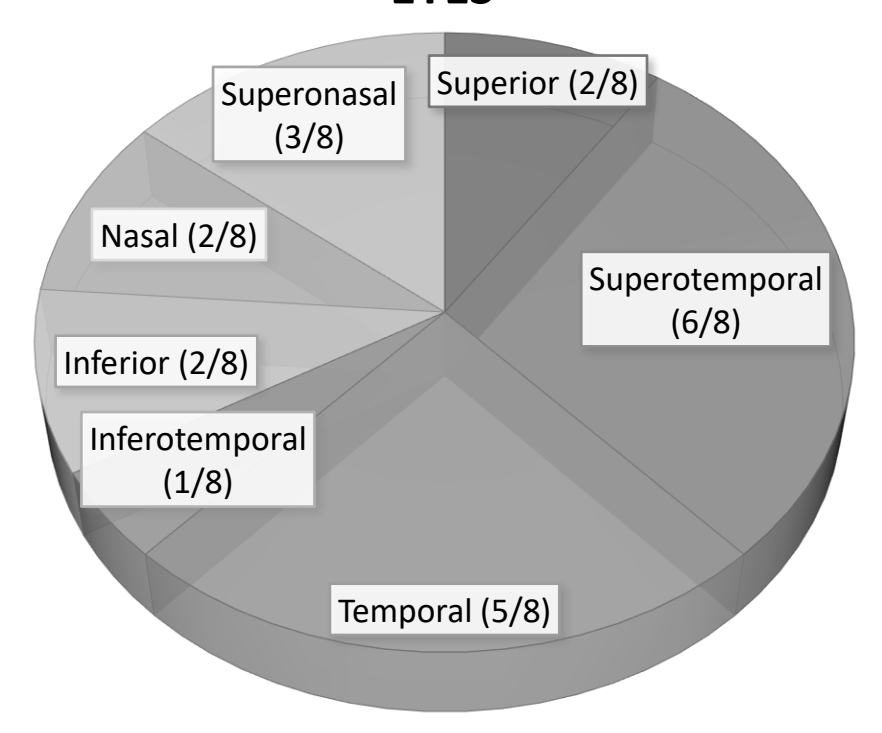


Figure 5. Schematic demonstrating the sectoral variation in visualization of fluorescent dye administered intracamerally (IC) in 10 ex vivo canine eyes. Fluorescence and visualization of the CAHO pathways was only seen in 8/10 of eyes.

#### 3.1.2 Experiment 2: In vivo aqueous angiography (AA) using a gravity-fed trocar system

Four eyes from 3 intact female beagles and 1 intact male mixed breed dog underwent *in vivo* AA using the gravity-fed trocar system (data not shown). Visualization of ICG fluorescence was absent in all visible scleral quadrants and the sectors in between those quadrants in the 4 eyes imaged. No cross-sectional OCT imaging was performed due to lack of visibility of ICG fluorescence (data not shown). This approach was found to be impractical and cumbersome, with the disadvantage of not producing any visible dye movement into the CAHO pathways and vascular channels. This experiment was performed to validate the *ex vivo* method for *in vivo* use.

To improve accessibility of the procedure, the gravity-fed trocar system was replaced with a single bolus injection protocol (Experiment 3).

## 3.1.3 Experiment 3: *In vivo* aqueous angiography (AA) via single intracameral (IC) injection

A total of 12 dogs were utilized for conducting AA following a single IC injection of dye (Table 5). Heavy sedation in conjunction with topical anesthesia provided adequate restraint and immobilization necessary for stay suture placement and conducting IC administration of ICG. Four dogs underwent Experiment 2 as well as Experiment 3; no differences in imaging quality were noted as compared to the 8 dogs that only underwent Experiment 3. Intraocular pressure was measured immediately prior to IC injection of ICG and within 15 minutes post-injection of dye. Individual pre and post IOP results, absolute differences, individual standard deviations, and relative change in IOP are listed in Table 2. An average of 25 still images were obtained for each eye using the Heidelberg Spectralis®.

**Table 5.** Summary of time to fluorescence, vessel location, vessel pattern, and vessel lumen diameters visualized after in vivo aqueous angiography (AA) in normal dog eyes

ID	Sex*	Age (years)	Body Weight (kg)	Eye †	Onset of fluorescence (sec post- injection)	Vessel Location	Vessel Complexity and Pulsation	Vessel Lumen Diameter (mm)	Vessel Lumen Depth (mm)
1	F	3.87	10	OD	30	Superotemporal	Complex, bifurcations	364.71	262.75
2	F	3.89	10	OD	45	Superotemporal	Complex, bifurcations	288.89	266.67
3	M	5.87	20.6	OD	35	Superotemporal- temporal	Single vessel	352.94	304.58
4	F	3.90	9	OD	35	Superotemporal	Complex, bifurcations, bidirectional pulsation	166.01	142.48
5	M	2.17	11	OD	35	Not visualized	None	-	-
6	F	2.38	11.5	OS	35	Superotemporal and temporal	Complex, bifurcations, pulsation	244.44	325.49
7	F	1.55	9	OS	30	Superotemporal	Complex, bifurcations	207.84	295.42
8	F	1.57	9	OS	35	Superotemporal	Complex, bifurcations	169.93	233.99
9	M	2.61	12.9	OS	30	Superotemporal, temporal, inferotemporal	Complex, bifurcations, bidirectional pulsation	269.28	287.58
10	F	2.61	11.5	OS	35	Faint superotemporal and temporal vessels	Complex, bifurcations	263.01	279.98
11	M	1.60	15.2	OS	40	Superotemporal, temporal, inferotemporal	Complex, bifurcations, pulsation	253.12	249.75
12	F	1.60	12	OD	35	Not visualized	None	-	-
Mea	n	2.80	11.81		35.00			258.0	264.9
SD		1.33	3.32		4.26			9.1	16.2

<sup>\*</sup>Gender defined as male (M) or female (F)

†Eye imaged was either right (OD) or left (OS)

Following IC injection of ICG, diffuse fluorescence throughout the anterior chamber was readily observed. Shortly thereafter, dye fluorescence was observed emanating into various scleral sectors in 10 out of the 12 eyes imaged. Two eyes failed to demonstrate fluorescence within any scleral sectors evaluated. Upon exiting the anterior chamber, initial dye fluorescence was noted to occur within intra-scleral channels, occurring on average  $35.0 \pm 4.3$  seconds post-IC injection of ICG. While no statistical analysis was performed, the means provided by the two graders were consistent. The mean absolute difference between the two graders was 0.4 seconds, while the mean individual standard deviation was 0.27 seconds. Progressive and rapid filling of

larger, complex radially oriented luminal networks was noted shortly thereafter (Figure 6). The most common scleral sector to exhibit dye fluorescence associated with the CAHO pathways was the superotemporal sclera. Results demonstrating regional fluorescence among the eyes imaged are summarized in Figure 7. Numerous bifurcations and intricate collateral pathways were present in 9 eyes with 1 eye exhibiting a single lateral vessel. In 6 out of 10 eyes which demonstrated intra-scleral fluorescence, dye movement was noted to exhibit progressive and complete delineation of the vessel walls once observed. (Figure 8) Thereafter, observed fluorescence intensity remained uniform and static. In 4 out of the 12 eyes (33.3%), pulsatile and turbulent movement of dye was observed, demonstrating a unidirectional movement in 2 (16.7%) eyes, while the other 2 (16.7%) eyes exhibited bidirectional movement. Noted pulsations were intermittent throughout the angiograms, when present, but appeared to coincide with the heart rate of the dog.

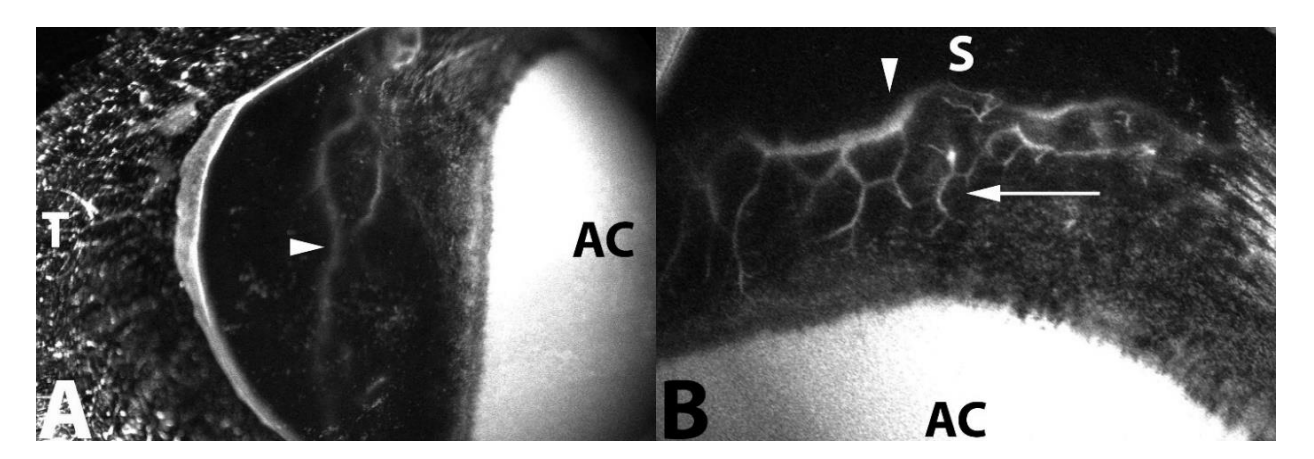


Figure 6. Representative *in-vivo* aqueous angiography (AA) image following intracameral (IC) injection of indocyanine green (ICG) into the right eye of a 3-year old intact female beagle dog. Fluorescence with deep intra-scleral vessels (arrow) and a large circumferential vessel (arrow head) is readily visualized within the temporal (A; 9 minutes post injection) and superior (B; 15 minutes post injection) scleral quadrants. AC = anterior chamber, S = superior, T = temporal.

## **EXPERIMENT 3 SEGMENTAL VARIATION**

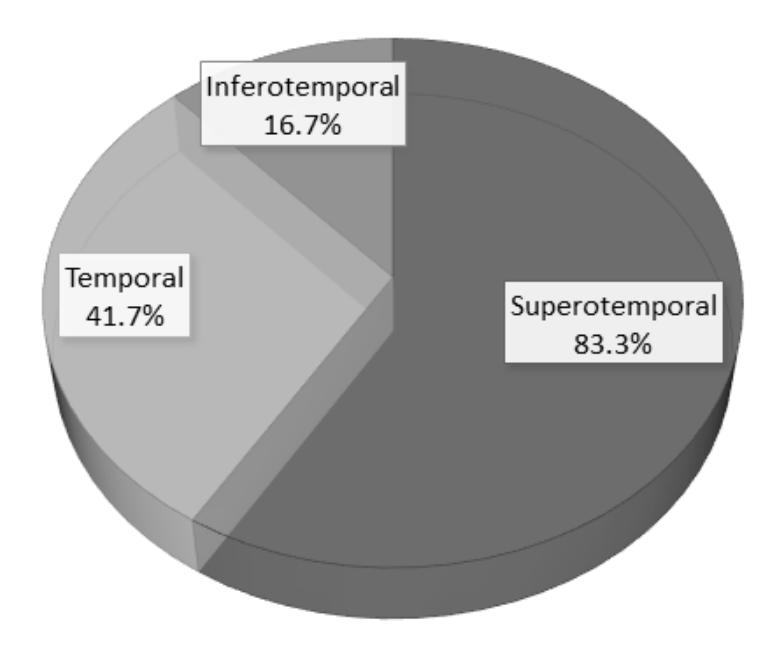


Figure 7. Schematic demonstrating the sectoral variation in fluorescent dye outflow after aqueous angiography (AA) in 12 live dogs. The most frequent scleral sector to exhibit dye fluorescence associated with the conventional aqueous humor outflow (CAHO) pathways was the superotemporal scleral aspect (10 out of 12 eyes; 83.3%). This location was the first to show fluorescence and exhibited the most intense dye fluorescence. Five eyes (41.7%) also demonstrated fluorescence of indocyanine green (ICG) within the temporal scleral quadrant, while 2 (16.7%) additional eyes also displayed fluorescence within the inferotemporal scleral sector.

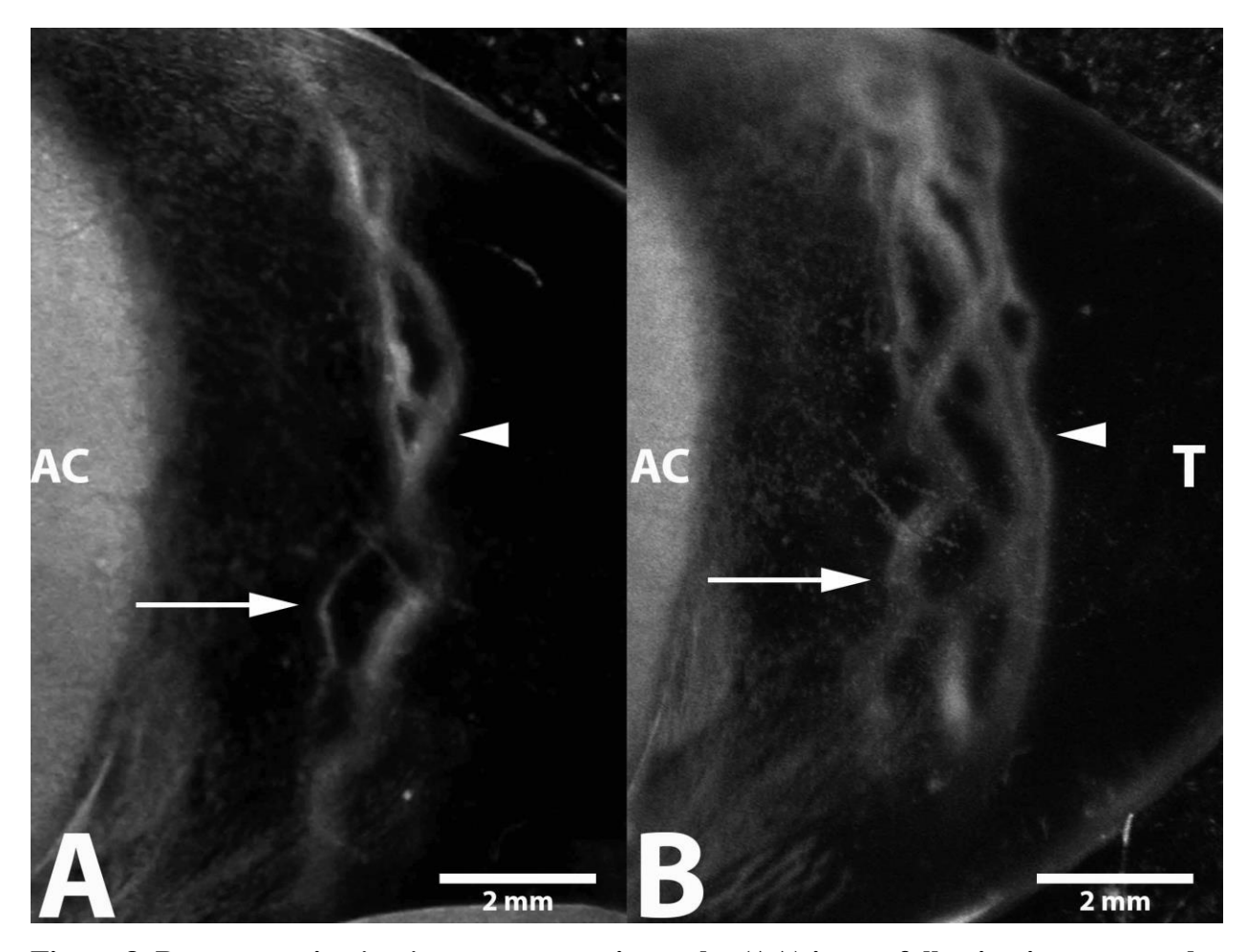


Figure 8. Representative *in-vivo* aqueous angiography (AA) image following intracameral (IC) injection of indocyanine green (ICG) into the left eye of a 1-year old intact female beagle dog. Initial fluorescence at 1 minute (A) and progressive filling at 4 minutes (B) post injection is depicted within deep intra-scleral vessels (arrow) and larger circumferential vessels (arrowhead). AC=anterior chamber.

All outflow channels which exhibited fluorescence following IC administration of ICG were readily identifiable on cross sectional OCT as vessels.

## 3.1.4 Experiment 4: *In vivo* intravenous (IV) scleral angiography (SA)

Following a 7-day recovery period, the same eyes of all 12 dogs that underwent AA via a single IC injection were evaluated using conventional IV administration of ICG and scleral imaging (Table 6). All eyes prior to imaging were considered clinically normal and did not

exhibit any evidence of intraocular inflammation or dye fluorescence (i.e. following prior ICG administration from Experiment 3). Intraocular pressure was measured immediately prior to IV injection of ICG and within 15 minutes post-injection of dye.

**Table 6.** Summary of normal dogs utilized and intraocular pressure measured before and after

conducting conducting in vivo scleral angiography (SA)

ID	Eye*	Onset of fluorescence (sec post-injection)	Pre IOP (A) (mmHg)	Post IOP (B)(mmHg)	Relative Change [B-A]/A
1	OD	30	14	18	0.29
2	OD	45	9	7	-0.22
3	OD	35	13	8	-0.38
4	OD	35	10	7	-0.30
5	OS	30	15	11	-0.27
6	OS	35	16	9	-0.44
7	OD	35	19	12	-0.37
8	OS	35	23	20	-0.13
9	OS	30	7	4	-0.43
10	OS	35	16	13	-0.19
11	OS	40	14	12	-0.14
12	OD	30	17	11	-0.35
Mean		34.58	14.42	11.00	-0.24
SD		4.50	4.40	4.57	0.20

<sup>\*</sup> Eye imaged was either right (OD) or left (OS)

Filling patterns amongst the 12 eyes imaged were noted to be highly variable. Common trends were observed and characterized by the rapid and progressive filling of large circumferential intra-scleral vessels, consistent with the venous circle of Hovius, 3-5 mm from the limbus (Figure 9). Numerous anastomoses were observed between these large caliber vessels.

Shortly thereafter, filling of smaller, deeper intra-scleral vessels was observed. These vessels were thought to represent components of the intra-scleral venous plexus. Simultaneously during this later filling period, fluorescence within both superficial and deep conjunctival arteries followed by their venular counter parts occurred. In all but 1 eye imaged, visualization of fluorescence within the vasculature was progressive and uniform. In this 1 eye, visible pulsation and turbulent flow was observed within the deeper intra-scleral vessels. Dye movement during this early filling period also demonstrated bi-directional movement. All dogs recovered uneventfully following imaging.

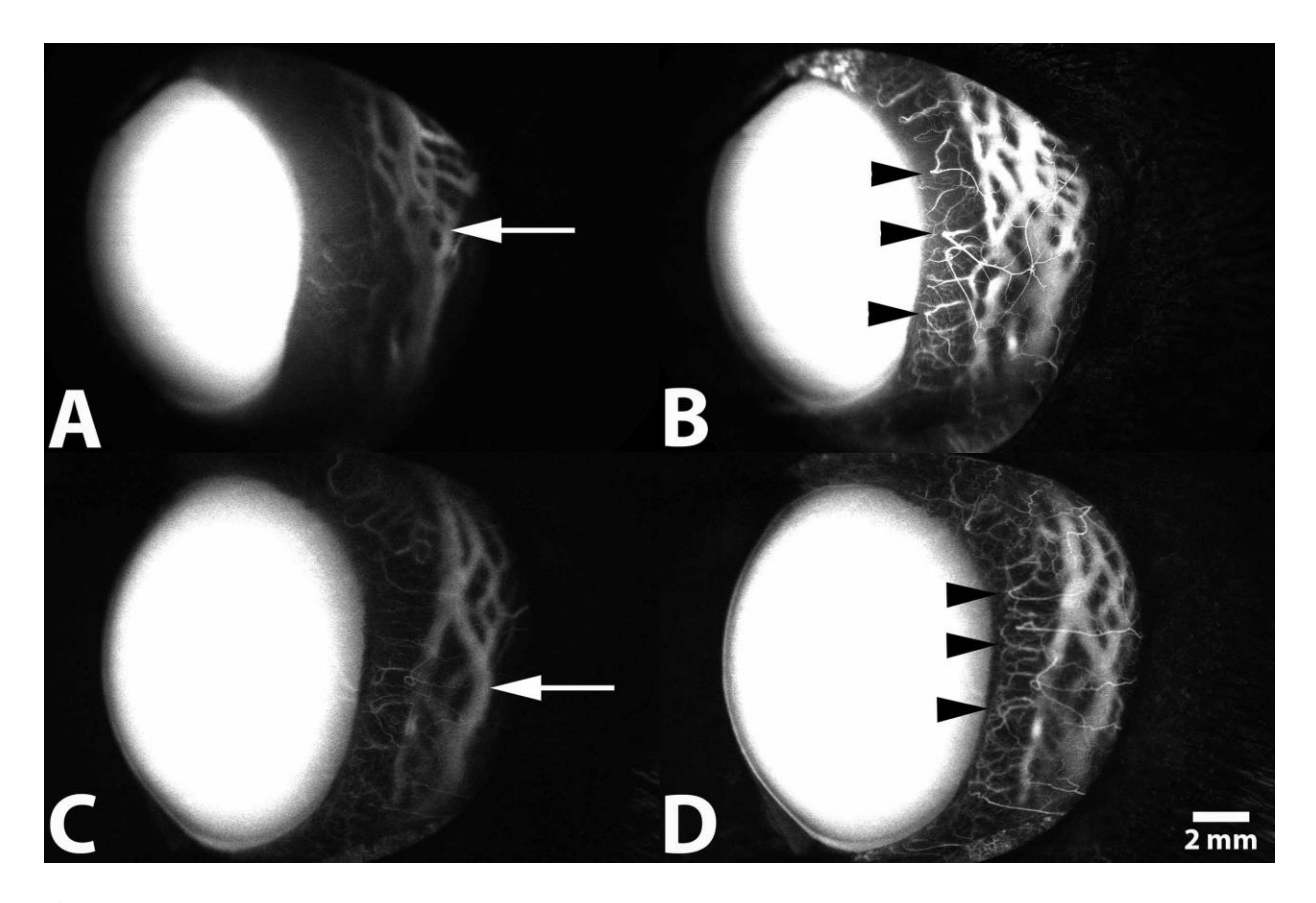


**Figure 9**. Representative scleral angiography (SA) following intravenous (IV) administration of indocyanine green (ICG) of the left eye from a 1-year old intact female beagle dog (A, B) and 2-year-old male beagle dog (C, D). A, C- Filling within deep circumferential ciliary arteries, the intra-scleral venous plexus, and venous circle of Hovius within the lateral scleral quadrant are visualized 30 seconds post injection (arrow). B, D- Filling of terminal ciliary arterioles, capillary beds, and venular counterparts are visualized 1-minute post injection (arrow heads).

### 3.2 Comparison of intracameral (IC) and intravenous (IV) routes of injection

When qualitatively comparing noted intrascleral vessels, IC ICG injection corresponded with IV routes of ICG administration in 10 of 12 (83.3%) eyes imaged (Figures 10 and 11). Two dogs could not be assessed due to a lack of visualization of dye fluorescence following IC administration. When visible, the IC route of administration allowed for visualization of the intra-scleral venous plexus, in addition to regional components of the venous circle of Hovius. Additionally, using this modality, pulsatile motion of dye was readily observed. One of the dogs exhibited pulsatile movement of dye following IC administration and transient movement following IV administration. In contrast, IV administration of ICG accommodated rapid visualization of both the intra-scleral venous plexus and venous circle of Hovius, in addition to, the conjunctival and episcleral vasculature. However, no significant movement of dye, suggestive of aqueous humor outflow was readily visible beyond the initial luminal filling of the vessels with this technique. In all eyes where fluorescence of ICG was noted following IC administration, similar vascular components were identifiable on side by side comparison following an IV route of administration. Cross sectional OCT scans qualitatively verified congruency of luminal pathways seen in both the IC and IV routes of dye administration (Figure 12). Using the OCT scans and computer software, the mean  $\pm$  SD luminal diameter of intrascleral vessels were measured to be 258.0±9.1 µm, occurring at mean depth of 264.9±16.2 um. Direct overlay, comparing routes of administration and color rendering, using a commercially available software, demonstrated slight variation between fluorescent patterns observed (Figure 10). Luminal fluorescence following IV administration demonstrated complete filling of the vascular channels observed. Partial and/or incomplete fluorescence, specifically

along the luminal walls of the larger vascular channels associated with the venous circle of Hovius was noted following IC administration.

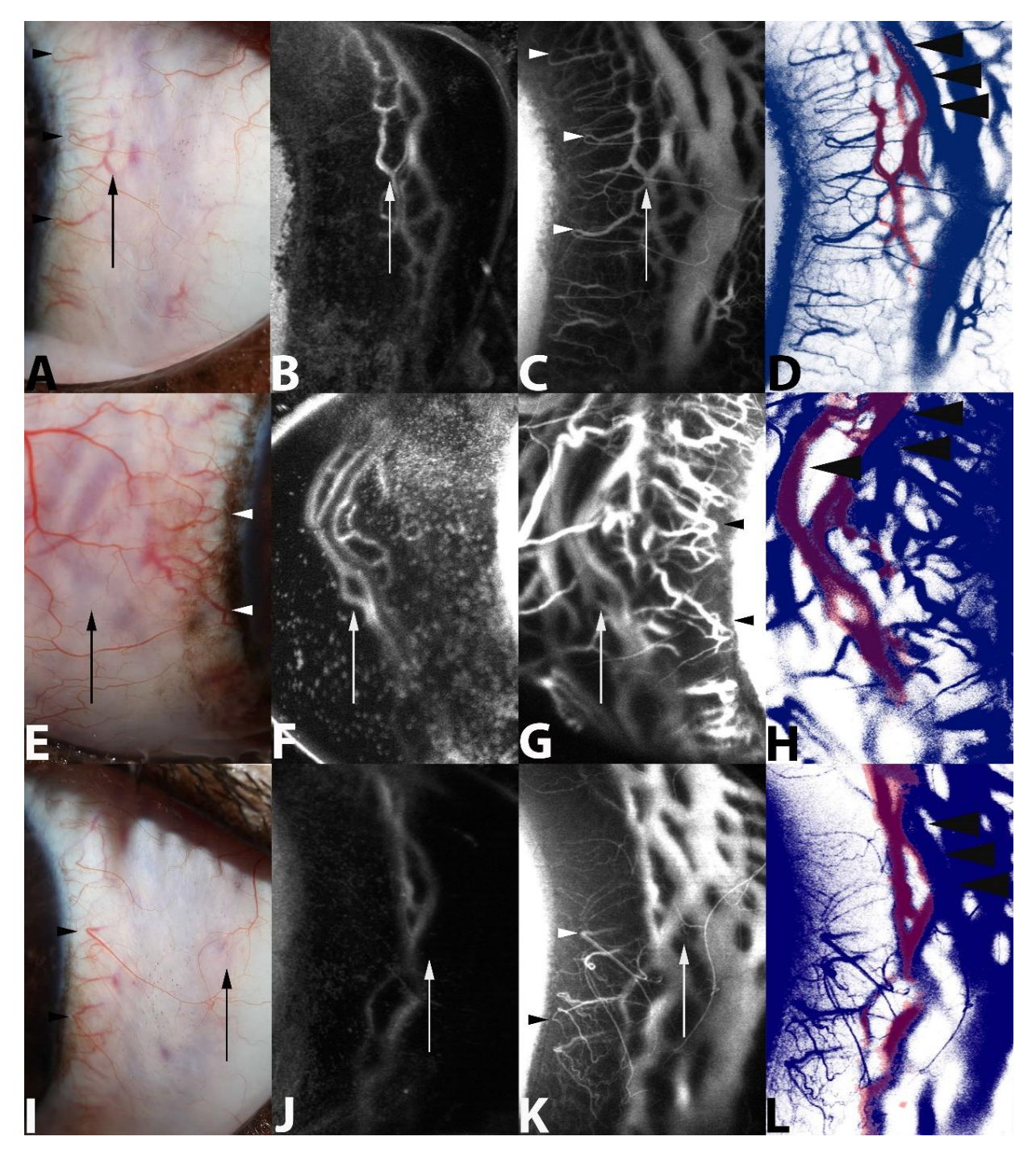


Figure 10. Representative standard color (A, E, I), *in-vivo* intracameral (IC) aqueous angiography (AA) (B, F, J), and intravenous (IV) scleral angiography (SA) (C, G, K) using indocyanine green (ICG) dye from the left eye of a 1-year old intact female beagle dog (A, B, C), the right eye (E, F, G) of a 3-year-old intact female beagle, and the left eye of a 1-year old intact female beagle dog (I, J, K), respectively. Venular components of the

## Figure 10 (cont'd)

conventional aqueous humor outflow (CAHO) pathways are readily visualized following both angiographic techniques and depicted by the arrows. Visualization of terminal ciliary arterioles and conjunctival vasculature (arrow heads) is noted following IV angiography alone. For comparative purposes, representative digital overlay and color rendering of angiographic images were generated following IC AA and IV SA utilizing ICG (D, H, L). Digital overlay and color rendering of images were performed utilizing an imaging editing software. Color rendering was performed using the color range tool (entire image), isolating observed fluorescence patterns. Red depicts fluorescence observed following IC AA and blue following IV SA. Note partial luminal filling of the larger vascular channels following IC AA (black arrows), suggestive of laminar flow. Image acquisition time following ICG injection includes the following; B (5 minutes), C (5 minutes), F (8 minutes), G (1 minute), J (1 minute), and K (2 minutes).

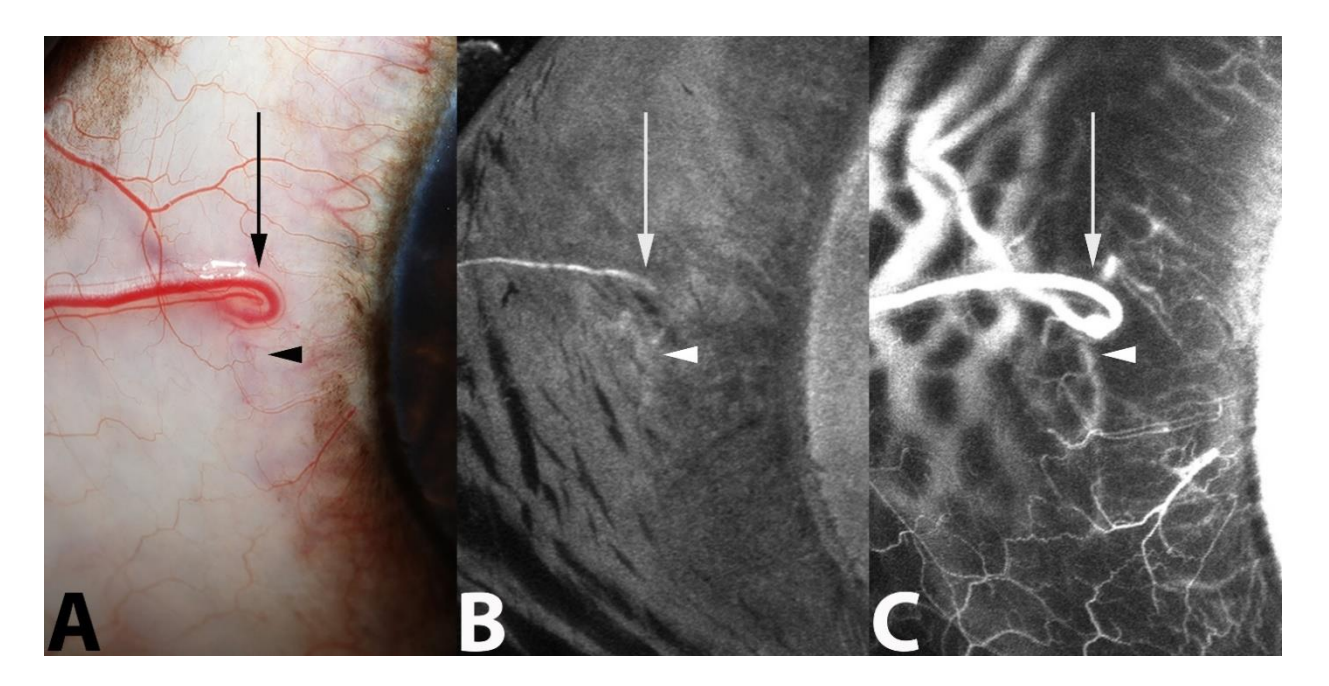


Figure 11. Representative standard color (A), IC aqueous angiography (AA) (B), and IV scleral angiography (SA) (C) from the right eye of a 4-year old male Mixed breed dog. This eye demonstrated minimal visualization of the CAHO pathways following IC administration of ICG. Outflow occurred via a component of the intra-scleral plexus (arrow head) and an episcleral vein (arrow). These components are similarly visible using standard color and IV ICG angiography.

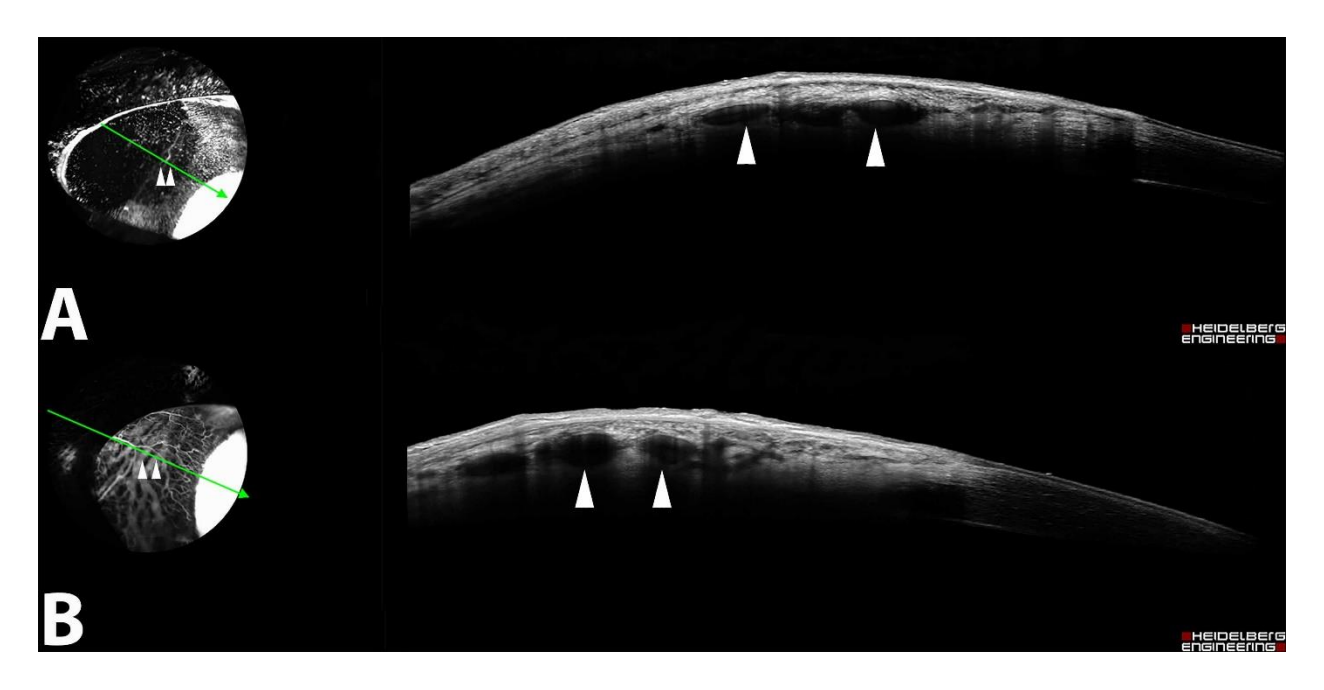


Figure 12. Cross sectional OCT scans from the right eye of a normal 3-year old intact female beagle dog following intracameral (IC) (A) and intravenous (IV) (B) indocyanine green (ICG) angiography. The orientation of the scan (green arrow) depicts luminal vessels which demonstrated fluorescence following both angiographic modalities (arrow heads) in similar locations within the tissue. AA, aqueous angiography; SA, scleral angiography.

#### 3.3 Safety

No aqueous flare (0 on the SUN scale) was observed in any eye prior to IC injections. All 12 dogs recovered from sedation and administration of ICG without significant complications. One day following the procedure all eyes were noted to exhibit 1+ aqueous flare, which resolved with medical therapy 2 days post procedure. Two dogs were observed to have developed a small amount of fibrin and mild generalized flare (4+ grading on the SUN scale) that subsequently resolved over a course of 10 days. Following IV SA, no adverse systemic or ocular signs were observed.

#### 3.4 Discussion

To the authors' knowledge, this is the first study documenting distal aqueous humor outflow in live dogs with no known ocular abnormalities. The results of this study demonstrated that AA, using similar delivery techniques as in humans 127,132,142, was easy to perform in cadaver eyes of dogs and permitted visualization of the CAHO pathways. This is consistent with recent studies in *ex vivo* canine and feline models. 126 (Telle MR, et al. Vet Ophthalmol 2019:22: ACVO E-Abstract E32; McLellan GJ, et al. IOVS 2019:60: ARVO E-Abstract 3184) Unfortunately, utilizing the same approach and delivery system, the authors were unable to attain comparable results in live dogs. Modification of the IC delivery to a more clinically applicable single bolus injection technique permitted visualization of the angiographic dye within the CAHO pathways.

Similarities were observed in the location, size, pattern, and redundancy of vascular components associated with CAHO pathways between IC and IV dye administration, consistent with those of previous corrosion casting techniques.<sup>3,158</sup> Cross-sectional OCT images supported the notion that vessels observed were the deep intra-scleral plexus and venous circle of Hovius.<sup>1,3</sup> While the use of SF and ICG permitted clear visualization of the CAHO pathways *ex vivo*, rapid diffusion of SF, presumably due to its small molecular size and binding properties<sup>133,156,159,160</sup> occurred. As such, ICG was employed for subsequent *in vivo* AA.

Use of the gravity-fed trocar system was shown to be effective for administering ICG into the anterior chamber of the living dog eye; however, no subsequent flow of dye within the CAHO pathways or its vascular components could be visualized. This finding may have simply reflected the dynamic nature of aqueous humor outflow and the variation in CAHO pathways. As demonstrated in humans, visualization of the CAHO pathway is often intermittent, not continuous<sup>7</sup>. It is possible sectors exhibiting outflow did not coincide with the area being

observed. Interindividual differences in vascular patterns, and scleral or conjunctival pigmentation as well as species differences in sectoral outflow of aqueous humor may also have hindered visualization of the angiographic signal<sup>70,71</sup> While the above are all possible explanations, the authors believe the lack of observation of dye fluorescence most likely reflected the experimental set up itself and its inability to be directly transferred for use in dogs due to anatomical differences. Placement of the trocars was limited to the temporal half of the globe due to the natural degree of scleral exposure, while permitting safe insertion into the globe, the collar of the trocars often interfered with the eyelid speculum and/or with the eyelids themselves. As a result, compressive effects on the sclera may have occurred by the trocar collars alone or in conjunction with the eyelid and/or eyelid speculum, leading to a lack of detectable fluorescence within the CAHO pathways.

Modification to an *in vivo* single bolus IC injection resulted in clear visualization of dye within CAHO pathways. The volume of ICG dye administered was comparable between dogs of similar body weights and the rate of dye administration was approximately the same when introduced under steady pressure as a bolus injection. This bolus approach was significantly less time-consuming, relied on a simplified experimental set up, and resulted in subjectively lower scores of post-procedure intraocular inflammation as compared to the gravity-fed delivery system. While human eyes are more tolerant and generate less of an inflammatory response to such procedures<sup>127</sup>, dog eyes are known to exhibit a significantly greater inflammatory response, even following minimally invasive intraocular procedures.<sup>161</sup> As such, the IC approach may be more advantageous in clinical veterinary practice, permitting AA to be more readily performed with less intraocular irritation or trauma. Additionally, use of heavy sedation in lieu of general anesthesia was effective for patient positioning, rotation of the globe, and conducting AA. Sedation facilitated a faster recovery of the dogs and reduced associated costs, thereby enhancing the feasibility of AA as a potential clinical diagnostic tool.

In contrast to human studies, <sup>127</sup> the presence of a nictitating membrane nasally, a deeper orbit, and a larger corneal diameter, scleral exposure of the dog eyes was limited and prohibited visualization of the inferior, nasal, and superonasal scleral sectors. (Telle MR, et al. Vet Ophthalmol, 2019;22:E32; McLellan GJ, et al. IOVS 2019:60: ARVO E-Abstract 3184) Based on eyelid conformation, the temporal scleral sector was the easiest to image in dogs, followed by the superotemporal and inferotemporal sectors. The superior and inferior scleral sectors were the most challenging to clearly visualize. In lieu of an eyelid speculum, 2 conjunctival stay sutures were utilized to help manipulate the globe, while relying on manual retraction of the eyelids with careful attention not to apply pressure to the globe or to the eyelids. Although there are limitations to this method of scleral exposure, including possible distortion or compression of aqueous humor outflow pathways, the authors had little other option to open the eyelids in sedated and/or anesthetized dogs.

As the superonasal sector was injected, we anticipated strong dye fluorescence in the inferotemporal sector due to its location directly opposite the injection site; however, this was not the case. Sectoral variation in dye fluorescence was noted, with the most common site of dye visualization in the superotemporal sector of the sclera. Two dogs, 1.6 and 2.2 years old, demonstrated no fluorescence of dye after IC administration of ICG. At this time, we can only speculate on reasons for the lack of dye visibility in 2 of the 12 eyes (16.7%), such as low levels of aqueous outflow, sectoral outflow, or dilution of dye within the anterior chamber. Fluctuations in IOP could cause sudden collapse of the outflow pathways and/or possible dye leakage following IC injection, resulting in varied concentrations of dye within the anterior chamber. Approximately 98% of ICG dye in plasma appears protein-bound and is consistent with our observation of steady fluorescence within the scleral vasculature after an initial flux in the

intensity of ICG dye and minor leakage into the surrounding tissues. Despite there being no apparent differences in permeability of ICG dye associated with age, it is possible that the age of the dogs could also have played a role. Although 2 cadaver eyes originated from a 2-month old puppy, all the live dogs evaluated in this study were adults under the age of 5.9 years. It is unknown at this time if older dogs have an observable difference in sectoral outflow of ICG dye compared to juvenile dogs. Given this information, the authors are working towards a quantitative method to measure intensity signals of fluorescent dye to allow for objective evaluation and comparison of dye outflow.

While not a primary focus, 2 interesting observations noted during the current study included pulsatile dye movement within the CAHO pathways during AA and varied fluorescent patterns following direct comparisons between IC and IV routes of dye administration. Of the 10 eyes that demonstrated progressive fluorescence post IC administration of ICG, 4 eyes exhibited visible pulsation and turbulent movement of ICG, while 2 eyes demonstrated visible bidirectional flow of dye. These observations were similarly described in human subjects, <sup>127,132</sup> highlighting the dynamic nature of these outflow pathways. The pulsatile dye movement, given its rhythmic nature with the heart rate of the dog, was believed to reflect transient and minute IOP fluctuations generated by alterations in blood pressure during systole. <sup>163</sup> In humans, this pulsatile movement has been demonstrated *in vivo* and was suspected to be linked to a cyclic flow pattern of aqueous initially induced by elevations in IOP from blinking and eye movement followed by a piston-like action of the choroid as a result of cardiac pulsation. <sup>150</sup> The result of this cyclic flow was a surge of aqueous humor into systemic circulation during the peak radial pulse. <sup>165</sup> While this study evaluated normal dogs, we speculate the degree and

frequency of this pulsatile dye movement may be reduced and/or eliminated during elevations in IOP.

In the current study only a small volume of dye was administered IC. Although IOP was unable to be measured immediately post-injection due to limitations in the time frame to obtain angiogram images, IOP was measured 15 minutes following completion of angiography.

Intraocular pressure only exceeded the upper limits of the normal reference range (22 mmHg) in 1 eye (25 mmHg), 154 which returned to normal (below 22 mmHg) within 1 hour. While alterations in dye concentration within the aqueous humor may have occurred using a single bolus approach, variations were considered minimal and were not believed to have affected the study results. Scleral imaging following IV administration of ICG readily identified the venous components associated with the CAHO pathways, similar to IC administration, including the intrascleral plexus and the venous circle of Hovius. Results herein were consistent with corrosion casts, which identified ciliary vessels running circumferentially through the sclera, immediately anterior to the scleral venous plexus; these vessels branched into anterior ciliary arteries, then split into various arteriolar branches before forming a capillary bed at the limbus.<sup>3</sup>

Direct comparison between IC and IV dye administration demonstrated stratification of dye, specifically following IC administration as dye entered into the systemic circulation at the level of the circle of Hovius. In contrast, IV administration resulted in progressive and uniform luminal filling of the observed vasculature. This suggested laminar aqueous humor outflow was occurring with IC administration of dye, findings similarly noted in human and porcine eyes. 149,164,166,167 This was thought to reflect the movement and bipartite separation of aqueous humor from the sanguineous components of blood (blood corpuscles), as it entered into hematogenous circulation. 165 This observation was inconsistent and its absence may have simply

reflected anatomical variations between subjects resulting from 2 distinct but intimately associated intervening small vessels, separated by a minute physical distance. Alternatively, the absence of laminar flow may have occurred due to the formation of a smooth and continuous solitary column of aqueous humor within a single larger vessel, resulting in a tripartite stratification pattern and the appearance of two vascular channels.<sup>149</sup>

An additional challenge of AA is the standardization of numerous parameters. Identical scleral sectors between subjects need to be imaged, utilizing identical dye volume, dye concentration, rate of infusion, illumination and filter settings. Additionally, IOP is an important variable which needs to be considered when evaluating aqueous humor outflow. Normal morphology, structural composition, and the array of dynamic physiologic changes that can arise in different ages and/or breeds of dogs should also be considered. The heterogenous results recorded herein pre and post AA and SA imaging indicated poor control of IOP between eyes and is a limitation of this study. Alterations in IOP may be an effect of the drugs employed for conducting angiography or the technique itself. Numerous sedative and anesthetic drug protocols have demonstrated alterations in IOP and aqueous outflow. 6,23 IC administration may have induced a rise in IOP accounting for transient elevations following bolus dye administration. Alternatively, minute leakage via the needle tract and/or induction of mild anterior uveitis following IC injection may have accounted for lower IOPs noted in some cases. It has been speculated that rapid influx of fluid into the anterior chamber results in incomplete mechanical disruption of the aqueous outflow barriers, including the blood aqueous barrier 158, however the significance of these IOP alterations and their true impact on aqueous humor outflow facility is unknown. Controversy exists within the literature, regarding canine IOPs and their correlation with aqueous humor outflow. Tonography and fluorophotometery studies have demonstrated

elevations in IOP yield and decreased rates of aqueous humor outflow.<sup>6,23</sup> Conversely, using a perfusion model, outflow facility has been reported to be relatively stable and independent of IOP alterations.<sup>158</sup>

The washout effect may contribute to changes in aqueous humor outflow. This phenomenon has been well described in many species<sup>169</sup> to take effect as early as 30 minutes after perfusing the globe<sup>170,171</sup>;In canines, washout is suspected to be primarily due to disruption and/or removal of the hyaluronidase-sensitive component of the barriers to aqueous outflow and not a direct IOP effect.<sup>2,158</sup> As such, it is possible that perfusion for 1 hour prior to angiography may have impacted aqueous outflow in *ex vivo* eyes. To limit the impact on eyes evaluated in this study, all eyes were treated similarly. It is also reasonable to conclude that transient IOP alterations likely impact aqueous outflow facility to some degree in the eyes of live dogs.<sup>158</sup> This, coupled with highly variable IOP values in this study could be potential confounders of aqueous outflow which could have altered the angiographic signal visualized and the timing observed. Future studies are required to address these limitations, wherein IOP is less varied in order to determine if IOP and/or washout have a true impact on aqueous humor outflow.

#### 3.6 Conclusion

Descriptive findings of CAHO pathways *ex vivo* and *in vivo* in normal dogs were provided. SA with ICG appears to be an effective means for identifying the vascular components associated with the distal CAHO pathways, while AA permits visualization and qualitative assessment of aqueous humor outflow. This study demonstrated the capacity to visualize distal CAHO pathways following AA in dogs using the proposed IC experimental set up and imaging device. The information provided herein offers new insights into the fluid characteristics associated with the CAHO pathways of dogs, which could serve as the foundation for subsequent

studies. This imaging modality could have an immediate benefit in dogs by identifying a clinically applicable tool to evaluate the CAHO pathways *in vivo*. This could shed new insights into the characteristics associated with CAHO pathways and how they may become altered in a variety of sight threatening conditions. Ultimately, it may allow for patient specific therapeutic approaches aimed at controlling IOP and preserving vision.

## **CHAPTER 4**

# AQUEOUS ANGIOGRAPHY IN *ADAMTS10*-OPEN ANGLE GLAUCOMA BEAGLE DOG EYES BEFORE AND AFTER DEVELOPMENT OF GLAUCOMA

## 4.1 Results

## 4.1.1 Intravenous (IV) scleral angiography (SA)

SA was performed on one eye each in  $10 \, ADAMTS10$ -OAG beagles. Six eyes were classified as glaucomatous and exhibited a baseline IOP  $\geq$ 20 mmHg (mean 27.5 mmHg; range 20.0-39.3 mmHg) and optic nerve head changes, while 4 pre-glaucomatous eyes were measured to have a baseline IOP <20 mmHg (mean 18.3 mmHg; range 16.3-19.7 mmHg) and no optic nerve head changes. These same eyes had mean immediate pre- and post-procedure IOP values of  $23.2\pm10.4$  mmHg and  $17.1\pm8.6$  mmHg, respectively. These values varied slightly from the baseline measurements with 5 eyes exhibiting IOP  $\geq$ 20 mmHg (range 20.0-43.0mmHg) and 5 eyes demonstrating IOP <20 mmHg (range 7.0-19.0 mmHg). (Table 7) There was no statistically significant difference between the pre- and post-SA IOP values when compared using a paired t-test (alpha = 0.05, p-value = 0.17). Individual pre- and post-SA IOP results including their absolute differences, individual standard deviations, and relative absolute differences are listed in Table 7.

**Table 7.** Summary of ADAMTS10-open angle glaucoma (ADAMTS10-OAG) dogs utilized for conducting scleral angiography (SA)

ID	Sex	Age (years)	Body Weight (kg)	Eye	Vessel Lumen Diameter (µm)	Vessel Lumen Depth in Sclera (µm)	Turbulence and Bi-Directional Flow within Circle of Hovius	Baseline IOP (mmHg)	A (mm Hg)	B (mm Hg)	Change in IOP	Absolute difference (A vs B)	Individual SD (A vs B)	Relative % difference (A vs B)
1	M	4.00	14.00	OS	-	-	None	20.0	23	15	<b>↓</b>	8	5.66	32.10(↓)
2	M	4.00	13.00	OS	146.80	349.87	None	31.3	31	32	1	1	0.71	3.17(↑)
3	F	4.00	11.50	OS	137.63	352.32	None	27.3	34	25	<b>↓</b>	9	6.36	30.51(↓)
4	M	3.00	15.00	OS	91.75	289.93	None	39.3	43	26	<b>↓</b>	17	12.02	49.27(↓)
5	F	3.00	9.65	OS	113.77	333.97	None	26.0	20	15	<b>↓</b>	5	3.54	28.57(↓)
6	F	1.00	9.55	OD	154.14	275.25	Bi-directional flow	19.7	16	9	<b>↓</b>	7	4.95	56.00(↓)
7	M	1.00	10.60	OD	-	-	Laminar flow	19.0	19	12	<b>↓</b>	7	5.95	45.16(↓)
8	M	1.00	14.30	OD	150.47	326.63	Bi-directional and laminar flow	18.1	23	20	<b>↓</b>	3	2.12	13.95(↓)
9	M	1.00	15.00	OD	157.81	300.94	None	16.3	7	4	<b>↓</b>	3	2.12	54.55(↓)
10	F	3.00	9.70	OS	155.98	306.45	Laminar flow	21.3	16	13	<b>1</b>	3	2.12	20.69(\)
Mea	n	2.5	12.2		138.54	316.92		23.8	23.2	17.1		6.3	4.45	34.40
SD		1.4	2.3		5.63	7.59		7.2	10.4	8.6		4.57	3.23	17.95

<sup>\*</sup>Gender defined as male (M) or female (F)

<sup>†</sup>Eye imaged was either right (OD) or left (OS)

<sup>‡</sup>Baseline IOP values over 6 months prior to the start of the study were calculated as a mean

<sup>§</sup> Absolute difference =|A-B|

<sup>|</sup> Individual SD =  $\sqrt{(A-B)^2/2}$ 

<sup>¶</sup> Relative absolute difference (given a % change) = |A-B|/[(A+B)/2]; A=pre IOP, B=post IOP

The sedation protocol, in addition to topical anesthesia, employed permitted adequate placement of stay sutures and performance of SA. Imaging of the left eye was randomly selected for the first 5 dogs, and the right eye was assigned to 4 dogs. The remaining eye was assigned to the left eye due to the right eye being used in a separate study. No eye imaged was receiving any topical therapy at the time of performing angiography.

For each eye, an average of 6.7 still images and 4.3 video clips were obtained following the initial 40 second video sequence. Progressive filling of intrascleral, episcleral, and conjunctival vessels were clearly visualized in all 10 eyes, with an average initial onset of filling time occurring at 35.8±10.6 seconds. The mean absolute difference between the two graders was 0.80 seconds, while the mean individual standard deviation was 0.92 seconds.

Complex, branching patterns with multiple anastomoses involving the scleral, episcleral, and conjunctival vasculature were observed post-injection. Clear visualization of deep intrascleral vessels, consistent with the circle of Hovius, was observed within the temporal (10/10), superotemporal (6/10), superior (1/10), and inferotemporal (1/10) scleral sectors. (Figure 13) Six eyes exhibited an elevated baseline IOP; these eyes demonstrated stagnancy in movement of dye once filling was complete (2/6), and visualization of laminar flow (4/6). One of the 2 eyes that had stagnant dye movement also demonstrated markedly delayed filling. The remaining 4 eyes had baseline IOPs within the normal range; of these, notable findings included bi-directional dye movement during the filling phase (2/4), laminar flow (1/4), and stagnancy of dye movement (1/4). Bi-directional flow was visible as turbulence of dye movement upon mixture with blood in vessel lumens. Upon complete filling of all luminal vessels, no variation of the fluorescent signal intensity was observed during the remainder of the imaging time period.

The mean  $\pm$  SD luminal diameter of intrascleral vessels, was noted to be 138.54 $\pm$ 5.63  $\mu$ m, occurring at mean depth of 316.92 $\pm$ 7.59  $\mu$ m.

# SCLERAL ANGIOGRAPHY SEGMENTAL VARIATION

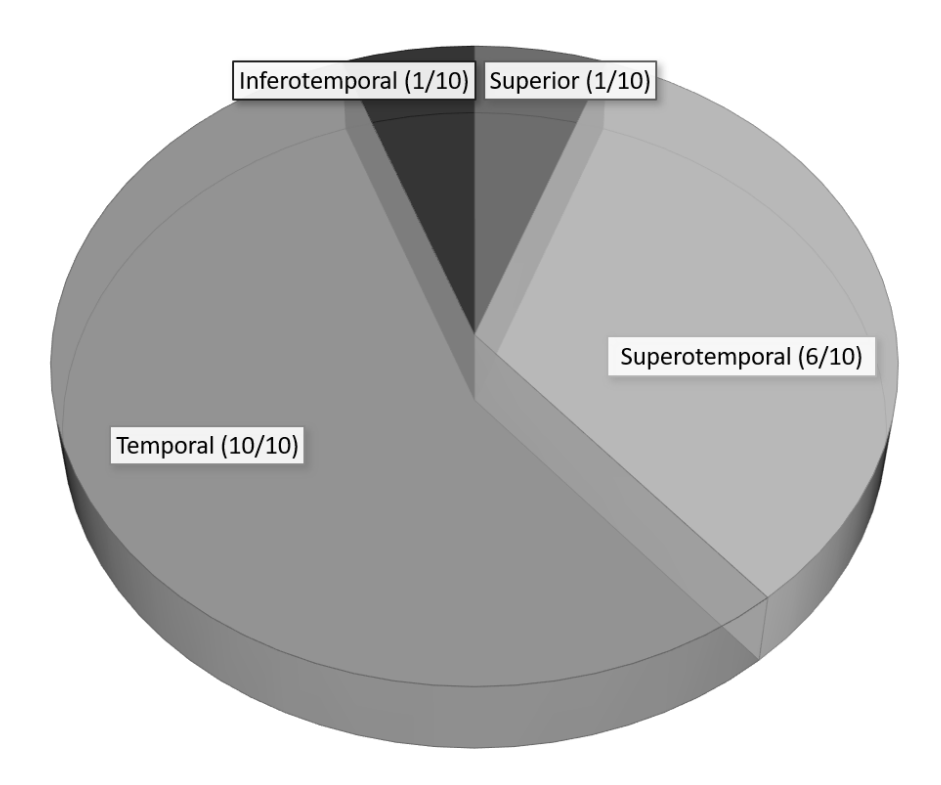


Figure 13. Schematic demonstrating the segmental variation in fluorescent dye outflow observed after scleral angiography (SA). Clear visualization of deep intrascleral vessels, consistent with the circle of Hovius, was observed within the temporal (10/10), superotemporal (10/10), superior (1/10), and inferotemporal (1/10) scleral sectors.

# 4.1.2 Intracameral (IC) aqueous angiography (AA)

AA was performed on the same eye of the same 10 *ADAMTS10*-OAG beagles as above after a recovery period of at least 24 hours (mean time of 5.8±1.6 days). (Table 8) All dogs were deemed to be systemically healthy prior to performing AA. No eyes demonstrated evidence of

residual ICG fluorescence from recent SA. The mean IOP measured pre- and post-ICG administration of all 10 eyes imaged were  $22.7\pm5.6$  mm Hg and  $10.5\pm8.5$  mm Hg, respectively. Immediate pre-procedure IOP was measured to be  $\geq$ 20 mmHg in 5 eyes (range 21.0-35.0 mmHg), and <20 mmHg in 5 eyes (range 18.0-19.0 mmHg). Pre- and post-IOP results were compared using a paired t-test and a clinically significant difference was observed (alpha = 0.05, p-value = 0.001). Individual pre- and post-procedure IOP results, including their absolute differences, individual standard deviations, and relative absolute differences are listed in Table 8.

**Table 8.** Summary of ADAMTS10-open angle glaucoma (ADAMTS10-OAG) dogs utilized for conducting aqueous angiography (AA)

ID	Eye	Vessel Location	Vessel Lumen Diameter (µm)	Vessel Lumen Depth in Sclera (µm)	Vessel Complexity and Pulsation	Baseline IOP (mmHg)	A (mm Hg)	B (mm Hg)	Change in IOP	Absolute Difference (A vs B)	Individual SD (A vs B)	Relative % difference (A vs B)
1	OS	Superotemporal	173.71	349.87	Complex, bifurcations, mild pulsation	20.0	18	7	<b>↓</b>	11	7.78	88.00(↓)
2	OS	Superotemporal	148.64	348.65	Complex, bifurcations, moderate pulsation, laminar flow	31.3	28	9	1	19	13.44	102.70(↓)
3	OS	Superotemporal	135.79	313.79	Complex, bifurcations, mild pulsation	27.3	19	5	<b>↓</b>	14	9.90	116.67(↓)
4	OS	Superotemporal	91.75	289.93	Complex, bifurcations, no pulsation	39.3	35	33	<b>↓</b>	2	1.41	5.88(↓)
5	OS	Superotemporal	102.76	350.49	Complex, bifurcations, slow filling with no pulsation	26.0	21	3	1	18	12.72	150.00(↓)
6	OD	Superotemporal	165.15	385.35	Complex, bifurcations, mild pulsation	19.7	18	13	<b>↓</b>	5	3.54	32.26(↓)
7	OD	Superotemporal	156.59	330.30	Complex, bifurcations, moderate pulsation, laminar flow	19.0	27	10	<b>1</b>	17	12.02	91.89(↓)
8	OD	Superotemporal	168.82	269.13	Single vessel, weak progression, mild pulsation	18.1	19	5	<b>\</b>	14	9.90	116.67(↓)
9	OD	Superior	154.14	313.79	Three vessels with little branching, no pulsation	16.3	19	10	1	9	6.36	62.07(↓)
10	OS	Superotemporal	150.47	300.94	Complex bifurcations, weak progressive filling, mild pulsation	21.3	23	10	1	13	9.19	78.79(↓)
Mea	'n		144.78	325.22	<i>g,</i>	23.8	22.7	10.5		12.2	8.27	84.49
SD			5.70	6.43		7.2	5.6	8.5		5.55	3.93	42.43

<sup>\*</sup> Eye imaged was either right (OD) or left (OS)

<sup>†</sup> Baseline IOP values over 6 months prior to the start of the study were calculated as a mean

<sup>‡</sup> Absolute difference =|A-B|

<sup>§</sup> Individual SD =  $\sqrt{(A-B)^2/2}$ 

<sup>||</sup> Relative absolute difference (given a % change) = |A-B|/[(A+B)/2]; A=pre IOP, B=post IOP

An average of 5.4 still images and 11.2 video clips after the initial 40 second video sequence were captured for each eye. Diffuse and uniform fluorescence of ICG within the anterior chamber was visualized, immediately following IC injection, in all eyes. The average time to observe initial dye fluorescence within the intra-scleral channels was 34.3±11.0 seconds post injection. The mean absolute difference between the two graders was 0.9 seconds, while the mean individual standard deviation as 1.29 seconds. All 10 eyes imaged demonstrated dye fluorescence within various scleral sectors. (Figure 14) Fluorescence was visualized within the superotemporal sclera most commonly, displaying complex intra-scleral branching patterns in 9/10 eyes (90%). Initial fluorescence observed typically occurred within a large deep intrascleral vessel and rapidly progressed into numerous complex branching intrascleral luminal vessels. The intensity of fluorescence within these intrascleral vessels was progressive over time, particularly as dye flowed into neighboring draining pathways, both intrascleral and conjunctival. One eye imaged (10%), demonstrated fluorescence within 3 solitary conjunctival vessels located in the superior scleral sector, and one eye (10%) demonstrated fluorescence in the temporal scleral sector.(Figure 15) Pulsatility of dye was visualized in a total of 7/10 eyes imaged. When visualized, pulsation was noted to occur within larger intrascleral vessels, the frequency of which appeared to align with the dog's heart rate. Five of the seven eyes demonstrating pulsation were subjectively graded as exhibiting mild pulsatile action and had normal to moderately elevated pre-procedure IOP values (baseline IOP range: 18.1-31.3mm Hg and pre-procedure IOP range 18-28 mmHg). Of these 7 eyes, 4 were glaucomatous and 3 were pre-glaucomatous. Two eyes with elevated baseline and immediate pre-procedure IOP values (19.0 mmHg and 27.0 mmHg, and 31.3 mmHg and 28.0 mm Hg, respectively) exhibited moderate pulsatile action, in addition to, laminar flow. Five eyes with baseline and immediate pre-procedure IOP values (20.0 mmHg

and 18.0 mmHg, 27.3 mmHg and 19.0 mmHg, 19.7 mmHg and 18.0 mmHg, 18.1 mmHg and 19.0 mmHg, 21.3 mmHg and 23.0 mmHg, respectively) were observed to have both mild pulsatile movement of dye as well as laminar flow. The 3/10 eyes that did not demonstrate pulsatility were from eyes with baseline IOP values of 16.3 mmHg, 26.0 mmHg, and 39.3 mmHg, and immediate pre-procedure IOPs of 19.0 mmHg, 21.0 mmHg, and 35.0 mmHg, respectively. Vessel luminal diameters, as measured on cross sectional OCT (Figure 16), were recorded at a mean±SD value of 144.78±5.70 μm and occurred at a depth of 325.22±6.43 μm within the scleral tissue.

# AQUEOUS ANGIOGRAPHY SEGMENTAL VARIATION

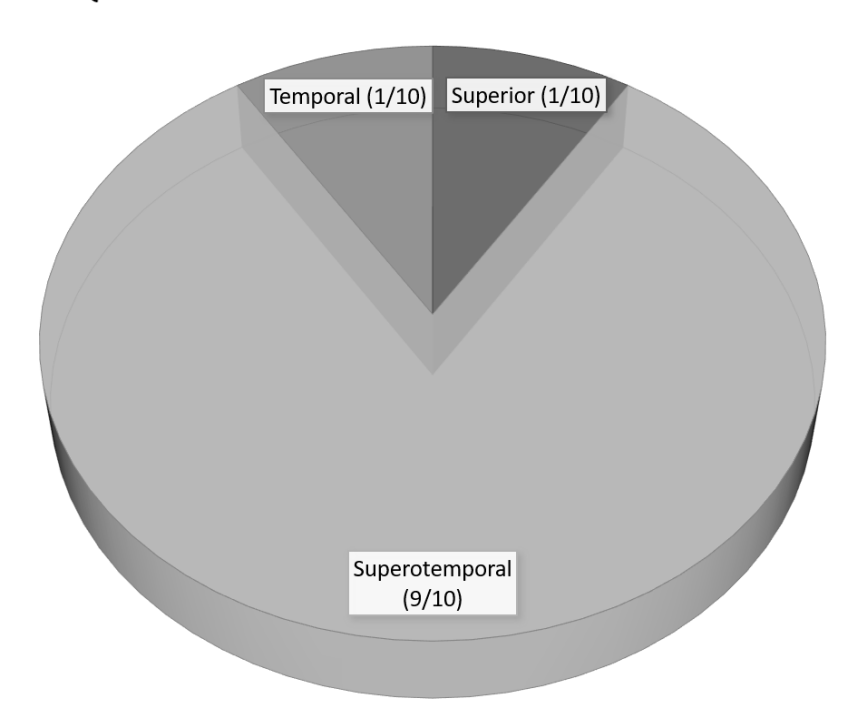


**Figure 14. Schematic demonstrating the segmental variation in fluorescent dye outflow observed after performing aqueous angiography (AA).** Complex, intra-scleral branching patterns with multiple anastomoses were visualized most frequently within the superotemporal sclera (9/10 eyes; 90%). One eye (10%) also demonstrated fluorescence of indocyanine green dye within 3 solitary conjunctival vessels located in the superior scleral segment, and one eye (10%) exhibited a fluorescent signal within the temporal sclera.

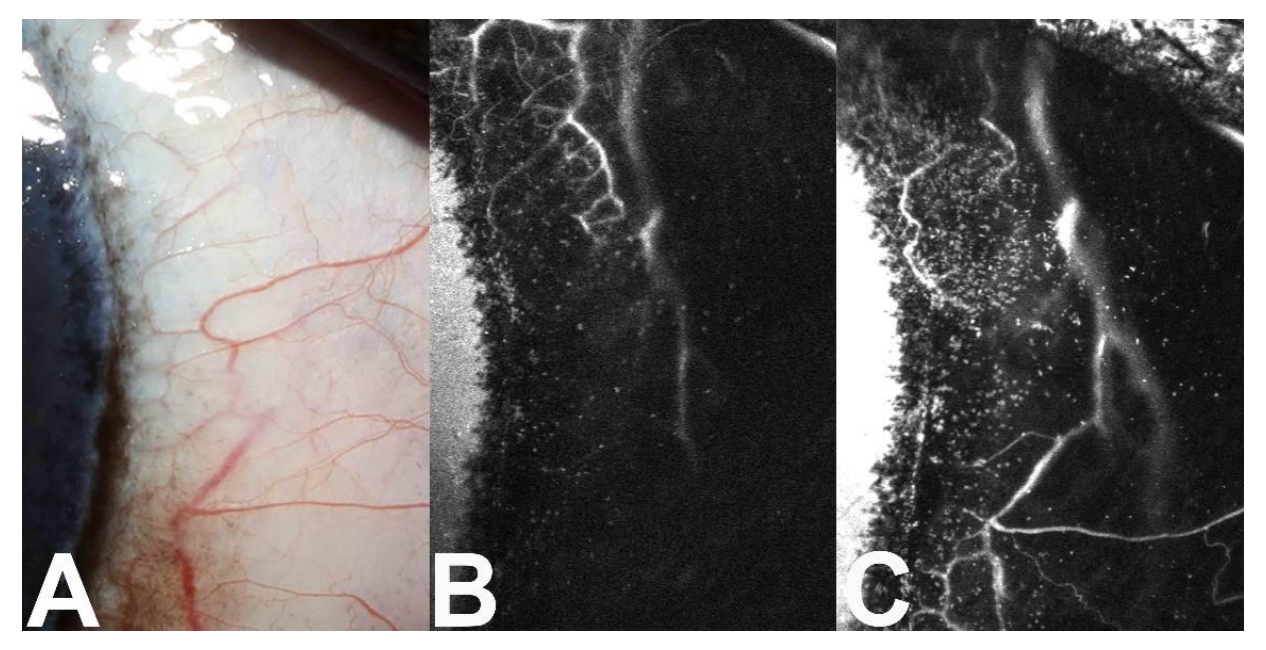


**Figure 15.** Standard color image of the temporal sclera of the left eye (A), aqueous angiography (AA) of the same area showing the appearance of 0.25% indocyanine green dye fluorescence 1 minute after intracameral (IC) injection (B), and the same location 20 minutes after initial dye injection (C), demonstrating progression of dye fluorescence and the presence of laminar flow within the scleral vessel over time in a 4-year-old female beagle dog.

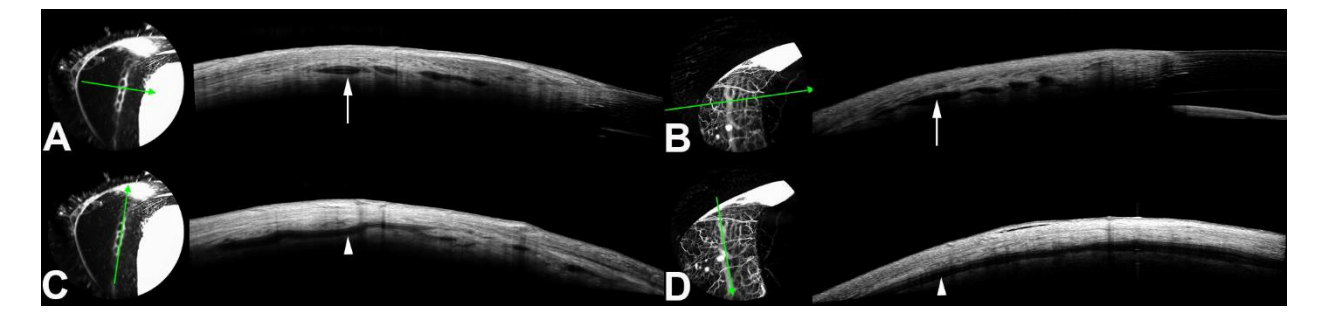
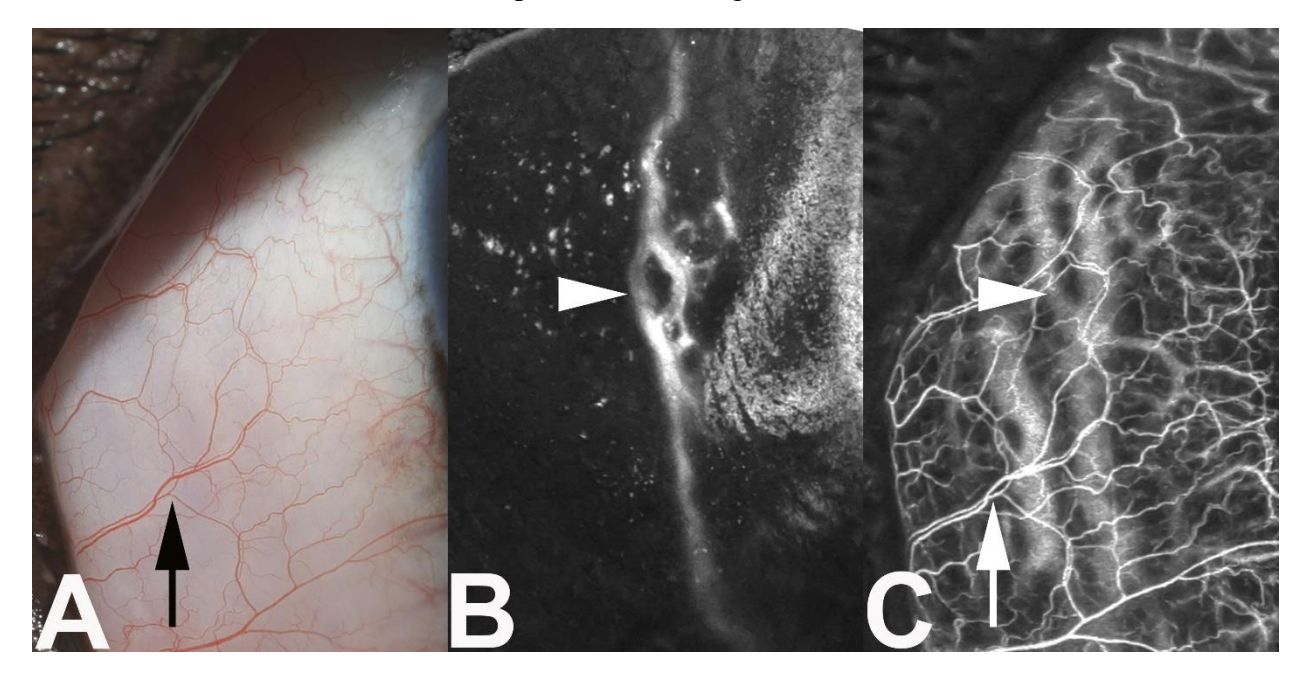


Figure 16. OCT imaging was performed in conjunction with intracameral aqueous angiography (A, C) and intravenous scleral angiography (B, D) in the left eye of a 1-year-old pre-glaucomatous female beagle dog. Cross-sectional scans (A, B) and longitudinal scans of the scleral tissue (C, D) were performed. The orientation of each scan is indicated by the direction of the green arrows. The presence of scleral vessels in the mid-to-deep stromal tissue were seen in cross section (arrow) (A, B) and in longitudinal section (arrowhead) (C, D). Measurements of the vessels were taken through the vertical axis of each vessel lumen, using computer software.

## 4.2 Comparison of intracameral (IC) and intravenous (IV) routes of injection

Representative color, AA and SA images (Figure 17), depicting identical scleral sectors, illustrate consistencies between the two angiographic techniques. Both angiographic modalities permitted visualization of luminal vessels within the sclera in most dogs, consistent with the intra-scleral venous plexus and the venous circle of Hovius. AA highlighted movement of dye from within the anterior chamber into the vascular components affiliated with the CAHO (intrascleral plexus and circle of Hovius). While SA routinely permitted visualization of similar vasculature components of the CAHO, this modality also highlighted the more superficial episcleral and conjunctival vasculature. Stagnancy in visibility of dye movement beyond the initial filling of vessels was noted in 7/10 eyes with SA (70%). One dog also had delayed filling of scleral vasculature with SA as compared to AA (Dog 4).



**Figure 17.** Standard color image of the temporal sclera in a 1-year-old male beagle dog showing branching of conjunctival vessels (arrow) (A). Imaging of the same location after intracameral (IC) injection of 0.25% indocyanine green dye yields fluorescence of a deep scleral vessel (B). Scleral angiography (SA), using 1 mg/kg indocyanine green, of the same region confirms the presence of the same deep scleral vessel (arrowhead), along with numerous thinner, branching conjunctival vessels (arrow) (C).

Intrascleral vessels were variable both in their luminal diameter and location within the sclera. Variability in vessel lumen size from 91.75  $\mu$ m to 157.81  $\mu$ m (mean 138.54  $\mu$ m) in diameter was noted in dogs imaged with SA, and 91.75  $\mu$ m and 173.71  $\mu$ m (mean 144.78  $\mu$ m) in diameter was noted in dogs imaged with AA. Larger diameter vessels were located an approximate distance of 5 mm from the limbus. The depth of vessels was relatively constant, with visualization in the mid-to-deep stromal tissue ranging from 275.25  $\mu$ m to 352.32  $\mu$ m (mean 316.92  $\mu$ m) in dogs imaged with SA, and 269.13  $\mu$ m to 385.35  $\mu$ m (mean 325.22  $\mu$ m) in dogs imaged with AA. No statistically significant difference was seen in mean vessel lumen diameters (a=0.05, p=0.62) between IC and IV routes of ICG dye administration. Similarly, no statistically significant difference was observed in mean vessel depth (a=0.05, p=0.52) within the sclera between IC and IV routes of ICG dye administration.

A series of chi-square tests were performed to evaluate the presence or absence of bidirectional flow, the complexity of branching of vessels, and the presence or absence of pulsatility of dye between pre-glaucomatous and glaucomatous *ADAMTS10*-OAG eyes. No statistically significant difference was seen in any of these parameters between groups. No statistically significant difference was noted in mean vessel lumen diameter using AA or SA between pre-glaucomatous and glaucomatous *ADAMTS10*-OAG eyes (a=0.05, p=0.62). No statistically significant difference was noted in mean vessel depth using AA or SA between preglaucomatous and glaucomatous *ADAMTS10*-OAG eyes (a=0.05, p=0.52).

In eyes demonstrating laminar flow, the digital overlay supported visualization of dye movement out of the CAHO pathways along the periphery of the vessels, creating a multipartite stratification pattern using 2 different colors.(Figure 18) A digital color overlay of all eyes was performed, which yielded evidence of laminar flow in only 5 eyes; four eyes exhibited an

elevated IOP and 1 eye had a measured baseline and immediate pre-procedure IOP under 20.0 mmHg.

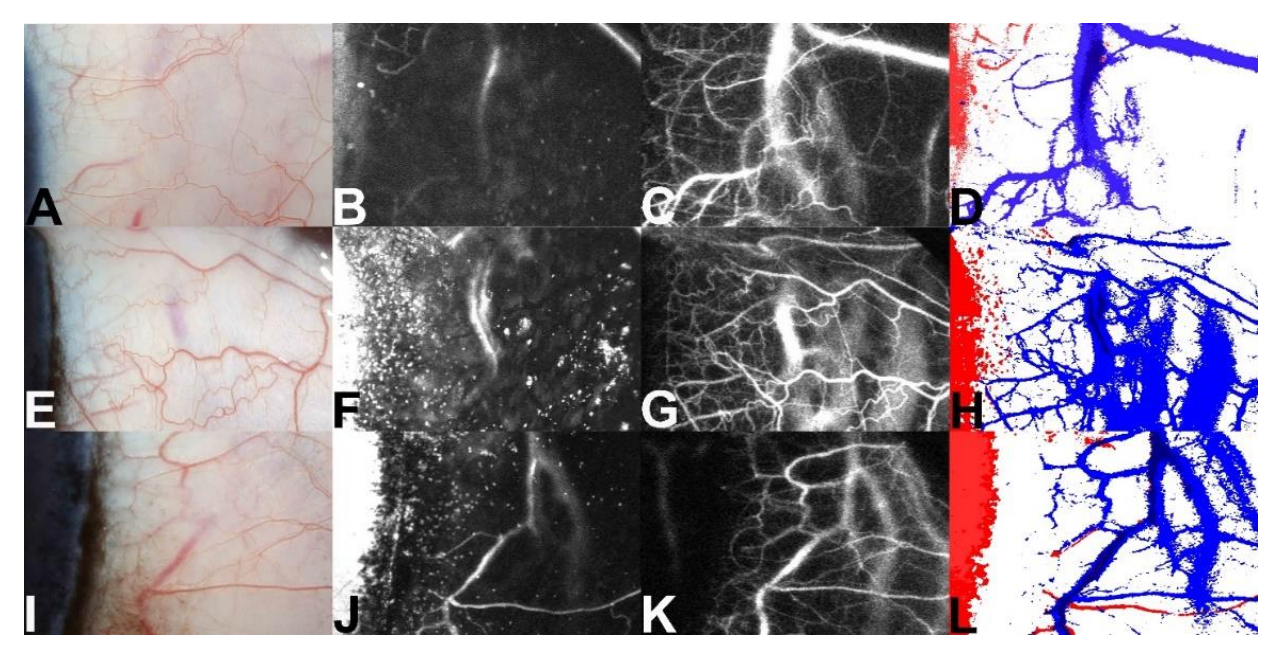


Figure 18. Standard color images of the temporal sclera of the left eye in 3 different *ADAMTS10*-open angle glaucoma (*ADAMTS10*-OAG) beagle dogs with IOP greater than 20 mmHg: a 4-year-old male (A), a 4-year-old male (E), and a 4-year-old female (I) with fluorescence of indocyanine green dye in the deep scleral vessels after aqueous angiography (AA) (B, F, J, respectively) and after scleral angiography (SA) (C, G, K, respectively). SA demonstrates the presence of a complex branching pattern of deep scleral vessels, with thinner, superficial conjunctival vessels in the overlying tissue. Color maps were made to show simultaneous SA and AA results for each dog (D, H, L); AA highlights vessels in red, while SA shows vessels highlighted in blue.

## 4.3 Safety

No complications were observed with the sedation protocol employed to conduct these angiographic techniques in any of the dogs. However, complications associated with SA and AA were observed. All dogs demonstrated mild aqueous flare the day following the procedure (1+ flare using the SUN scale)<sup>172</sup>. Clinically detectable signs of intraocular inflammation were noted to resolve following SA and AA 24 hours and 48 hours, respectively. A small fibrin tag was visualized in 2 eyes, following AA, which resolved with ongoing topical treatment for 10 days.

The fibrin resolved in both dogs with topical neomycin-polymyxin-B-dexamethasone ophthalmic ointment administered for a duration of 7 days.

#### 4.4 Discussion

The techniques used to deliver ICG dye and to image the CAHO pathways were identical to those used in a recent in vivo study to evaluate 12 normal dogs. 89 Similar limitations were noted, including difficulty imaging the nasal sclera due to the presence of the nictitating membrane. The location and complex branching patterns seen with AA and observing fluorescent patterns of ICG in the pre- and post-glaucomatous ADAMTS10-OAG dogs were in alignment with results obtained from our recent work (Burn JB et al., Vet Ophtho 2020:22:6: ACVO E-Abstract E46), in addition to, ex vivo studies evaluating a subset of glaucomatous dogs and cats. 126,143,149 Dye fluorescence was consistently observed in the superotemporal sclera in ADAMTS10-OAG dogs, in contrast to normal dogs, which demonstrated greater variation in location of dye fluorescence. (Burn JB et al., Vet Ophtho 2020:22:6: ACVO E-Abstract E46) The reduction in location of dye visualization in ADAMTS10-OAG dogs could have resulted from a change driven by elevated IOP levels or morphologic changes to the outflow pathways as a result of the disease process itself. Two of the three eyes in which no visualization of dye was observed were glaucomatous (26.0 and 39.3 mmHg), while the one remaining eye was preglaucomatous with a baseline IOP of 16.3 mmHg. Although the underlying reason for these differences in visualization of dye and the effect IOP may have remains unknown at this time, it is speculated that the variation observed between eyes in this study may be attributed to a subtle decrease in the amount of aqueous humor that exited the anterior chamber in eyes that exhibited elevated IOP. It was also plausible that intermittent spikes in IOP could have been occurring between IOP measurements, such that they were not detected at the time of measurement.

This study identified 3 characteristics of aqueous humor outflow: pulsation, laminar flow, and turbulent bi-directional flow. Pulsatile movement of fluorescent dye has been observed as a rhythmic movement of dye within the vessel lumens, consistent with the cardiac rhythm of the dog being imaged, while laminar flow has been described as a continuous and smooth column of dye filling a single larger vessel in a bipartite stratification pattern. Turbulent flow has been defined as irregular flow of fluorescent dye as it mixes with blood upon entering the vascular channels. 149

In this study, pulsatile movement of ICG dye was a frequent observation in eyes (7/10; 70% eyes) imaged with AA, as compared to a previous study of normal dogs (4/12; 33%).(Burn JB et al., Vet Ophtho 2020:22:6: ACVO E-Abstract E46) This difference could be due to an elevation in IOP, which creates a surge that drives the choroid piston effect<sup>150</sup> thereby allowing for more prominent visualization of fluid pulsation within the outflow vessels. Upon imaging with AA, 2 eyes with baseline IOP ≤20 mmHg (18.1 and 19.7 mmHg) and 3 eyes with baseline  $IOP \ge 20 \text{ mmHg}$  (20.0, 21.3, and 27.3 mmHg) demonstrated mild pulsatile movement of dye, while moderate pulsatility of dye was seen in one pre-glaucomatous eye (19.0 mmHg) and one glaucomatous eye (31.3 mmHg). As the eye with the highest documented IOP in this study did not demonstrate any pulsatility of dye, it is possible that an upper threshold of IOP exists in observing this phenomenon. Thus, a lack of pulsatility may play a potential role as a useful marker to identify early stages of impaired outflow of aqueous humor in dogs with open angle glaucoma. This finding might also reflect structural alterations to the CAHO pathways already in place, given the animal model being used. Another explanation of this dynamic movement of dye could be related to increased ocular perfusion pressure, as seen in humans with open angle glaucoma.<sup>173</sup> Although systemic blood pressure was not measured in this study and it is therefore

unable to be verified, it is plausible that ocular perfusion could be reduced with systemic hypertension and this could occur even before elevations in IOP are recorded.

Four glaucomatous and one pre-glaucomatous eye each demonstrating pulsatility of dye also demonstrated laminar flow characteristics. The left eye of a 4-year-old glaucomatous male beagle dog with a baseline IOP of 20.0 mmHg and a pre-procedural IOP of 18.0 mmHg, the left eye of a 4-year old glaucomatous male beagle dog with a baseline IOP of 31.3 mmHg and a preprocedural IOP of 28.0 mmHg, the left eye of a 4-year-old female beagle dog with a baseline IOP of 27.3 mmHg and a pre-procedural IOP of 19.0 mmHg, the left eye of a 3-year-old glaucomatous female beagle dog with a baseline IOP of 21.3 mmHg and a pre-procedural IOP of 23.0 mmHg, and the right eye of a pre-glaucomatous 1-year-old male beagle dog with a baseline IOP of 19.0 mmHg and a pre-procedural IOP of 27.0 mmHg exhibited laminar flow of dye when imaged with AA. Laminar flow was further highlighted in the same eyes using a digital overlay that demonstrated ICG streaming into the vessel in a thin column immediately adjacent to the vessel wall (Figure 17). Although it did not help with measuring signal intensity, the use of digital color overlays may be useful in delineating laminar flow in future studies. Compared to normal eyes, glaucomatous eyes demonstrated a subjectively less pronounced but obvious difference in the degree of lamination observed within vessel lumens.<sup>89</sup> This could be explained by a decreased volume of aqueous humor outflow or a possible decrease in luminal size in glaucomatous eyes. In this study, vessel lumen diameters from AA imaging measured a mean of  $144.8\mu m \pm 5.7\mu m$ , while the same measurements from normal eyes performed in a separate study measured a mean of 258.0 ± 9.1 µm. A statistically significant difference was found between the caliber of vessel size measured from AA imaging in eyes of ADAMTS10-OAG dogs

as compared to eyes from unaffected normal dogs (a=0.05, p=0.00034). (Burn JB et al., Vet Ophtho 2020:22:6: ACVO E-Abstract E46)

Bi-directional or turbulent flow of aqueous humor was observed to mix with blood in the scleral vessels of the right eye of a pre-glaucomatous 1-year-old female beagle dog and the right eye of a pre-glaucomatous 1-year-old male beagle dog with baseline and pre-SA IOP values of 19.7 mmHg and 16 mmHg, and 18.1 mmHg and 23 mmHg, respectively. This movement of fluid was not useful in measuring signal intensity, but allowed for direct visualization of the location of dye entering into the blood stream.

The highest IOP value documented in this study was in the eye of a glaucomatous 3-year-old male beagle dog that did not exhibit any pulsatile movement of ICG, turbulence, or laminar flow: baseline IOP was measured to be 39.3 mmHg (pre-SA and pre-AA IOP were 43.0 and 35.0 mmHg, respectively). A second eye from a glaucomatous 4-year-old male beagle dog had an elevated baseline IOP of 31.3 mmHg (pre-SA and pre-AA IOP of 31 mmHg and 28 mmHg, respectively) and displayed moderate pulsation of dye and laminar flow in AA. These values were consistent with a slow rise in IOP associated with progression of open angle glaucoma. In concurrence with a slow rise in IOP, aqueous humor has been documented to move out of the eye at a decreased rate in dogs with open angle glaucoma<sup>174,175</sup>; this is in alignment with the diminished fluorescent signal seen with both AA and SA in the eye from the beagle with a markedly elevated baseline IOP of 39.3 mmHg.

The lowest baseline IOP in the AA group was measured in the eye of a pre-glaucomatous 1-year-old male beagle dog (16.3 mmHg; pre-SA IOP 7 mmHg; pre-AA IOP 19.0 mmHg) in which three vessels with little branching and no movement of dye were observed. Although this eye was classified as being in a pre-glaucomatous stage, it is possible that intermittent IOP

elevations may have occurred and could have led to the decreased visualization of aqueous humor outflow activity. Alternately, this observation may have been due to individual variation.

Although the techniques applied were effective in clearly demonstrating dye fluorescence and the time to visualization of fluorescence was similar between AA and SA, the onset of fluorescence observed was subjectively delayed and there was a weaker fluorescent signal in eyes of dogs with elevated baseline IOPs compared to those eyes imaged in normal dogs. IOP measured pre-and post-administration of dye was not statistically significant in the SA group, however, there was a substantial decrease in IOP after AA was performed and this was statistically significant. This introduces the possibility of leakage of dye from the anterior chamber via the paracentesis site. Early leakage of dye would have diluted the concentration of ICG administered into the anterior chamber, potentially weakening the fluorescent signal and reducing ICG visibility in the scleral vessels. Although this may have been a concern for quantifying the fluorescent signal, this was not a clinically relevant issue as fluorescence of dye was clearly visible in all eyes imaged. Pre- and post-procedure IOP variations may have also reflected disruptions in the blood aqueous barrier occurring as a sequelae to IC dye injection. Unfortunately, there was no way to quantify the fluorescent signal based on the variation in signal intensity between eyes and imaging modalities.

There is currently limited data regarding the caliber of scleral vessels observed *in vivo*, and the onset of dye filling and/or the time to complete dye filling within CAHO pathways of normal dog eyes.(Burn JB et al., Vet Ophtho 2020:22:6: ACVO E-Abstract E46) Overall, more eyes in this study with an elevated IOP had visible turbulent and/or pulsatile flow of aqueous humor when AA was performed as compared to normal dogs.(Burn JB et al., Vet Ophtho 2020:22:6: ACVO E-Abstract E46) Despite this finding, there was no association between vessel

lumen diameter and IOP values. As there was no notable difference in vessel size when compared to changes in IOP, it is speculated that there may be variations in the regional outflow of fluorescent dye, similar to the differences in regional outflow observed in human eyes.<sup>128</sup>

The weak evidence to support our initial hypothesis may have been a product of evaluating dogs with mild IOP elevation as opposed to dogs with markedly elevated IOP values. The theoretical threshold of IOP elevation to view changes in CAHO caliber and vessel number from the eye may not have been met in this experiment. It is also possible that changes in pressure or obstruction of aqueous outflow as a result of manual eyelid retraction or the use of conjunctival stay sutures may also have played a role. Alternatively, these results may simply have been due to the absence of conventional outflow abnormalities occurring in the open angle glaucoma model being used in this study. It is also possible that this experiment may have required additional eyes to identify common patterns of CAHO pathways and if there are changes in conventional outflow linked to age and/or breed of dogs. Differences, should they exist, may have been mild and difficult to detect using this imaging modality. Additionally, it was speculated that delayed rates of filling and/or sectoral changes in filling were present in ADAMTS10-OAG dogs; however, with a limited number of dogs with an elevated IOP, it was difficult to make any associations. Therefore, it is possible that the CAHO pathways could behave differently in ADAMTS10-OAG eyes as compared to those affected by angle closure glaucoma and more investigation is currently needed to support this claim.

Overall, this imaging technique may have application in the future in dogs to identify the threshold of IOP at which physiologic changes are seen with regards to aqueous humor outflow. This may help to tailor therapeutic treatments to preserve vision in both open and angle closure glaucomatous dogs. Thus, AA could be used to detect early functional abnormalities and to

implement patient-specific treatment approaches as it allows for the identification and functional characterization of the CAHO pathways *in vivo*.

#### 4.5 Conclusion

This study demonstrates the use of AA and provides baseline data regarding the CAHO pathways in *ADAMTS10*-OAG dogs. All eyes imaged in this study demonstrated visible aqueous humor outflow primarily within the superotemporal scleral sector. Pulsatility of fluorescent dye was visualized in 7/10 eyes undergoing AA, while SA yielded laminar flow visualization in 1/10 eyes and bidirectional movement of aqueous humor in 2/10 eyes. Three glaucomatous and 2 preglaucomatous eyes demonstrated mild pulsatility of dye, while moderate pulsatility was noted in one glaucomatous and one pre-glaucomatous eye with baseline IOP values of 31.3 mmHg and 19.0 mmHg, respectively. Three eyes showed no pulsatile activity; two eyes with an elevated baseline IOP (39.3 mmHg and 26.0 mmHg), and one eye with a normal baseline IOP (16.3 mmHg). These differences may be due to a threshold in IOP that must be reached before the amount of aqueous humor leaving the eye in *ADAMTS10*-OAG dogs is noted to make a clinical difference.

#### CHAPTER 5

## **CONCLUSION**

Although AA is already in clinical use in human medicine <sup>128</sup>, there is currently no imaging modality in veterinary medicine that allows for evaluation of CAHO outside of a research setting. <sup>126</sup> This manuscript provides a detailed account of a streamlined technique for AA and the descriptive findings of CAHO pathways *in vivo* in both normal and in *ADAMTS10*-OAG canine eyes. The research described herein has paved the foundation to move towards a clinically applicable technique that successfully evaluates CAHO pathways *in vivo* in both normal canine eyes and in *ADAMTS10*-OAG canine eyes pre- and post-development of glaucoma. The technique developed was minimally invasive and could be performed under sedation, which increased the feasibility of this protocol for use in a clinical setting.

A pilot study was developed to test the functionality of a gravity-fed trocar system to deliver fluorescent dye directly into the anterior chamber. The gravity-fed trocar system had a cumbersome set-up and required the use of specialized equipment (trocars). The set-up time for this protocol and the time required to deliver fluorescent dye into the anterior chamber using the gravity-fed system resulted in the need for this technique to be performed under general anesthesia. Upon imaging, this protocol did not allow for any visualization of dye outflow from the anterior chamber in the four eyes that were assessed *in vivo*. This was suspected to be due to a number of different factors, including tension applied to the sclera by the conjunctival stay sutures that were placed, compression of the eyelids from manual retraction, and/or compression of the scleral vasculature as a result of compression from the trocar collar or the eyelid speculum against the globe. For this system to truly be clinically applicable, the technique used must be

efficient and easy to set up, require minimal to no specialized equipment, be cost effective, and allow for visualization of fluorescence in the CAHO pathways.

To address these shortcomings and to improve the technique used, the gravity fed-trocar system was replaced with a single IC injection of fluorescent dye via paracentesis. This single IC injection technique was more effective and clinically practical compared to the gravity-fed trocar set-up. Upon refining the technique, a positive shift in visualization of the dye was also observed. The adjustments also allowed for the procedure to be performed using routine clinical equipment and with dogs under sedation, in lieu of general anesthesia. Sedation was not only useful in decreasing the risks associated with longer general anesthesia times, but this change made the procedure more cost-friendly, efficient, and less time-consuming, bringing SA and AA procedures another step closer to use in clinical practice.

Once the technique for IC delivery of fluorescent dye was streamlined, two separate imaging modalities, AA and SA, were compared. Although fluorescent dye was administered in a different location for AA compared to SA, both imaging modalities were complementary to each other and allowed for confirmation of dye movement out of the CAHO pathways and into venous circulation in a short period of time. Use of the IC experimental set up and the Heidelberg Spectralis imaging machine allowed for visualization of the distal CAHO pathways following AA in dogs, in addition to allowing for observation of characteristics of aqueous humor movement as it flowed back into venous circulation.

Upon performing AA, segmental outflow was visible in all 6 glaucomatous and 4 preglaucomatous *ADAMTS10*-OAG dog eyes and in 10 of 12 normal dog eyes. Fluorescence was noted most commonly in the superotemporal scleral sector in all normal eyes in which CAHO pathways were visualized, while pre-and post-glaucomatous eyes exhibited fluorescence of dye most commonly in the temporal (10/10 eyes) followed by the superotemporal scleral sectors (6/10 eyes). Given that there appeared to be prominent segmental outflow of aqueous humor in the superotemporal sector across all eyes, suggesting that the superotemporal sector may be an ideal location for placement of glaucoma shunts and/or performance of minimally invasive glaucoma surgery. However, further investigation is needed to confirm this.

ICG was observed after a mean time of 35.0±4.3 seconds in normal eyes and 35.8±10.6 seconds following IC administration in pre-and post-glaucomatous eyes, supporting that this modality can be used to rapidly identify fluorescence of dye within the CAHO pathways, its location, and characteristics associated with movement of the dye in a short period of time. Additionally, the use of different dyes may offer more information than with use of a single dye alone. Although SF diffused from the vasculature quickly, it was useful to evaluate the outline of the vascular structures, prior to diffusion into the surrounding tissue. ICG remained within the vessel lumens for a longer period of time, and therefore, was more useful to evaluate the CAHO pathways and the dynamics of aqueous humor as the fluid traveled back into venous circulation.

The most common dynamic characteristics of aqueous humor movement in normal eyes were pulsatility and turbulence (33.3%). Pulsation of dye was observed more frequently in preand post- glaucomatous eyes (70%). Mild pulsatility was observed in 2 pre-glaucomatous and 3 glaucomatous eyes, while moderate pulsatility was visualized in one pre-glaucomatous and one glaucomatous eye. Pulsatility was observed intermittently throughout the angiograms and appeared to coincide with cardiac cycle of the dog being imaged. It is unclear why pulsatility occurs more often in eyes with an elevated intraocular pressure. It is speculated that intermittent alterations in IOP or subtle reductions in aqueous humor exiting the eye via the CAHO pathways may have resulted in the noted changes and dynamic movement of dye. In comparison to

pulsatility, turbulence of dye was visualized as irregular or erratic movement of dye upon mixture with blood<sup>149</sup> within the venous Circle of Hovius. This finding was seen in 2 normal and 2 pre-glaucomatous eyes. Gentle compression of the eyelids was also noted to result in alterations in fluid outflow rates, pulsatility, turbulence, and visibility of dye. These findings suggest that alterations in IOP and or episcleral venous pressure, through internal or external compressive forces, may lead to changes in dye movement out of CAHO pathways.

Laminar flow has been used in previous studies to demonstrate flow characteristics of blood in scleral vessels. 149,163 AA performed in 2 normal eyes yielded stratification of dye, with a higher signal intensity closest to the vessel walls, as aqueous humor flowed back into systemic circulation; this was consistent with laminar flow. In contrast, 3 *ADAMTS10*-OAG eyes with low IOP and mild pulsatility and 2 *ADAMTS10*-OAG eyes with elevated IOP and moderate pulsatility also demonstrated laminar flow. After SA, lamination of dye within the scleral vessels was observed in only one *ADAMTS10*-OAG dog with low IOP and 4 *ADAMTS10*-OAG dogs with elevated IOP. The variances noted in aqueous humor dynamics may be due to the need to reach a minimum threshold in IOP before the amount of aqueous humor leaving the eye in *ADAMTS10*-OAG dogs would create a noticeably different angiographic pattern. The appearance of this phenomenon was emphasized using digital overlays in both normal and glaucomatous eyes. The digital overlays highlighted the movement of fluorescent dye into systemic circulation and shows the dye hugging the vessel walls. Interestingly, this movement was noted more frequently in eyes that demonstrated an elevated IOP.

IV delivery of dye into systemic circulation (SA) was used to verify the location of the distal outflow pathways of the globe. This modality was easy to perform, carried relatively low risk to the patient, and had a very short recovery period. When used in these studies, SA via ICG

appeared to be an effective means for identifying the vascular components associated with the distal CAHO pathways, while AA permitted visualization and qualitative assessment of aqueous humor outflow.

Rapid and progressive filling of vessels was observed in normal and glaucomatous eyes with an average initial onset of filling time occurring at 34.6±4.5 and 35.8±10.6 seconds, respectively. All eyes exhibited fluorescence of the scleral, episcleral, and conjunctival vasculature in complex, branching patterns with numerous anastomoses. Similar to AA, visualization of the sclera was limited to the superior, superotemporal, temporal, and inferotemporal sectors. Deep intrascleral vessels in a location and of a size consistent with the venous circle of Hovius, were observed mainly in the temporal and superotemporal sectors.

All outflow channels which exhibited fluorescence following AA and SA were readily identifiable on cross-sectional OCT as vessels. Vessel lumen diameters in normal dog eyes were measured to be comparable to previous corrosion cast studies. Vessel lumen diameters from AA imaging of normal and glaucomatous eyes were measured to be a mean  $\pm$  SD of 258.0  $\pm$  9.1  $\mu$ m and 144.8 $\mu$ m  $\pm$  5.7 $\mu$ m, respectively. (Figure 19) There was a statistically significant difference between the caliber of vessel lumens measured from AA imaging in eyes of *ADAMTS10*-OAG dogs as compared to eyes from unaffected normal dogs. These findings are suggestive of a decrease in luminal diameter in glaucomatous dogs, which is speculated to be one of the underlying mechanisms for resistance to aqueous humor outflow and subsequent IOP elevation in this canine model.

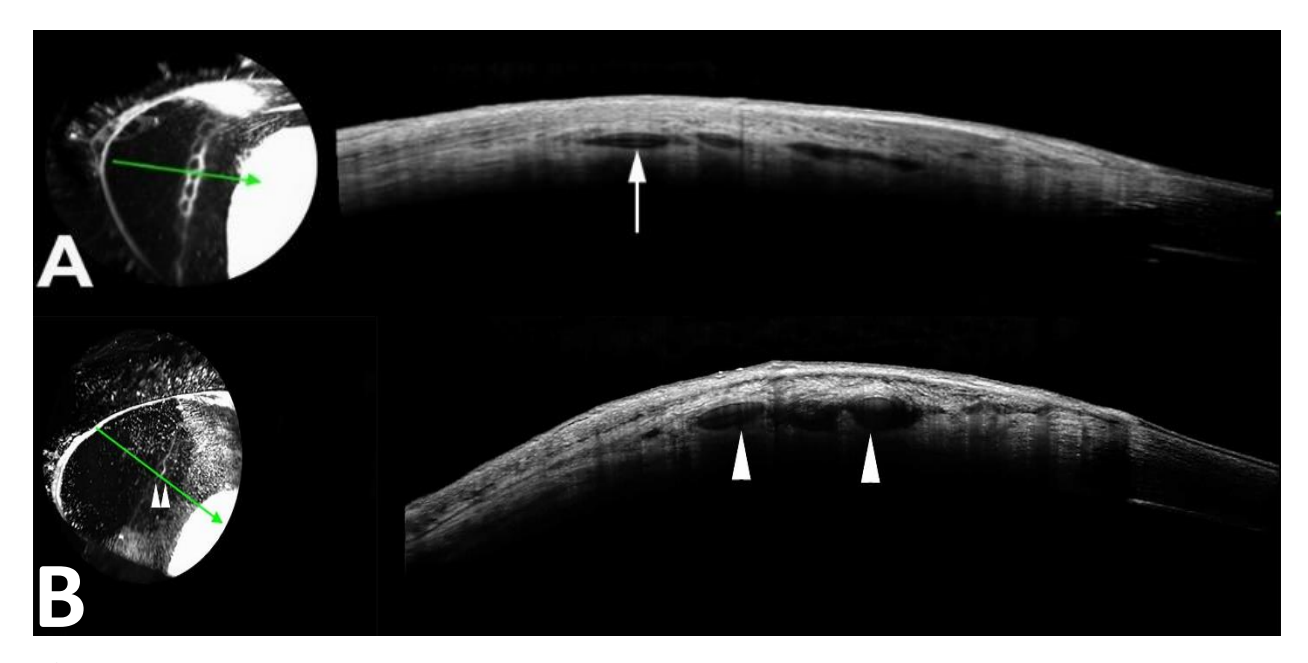


**Figure 19.** Cross sectional OCT scans from the left eye of a 1-year old intact female preglaucomatous beagle dog following intracameral aqueous angiography (A), and from the right eye of a 3-year old intact female normal beagle dog following intracameral aqueous angiography (B). The orientation of the scan (green arrow) depicts luminal vessels which demonstrated fluorescence.

Several anatomic limitations were encountered that may have limited observation of fluorescent dye in all regions of the sclera. The nictitating membrane was a major inhibitor and precluded observation of dye outflow in the nasal and inferior aspects of the globe. Although retraction of the nictitating membrane was possible, this still did not allow for clear visualization of the scleral segments in question and may have added another element of compression on the globe that could have led to alterations in aqueous humor outflow. As such, this may have inhibited visualization of possible dye fluorescence in the nasal and inferior scleral segments. In addition to the nictitating membrane, some dogs had tight palpebral fissures that made it difficult to manually retract the superior and inferior palpebrae to a degree where the sclera was visible. There was also the concern for inadvertent pressure to be placed on the globe with manual retraction and/or manipulation of the superior and inferior palpebrae. Given these obstacles, there

was no practical way to evaluate the nasal and inferior scleral segments clearly or consistently in live dogs.

Another limitation of this current work was the lack of ability to accurately measure the true volume of dye injected IC and to quantify the signal intensity of the fluorescent dye in the CAHO pathways. It is possible that the amount of dye injected IC was diluted by aqueous humor and/or flowed out of the anterior chamber at variable rates, leading to inconsistencies in signal intensity of the fluorescent dye seen in the anterior chamber and in the CAHO pathways.

Although not clinically significant, these parameters may help to identify the minimum quantity of dye that could be used as well as provide an objective measure of dye concentration as measured by signal intensity. This is an area which the authors hope to develop a protocol for and to be able to measure in future studies.

Overall, AA was shown to be a clinically applicable tool that may have practical utility for clinical veterinary ophthalmologists to evaluate dogs with glaucoma. This imaging modality could have an immediate benefit in dogs by identifying the location and dynamic characteristics of aqueous humor as it leaves the eye. This could shed new insights into the characteristics associated with CAHO pathways and how they may become altered in a variety of sight threatening conditions. Ultimately, it may allow for patient specific therapeutic approaches aimed at controlling IOP and preserving vision.

The use of *ADAMTS10*-OAG beagle dogs as an animal model for human glaucoma increases the emphasis of the clinical utility of this work. The work described herein details a protocol that could potentially be safely used across multiple species. The *ADAMTS10*-OAG beagle dog is an ideal model to study since they exhibit a slow rise in IOP and a morphologically normal ICA. The IOP in these dogs can be reasonably well controlled for some time with topical

medications, therefore, this is an ideal model to study the changes that arise with glaucomatous eyes over time. The information provided herein offers new insights into the fluid characteristics associated with the CAHO pathways of dogs, which could serve as the foundation for subsequent studies. Future studies that build on this foundation could provide insight into human glaucoma and ways to improve treatment efficacy and outcomes, including the potential for earlier initiation of prophylactic glaucoma medications based on aqueous humor dynamics, the ability to assess placement of glaucoma shunts and/or to determine the most suitable location for minimally invasive glaucoma surgeries based on fluorescence of dye in certain sectors of the globe, all with the goal of increasing the rate of retention of vision.

It is our intent to further evaluate changes to aqueous humor outflow in future studies, including changes to vessel lumen diameter and the rate of aqueous humor outflow in *ADAMTS10*-OAG beagles when treated with a prostaglandin analogue (latanoprost 0.005% ophthalmic solution). It is hypothesized that this treatment will increase visibility of dye outflow and pulsatility in dogs that have an IOP above 20 mmHg as topical prostaglandin analogue medications remodel the extracellular matrix of the ciliary body, which subsequently decreases uveoscleral outflow resistance. Other future directions include further evaluation of laminar flow and the aqueous humor outflow characteristics associated with this observation. It is the authors' hope that in future studies, vessel lumen measurements, pulsatility of dye, and alterations in dye outflow as a result of different ages, imaging techniques and sedation versus general anesthesia will be able to be objectively recorded.

**BIBLIOGRAPHY** 

#### **BIBLIOGRAPHY**

- 1. van Buskirk EM. The canine eye: the vessels of aqueous drainage. *Invest Ophthalmol Vis Sci.* 1979;18(3):223-230.
- 2. van Buskirk EM, Brett J. The canine eye: in vitro studies of the intraocular pressure and facility of aqueous outflow. *Assoc Res Vis Ophthalmol*. 1973;17(4):373-377.
- 3. Sharpnack DD, Wyman M, Anderson BG, Anderson WD. Vascular pathways of the anterior segment of the canine eye. *Am J Vet Res.* 1984;45(7):1287-1294.
- 4. McMaster PRB, Macri FJ. Secondary aqueous humor outflow pathways in the rabbit, cat, and monkey. *Arch Ophthalmol*. 1968;79(3):297-303.
- 5. Inomata H, Bill A, Smelser GK. Aqueous humor pathways through the trabecular meshwork and into Schlemm's canl in the cynomolgus monkey (Macaca irus). An electron microscopic study. *Am J Ophthalmol*. 1972;73(5):760-789.
- 6. Peiffer RL, Gelatt KN, Gum GG. Determination of the facility of aqueous humor outflow in the dog, comparing in vivo and in vitro tonographic and constant pressure perfusion techniques. *Am J Vet Res.* 1976;37(12):1473-1477.
- 7. Huang AS, Li M, Yang D, Wang H, Wang N, Weinreb RN. Aqueous angiography in living nonhuman primates shows segmental, pulsatile, and dynamic angiographic aqueous humor outflow. *Ophthalmology*. 2017;124(6):793-803.
- 8. Riley M, Meyer R, Yates E. Glutathione in the aqueous humor of human and other species. *Invest Ophthalmol Vis Sci.* 1980;19(1):94-96.
- 9. Hah Y, Chung HJ, Sontakke SB, et al. Ascorbic acid concentrations in aqueous humor after systemic vitamin C supplementation in patients with cataract: pilot study. *BMC Ophthalmol*. 2017;17(121):1-5.
- 10. Macknight ADC, Mclaughlin CW, Peart D, Purves RD, Carré DA, Civan MM. Formation of the Aqueous Humor. 2000;27:100-106.
- 11. Reddy VN, Giblin FJ, Lin L, Chakrapani B. The effect of aqueous humor ascorbate on ultraviolet B-induced DNA damage in lens epithelium. *Invest Ophthalmol Vis Sci*. 1998;39(2):344-350.
- 12. Consul B, Taunk J, Mathur G. Human aqeuous electrolytes. *J All India Ophthalmol Soc.* 1969;17(2):52-54.
- 13. Behar-Cohen FF, Savoldelli M, Parel J, et al. Reduction of corneal edema in endotoxin-induced uveitis after application of L-NAME as nitric oxide synthase inhibitor in rats by iontophoresis. *Invest Ophthalmol Vis Sci.* 1998;39(6):897-904.
- 14. Park GS, Kwon NS, Kim YM, Kim JC. The role of nitric oxide in ocular surface diseases. *Korean J Ophthalmol*. 2001;15:59-66.
- 15. Beyazyildiz E, Cankaya A, Beyazyildiz O, et al. Disturbed oxidant/antioxidant balance in

- aqueous humour of patients with exfoliation syndrome. *Jpn J Ophthalmol*. 2014;58(4):353-358.
- 16. Kars ME, Toklu Y, Yorgun MA, Neşelioğlu S, Eren F. Electrolyte, nitric oxide and oxidative stress levels of aqueous humor in patients with retinal detachment and silicone oil tamponade. *Curr Eye ResEye Res*. 2020:1460-2202.
- 17. Garweg JG, Garweg SL, Flueckiger F, Jacquier P, Boehnke M. Aqueous humor and serum immunoblotting for immunoglobulin types G, A, M, and E in cases of human ocular toxoplasmosis. *J Clin Microbiol*. 2004;42(10):4593-4598.
- 18. Civan MM, Macknight ADC. The ins and outs of aqueous humour secretion. *Exp Eye Res*. 2004;78:625-631.
- 19. van Buskirk EM, Grant WM. Influence of temperature and the question of involvement of cellular metabolism in aqueous outflow. *Am J Vet Res.* 1974;77(4):565-572.
- Mcdonnell F, Dismuke WM, Overby DR, Stamer WD. Pharmacological regulation of outflow resistance distal to Schlemm's canal. *Am J Physiol Cell Physiol*. 2018;315(1):44-51.
- 21. Barrie KP, Gum GG, Samuelson DA. Quantitation of uveoscleral outflow in normotensive and glaucomatous Beagles by 3H-labeled extran. *Am J Vet Res.* 1985;46(1):84-88.
- 22. Alm A, Nilsson SFE. Uveoscleral outflow A review. Exp Eye Res. 2009;88(4):760-768.
- 23. Ward DA, Cawrse MA, Hendrix DVH. Fluorophotometric determination of aqueous humor flow rate in clinically normal dogs. *Am J Vet Res.* 2001;62(6):853-858.
- 24. Gelatt KN, Mackay EO. Distribution of intraocular pressure in dogs. *Vet Ophthalmol*. 1998;1:109-114.
- 25. Giannetto C, Piccione G, Giudice E. Daytime profile of the intraocular pressure and tear production in normal dog. *Vet Ophthalmol*. 2009;12(5):302-305.
- 26. Leiva M, Naranjo C, Peña MT. Comparison of the rebound tonometer (ICare ®) to the applanation tonometer (Tonopen XL ®) in normotensive dogs. *Vet Ophthalmol*. 2006;9(1):17-21.
- 27. Andrade SF, Palozzi RJ, Giuffrida R, de Campos RJ, de Campos Santos G, Fukui RM. Comparison of intraocular pressure measurements between the Tono-Pen XL and Perkins applanation tonometers in dogs and cats. *Vet Ophthalmol*. 2012;15(Supplement 1):14-20.
- 28. Martin-Suarez E, Molleda C, Tardon R, Galn A, Gallardo J, Molleda J. Diurnal variations of central corneal thickness and intraocular pressure in dogs from 8:00am to 8:00pm. *Can Vet J.* 2014;55(4):361-365.
- 29. Kawata M, Tsukizawa H, Nakayama M, Hasegawa T. Rectification of width and area of the ciliary cleft in dogs. *J Vet Med Sci.* 2010;72(5):533-537.
- 30. Gelatt KN, Gum GG, Williams LW, Barrie KP. Uveoscleral flow of aqueous humor in the normal dog. *Am J Vet Res.* 1979;40(6):845-848.

- 31. Smith P, Samuelson D, Brooks D. Aqueous drainage paths in the equine eye: Scanning electron microscopy of corrosion cast. *J Morphol.* 1988;198:33-42.
- 32. Johnson M, Mclaren JW, Overby DR. Unconventional aqueous humor out flow: A review. *Exp Eye Res*. 2017;158:94-111.
- 33. Samuelson DA, Gelatt KN. Aqueous outflow in the beagle. II. Postnatal morphologic development of the iridocorneal angle: corneoscleral trabecular meshwork and angular aqueous plexus. *Curr Eye Res.* 1984;3(6):795-808.
- 34. Koudouna E, Young RD, Overby DR, et al. Ultrastructural variability of the juxtacanalicular tissue along the inner wall of Schlemm's canal. *Mol Vis*. 2019;21(25):517-526.
- 35. Pizzirani S, Gong H. Functional Anatomy of the Outflow Facilities. *Vet Clin North Am Small Anim Pract*. 2015;45(6):1101-1126.
- 36. Gelatt K, Gilger B, Kern T. Veterinary Ophthalmology: Two Volume Set.; 2013.
- 37. Rosenquist R, Epstein D, Melamed S, Johnson M, Grant WM. Outflow resistance of enucleated human eyes at two different perfusion pressures and different extents of trabeculotomy. *Curr Eye Res.* 1989;8(12):1233-1240.
- 38. Grant WM. Experimental aqueous perfusion in enucleated human eyes. *Arch Ophthalmol*. 1963;69:783-801.
- 39. Bill A, Svedbergh B. Scanning electron microscopic studies of the trabecular meshwork and the canal of schlemm An attempt to localize the main resistance to outflow of aqueous humor in man. *Acta Ophthalmol*. 1972;50(3):295-320.
- 40. Ethier CR, Coloma FM, de Kater AW, Allingham RR. Retroperfusion studies of the aqueous outflow system. Part 2: Studies in human eyes. *Invest Ophthalmol Vis Sci.* 1995;36(12):2466-2475.
- 41. Grant WM. Further studies on facility of flow through the trabecular meshwork. *Arch Ophthalmol.* 1958;60:523-533.
- 42. Maepea O, Bill A. The Pressures in the Episcleral Veins, Schlemm's Canal and the Trabecular Meshwork in Monkeys: Effects of Changes in Intraocular Pressure. *Exp Eye Res.* 1989;49:645-663.
- 43. Acott TS, Kelley MJ. Extracellular matrix in the trabecular meshwork. *Exp Eye Res*. 2008;86(4):543-561.
- 44. Knepper PA, Goossens W, Hvizd M, Palmbergf PF. Glycosaminoglycans of the human trabecular meshwork in primary open-angle glaucoma. *Invest Ophthalmol Vis Sci*. 1996;37(7):1360-1367.
- 45. Hubmacher D, Apte SS. Genetic and functional linkage between ADAMTS superfamily proteins and fibrillin-1: a novel mechanism influencing microfibril assembly and function. *Cell Mol Life Sci.* 2011;68:3137-3148.
- 46. Merwe EL Van Der, Kidson SH. The three-dimensional organisation of the post-

- trabecular aqueous out flow pathway and limbal vasculature in the mouse. *Exp Eye Res*. 2014;125:226-235. doi:10.1016/j.exer.2014.06.011
- 47. Carreon T, van der Merwe E, Fellman RL, Johnstone M, Bhattacharya SK. Aqueous outflow A continuum from trabecular meshwork to episcleral veins. *Prog Retin Eye Res*. 2017;57:108-133.
- 48. McDonnell F, Dismuke WM, Overby DR, Stamer WD. Pharmacological regulation of outflow resistance distal to Schlemm's canal. *Am J Physiol Cell Physiol*. 2018;1(315):C44-C51.
- 49. Toris CB, Fan S, Johnson T V, et al. Aqueous flow measured by fluorophotometry in the mouse. *Invest Ophthalmol Vis Sci.* 2016;57:3844-3852.
- 50. Kiel JW, Reitsamer HA. Paradoxical effect of phentolamine on aqueous flow in the rabbit. *J Ocul Pharmacol Ther*. 2007;23(1):21-26.
- 51. Toris CB, Risma JM, Gonzales-martinez J, Mclaughlin MA, Dawson WW. Aqueous humor dynamics in inbred rhesus monkeys with naturally occurring ocular hypertension. *Exp Eye Res*. 2010;91(6):860-865. http://dx.doi.org/10.1016/j.exer.2010.09.011.
- 52. Gelatt KN, Gum GG, Merideth RE, Bromberg N. Episcleral venous pressure in normotensive and glaucomatous beagles. *Invest Ophthalmol Vis Sci.* 1982;23(1):131-135.
- 53. Brubaker R. Determination of episcleral venous pressure in the eye. A comparison of three methods. *Arch Ophthalmol*. 1967;77(1):110-114.
- 54. Kiel JW, Kopczynski CC. Effect of AR-13324 on episcleral venous pressure in Dutch belted rabbits. *J Ocul Pharmacol Ther*. 2015;31(3):146-151.
- 55. Erickson-Lamy K, Rohen JW, Grant WM. Outflow facility studies in the perfused human ocular anterior segment. *Exp Eye Res.* 1991;52:723-731.
- 56. Goel M, Picciani RG, Lee RK, Bhattacharya SK. Aqueous humor dynamics : A review. *Open Ophthalmol J.* 2010;4:52-59.
- 57. Grant WM. Experimental aqueous perfusion in enucleated human eyes. *AMA Arch Ophthalmol*. 1958;60(4 Part 1):523-533.
- 58. Grant WM. Further studies on facility of flow through the trabecular meshwork. *AMA Arch Ophthalmol*. 1958;60(4 Part 1):523-533.
- 59. Bhattacharya SK, Rockwood EJ, Smith SD, et al. Proteomics reveal cochlin deposits associated with glaucomatous trabecular meshwork. *J Biol Chem.* 2005;280(7):6080-6084.
- 60. Knepper PA, Breen M, Weinstein HG, Blacik LJ. Intraocular pressure and glycosaminoglycan distribution in the rabbit eye: Effect of age and dexamethasone. *Exp Eye Res.* 1978;27:567-575.
- 61. Barany E. In vitro studies of the resistance to flow through the angle of the anterior chamber. *Acta Soc Med Upsalien*. 1953;59(3-4):260-276.

- 62. Park CY, Lee JK, Kahook MY, Schultz JS, Zhang C, Chuck RS. Revisiting ciliary muscle tendons and their connections with the trabecular meshwork by two photon excitation microscopic imaging. *Invest Ophthalmol Vis Sci.* 2016;57:1096-1105.
- 63. Rohen JW, Lutjen E, Bahany E. The relation between the ciliary muscle and the trabecular meshwork and its importance for the effect of miotics on aqueous outflow resistance. A study in two contrasting monkey species, Macaca irus and Cercopithecus aethiops. *Albr Von Graefes Arch Klin Exp Ophthalmol*. 1967;172(1):23-47.
- 64. Tamm E, Flugel C, Sefani FH, Rohen JW. Contractile cells in the human scleral spur. *Exp Eye Res.* 1992;54:531-543.
- 65. Barany E, Christensen RE. Cycloplegia and outflow resistance in normal human and monkey eyes and in primary open-angle glaucoma. *Arch Ophthalmol*. 1967;77(6):757-760.
- 66. Gabelt BT, Crawford K, Kaufman PL. Outflow facility and its response to decline in aging rhesus monkeys. *Arch Ophthalmol*. 1991;109(6):879-882.
- 67. Croft MA, Oyen MJ, Gange SJ, Fisher MR, Kaufman PL. Aging effects on accommodation and outflow facility responses to pilocarpine in humans. *Arch Ophthalmol.* 1996;114(5):586-592.
- 68. Belmonte C, Bartels SP, Liu JHK, Neufeld AH. Effects of stimulation of the ocular sympathetic nerves on IOP and aqueous humor flow. *Invest Ophthalmol Vis Sci*. 1987;28:1649-1654.
- 69. Waxman S, Wang C, Dang Y, et al. Structure Function Changes of the Porcine Distal Outflow Tract in Response to Nitric Oxide. *Invest Ophthalmol Vis Sci.* 2018;59(12):4886-4895.
- 70. Waxman S, Loewen RT, Dang Y, Watkins SC, Watson AM, Loewen NA. High-resolution, three-dimensional reconstruction of the outflow tract demonstrates segmental differences in cleared eyes. *Invest Ophthalmol Vis Sci.* 2018;59(6):2371-2380.
- 71. Wecker T, Oterendorp C Van, Reichardt W. Functional assessment of the aqueous humour distal outflow pathways in bovine eyes using time-of-flight magnetic resonance tomography. *Exp Eye Res.* 2018;166:168-173.
- 72. Tham YC, Li X, Wong TY, Quigley HA, Aung T, Cheng CY. Global prevalence of glaucoma and projections of glaucoma burden through 2040: A systematic review and meta-analysis. *Ophthalmology*. 2014;121(11):2081-2090. doi:10.1016/j.ophtha.2014.05.013
- 73. Quigley H, Broman AT. The number of people with glaucoma worldwide in 2010 and 2020. *Br J Ophthalmol*. 2006;90(3):262-267.
- 74. Gelatt KN, Mackay EO. Secondary glaucomas in the dog in North America. *Vet Ophthalmol*. 2004;7(4):245-259.
- 75. Gelatt KN, Mackay EO. Prevalence of the breed-related glaucomas in pure-bred dogs in North America. *Vet Ophthalmol*. 2004;7(2):97-111.

- 76. Oliver JAC, Ricketts SL, Kuehn MH, Mellersh CS. Primary closed angle glaucoma in the Basset Hound: Genetic investigations using genome-wide association and RNA sequencing strategies. *Mol Vis.* 2019;25:93-105.
- 77. Dubin AJ, Bentley E, Buhr KA, Miller PE. Evaluation of potential risk factors for development of primary angle-closure glaucoma in Bouviers des Flandres. *J Am Vet Med Assoc.* 2017;250(1):60-67.
- 78. Bjerkås E, Ekesten B, Farstad W. Pectinate ligament dysplasia and narrowing of the iridocorneal angle associated with glaucoma in the English Springer Spaniel. *Vet Ophthalmol*. 2002;5(1):49-54.
- 79. Oliver JAC, Ekiri A, Mellersh CS. Prevalence of pectinate ligament dysplasia and associations with age, sex and intraocular pressure in the Basset hound, Flatcoated retriever and Dandie Dinmont terrier. *Canine Genet Epidemiol*. 2016;3(1):doi: 10.1186/s40575-016-0033-1. eCollection 2016. http://dx.doi.org/10.1186/s40575-016-0033-1.
- 80. Ahonen SJ, Kaukonen M, Nussdorfer FD, Harman CD, Komaromy AK, Lohi H. A novel missense mutation in ADAMTS10 in Norwegian Elkhound primary glaucoma. *PLoS One*. 2014;9(11:e111941).
- 81. Oliver JAC, Rustidge S, Jenkins CA, Farias FHG, Giuliano EA, Mellersh CS. Evaluation of ADAMTS17 in Chinese Shar-Pei with primary open-angle glaucoma, primary lens luxation, or both. *Am J Vet Res.* 2018;79:98-106.
- 82. Oliver JAC, Forman OP, Pettitt L, Mellersh CS. Two independent mutations in ADAMTS17 are associated with primary open angle glaucoma in the Basset Hound and Basset Fauve de Bretagne breeds of dog. *PLoS One*. 2015;10(10:e0140436):doi:10.1371/journal.pone.0140436. doi:10.1371/journal.pone.0140436
- 83. Gould D, Pettitt L, Mclaughlin B, et al. ADAMTS17 mutation associated with primary lens luxation is widespread among breeds. *Vet Ophthalmol*. 2011;14(6):378-384.
- 84. Kuchtey J, Olson LM, Rinkoski T, et al. Mapping of the disease locus and identification of ADAMTS10 as a candidate gene in a canine model of primary open angle glaucoma. *PLoS Genet*. 2011;7(2):e1001306. doi:10.1371/journal.pgen.1001306
- 85. Johnson M. "What controls aqueous humour outflow resistance?" *Exp Eye Res*. 2006;82(4):545-557.
- 86. Gelatt KN, Peiffer RL, Gwin RM, Gum GG, Williams LW. Clinical manifestations of inherited glaucoma in the beagle. *Invest Ophthalmol Vis Sci.* 1977;16(12):1135-1142.
- 87. Gelatt KN, Gum G, Williams LW, Gwin RM. Ocular hypotensive effects of carbonic anhydrase inhibitors in normotensive and glaucomatous Beagles. *Am J Vet Res*. 1979;40(3):334-345.
- 88. Gwin RM, Gelatt KN, Gum GG, Peiffer Jr RL, Williams LW. The effect of topical pilocarpine on intraocular pressure and pupil size in the normotensive and glaucomatous beagle. *Invest Ophthalmol Vis Sci.* 1977;16(12):1143-1148.

- 89. Burn JB, Huang AS, Weber AJ, Komáromy AM, Pirie CG. Aqueous angiography in normal canine eyes. *Transl Vis Sci Technol*. 2020;9(9):1-17. doi:10.1167/tvst.9.9.44
- 90. Ekesten B, Narfstrom K. Correlation of morphologic features of the iridocorneal angle to intraocular pressure in Samoyeds. *Am J Vet Res.* 1991;52(11):1875-1878.
- 91. Hasegawa T, Kawata M, Ota M. Ultrasound biomicroscopic findings of the iridocorneal angle in live healthy and glaucomatous dogs. *J Vet Med Sci.* 2015;77(12):1625-1631. https://www.jstage.jst.go.jp/article/jvms/77/12/77\_15-0311/\_article.
- 92. Choppin A, Eglen RM. Pharmacological characterization of muscarinic receptors in dog isolated ciliary and urinary bladder smooth muscle. *Br J Pharmacol*. 2001;132(4):835-842.
- 93. Tachado SD, Virdee K, Akhtar RA, Abdel-latif AA. M3 muscarinic receptors mediate an increase in both inositol trisphosphate production and cyclic AMP formation in dog iris sphincter smooth muscle. *J Ocul Pharmacol*. 1994;10(1):137-147.
- 94. Grozdanic SD, Kecova H, Harper MM, Nilaweera W, Kuehn MH, Kardon RH. Functional and structural changes in a canine model of hereditary primary angle-closure glaucoma. *Invest Ophthalmol Vis Sci.* 2010;51:255-263.
- 95. Park S, Kang S, Lim J, et al. Effects of prostaglandin-mediated and cholinergic- mediated miosis on morphology of the ciliary cleft region in dogs. *Am J Vet Res*. 2018;79(9):980-985.
- 96. Yoshitomi T, Ito Y. Effects of indomethacin and prostaglandins on the dog iris sphincter and dilator muscles. *Invest Ophthalmol Vis Sci.* 1988;29(1):127-132.
- 97. Tsai S, Almazan A, Lee SS, et al. The effect of topical latanoprost on anterior segment anatomic relationships in normal dogs. *Vet Ophthalmol*. 2013;16(5):370-376. doi:10.1111/vop.12011
- 98. Sapienza JS, Kim K, Rodriguez E, DiGirolamo N. Preliminary findings in 30 dogs treated with micropulse transscleral cyclophotocoagulation for refractory glaucoma. *Vet Ophthalmol.* 2019;22:520-528.
- 99. O'Reilly A, Hardman C, Stanley RG. The use of transscleral cyclophotocoagulation with a diode laser for the treatment of glaucoma occurring post intracapsular extraction of displaced lenses: a retrospective study of 15 dogs (1995–2000). *Vet Ophthalmol*. 2003;6(2):113-119.
- 100. Graham KL, Donaldson D, Billson FA, Billson FM. Use of a 350-mm2Baerveldt glaucoma drainage device to maintain vision and control intraocular pressure in dogs with glaucoma: a retrospective study (2013–2016). *Vet Ophthalmol*. 2017;20(5):427-434.
- 101. Plummer CE, MacKay EO, Gelatt KN. Comparison of the effects of topical administration of a fixed combination of dorzolamide-timolol to monotherapy with timolol or dorzolamide on IOP, pupil size, and heart rate in glaucomatous dogs. *Vet Ophthalmol*. 2006;9(4):245-249.
- 102. Gelatt KN, MacKay EO. Changes in intraocular pressure associated with topical

- dorzolamide and oral methazolamide in glaucomatous dogs. *Vet Ophthalmol*. 2001;4(1):61-67.
- 103. Brooks AM V., Gillies WE. Ocular β-blockers in glaucoma management. *Drugs Aging*. 1992;2:208-221.
- 104. Gelatt KN, Gilger BC, Kern TJ. Chapter 19: The Canine Glaucomas.; 2013.
- 105. Krauss AHP, Impagnatiello F, Toris CB, et al. Ocular hypotensive activity of BOL-303259-X, a nitric oxide donating Prostaglandin F2a agonist, in preclinical models. *Exp Eye Res.* 2011;93(3):250-255. http://dx.doi.org/10.1016/j.exer.2011.03.001.
- 106. Borghi V, Bastia E, Guzzetta M, et al. A novel nitric oxide releasing prostaglandin analog , NCX 125, reduces intraocular pressure in rabbit, dog, and primate models of glaucoma. *J Ocul Pharmacol Ther*. 2010;26(2):125-131.
- 107. Gelatt KN, Mackay EO. Effect of different dose schedules of latanoprost on intraocular pressure and pupil size in the glaucomatous Beagle. *Vet Ophthalmol*. 2001;4(4):283-288.
- 108. Leary KA, Lin K-T, Steibel JP, Harman CD, Komáromy AM. Safety and efficacy of topically administered netarsudil (Rhopressa<sup>TM</sup>) in normal and glaucomatous dogs with ADAMTS10-open-angle glaucoma (ADAMTS10 -OAG). *Vet Ophthalmol*. 2019.
- 109. Maggio F, Bras D. Surgical Treatment of Canine Glaucoma: Filtering and End-Stage Glaucoma Procedures. *Vet Clin North Am Small Anim Pract*. 2015;45(6):1261-1282.
- 110. Westermeyer HD, Hendrix DVH, Ward DA. Long-term evaluation of the use of Ahmed gonioimplants in dogs with primary glaucoma: nine cases (2000-2008). *J Am Vet Med Assoc*. 2011;238(5):610-617.
- 111. Bras D, Maggio F. Surgical Treatment of Canine Glaucoma: Cyclodestructive Techniques. *Vet Clin North Am Small Anim Pract*. 2015;45(6):1283-1305. http://dx.doi.org/10.1016/j.cvsm.2015.06.007.
- 112. Hardman C, Stanley RG. Diode laser transscleral cyclophotocoagulation for the treatment of primary glaucoma in 18 dogs: a retrospective study. *Vet Ophthalmol*. 2001;4(3):209-215.
- 113. Sebbag L, Allbaugh RA, Strauss RA, et al. MicroPulse<sup>TM</sup> transscleral cyclophotocoagulation in the treatment of canine glaucoma: Preliminary results (12 dogs). *Vet Ophthalmol*. 2019;22:407-414.
- 114. Lutz E, Webb T, Bras I, et al. Diode endoscopic cyclophotocoagulation in dogs with primary and secondary glaucoma: 309 cases (2004-2013). *Vet Ophthalmol*. 2013;16(6):40.
- 115. Larocca R, Martin R. Early results of the veterinary implant glaucoma registry (VIGOR) a multicenter evaluation of the Brown glaucoma implant in canines (abstract). In: *49th Annual Conference of the American College of Veterinary Ophthalmologists*.; 2018:137.
- 116. Larocca R, Martin R. Interim results of the Veterinary Implant Glaucoma Registry (VIGOR) a multicenter evaluation of the Salvo glaucoma implant in canines. In: 50th Annual Conference of the American College of Veterinary Ophthalmologists.; 2019:E49.

- 117. Lutz E, Sapienza J. Combined diode endoscopic cyclophotocoagulation and Ex-press shunt gonioimplantation in four cases of canine glaucoma. In: *40th Annual Conference of the American College of Veterinary Ophthalmologists*.; 2009:396.
- 118. Sapienza JS, Van der Woerdt A. Combined transscleral diode laser cyclophotocoagulation and Ahmed gonioimplantation in dogs with primary glaucoma: 51 cases (1996–2004). *Vet Ophthalmol*. 2005;8(2):121-127.
- 119. Glover TL, Naisse MP, Davidson MG. Effects of topically applied mitomycin-C on intraocular pressure, facility of outflow, and fibrosi after glaucoma filtration surgery in clinically normal dogs. *Am J Vet Res.* 1995;56(7):936-940.
- 120. Gokce M, Akata R, Kiremitci-Gumusderelioglu M. 5-FU loaded pHEMA drainage implants for glaucoma-filtering surgery: device design and in vitro release kinetics\*. *Biomaterials*. 1996;17(9):941-994.
- 121. Pakravan M, Miraftabi A, Yazdani S, Koohestani N, Yaseri M. Topical mitomycin-C versus subconjunctival 5-Fluorouracil for management of bleb failure. *J Ophthalmic Vis Res.* 2011;6(2):78-86.
- 122. Andrew NH, Akkach S, Casson RJ. A review of aqueous outflow resistance and its relevance to microinvasive glaucoma surgery. *Surv Ophthalmol*. 2020;65(1):18-31.
- 123. Pirie CG, Alario A. Anterior segment angiography of the normal canine eye: A comparison between indocyanine green and sodium fluorescein. *Vet J.* 2014;199(3):360-364.
- 124. Alario AF, Pirie CG. Fluorescein gonioangiography of the normal canine eye using a dSLR camera adaptor. *Res Vet Sci.* 2015;100:277-282.
- 125. McLellan GJ, Telle MR, Nilles J, et al. Imaging post-trabecular outflow pathways in spontaneous canine glaucoma. *ARVO 2019 Conf.* 2019:3184-B0358.
- 126. Snyder KC, Oikawa K, Williams J, et al. Imaging distal aqueous outflow pathways in a spontaneous model of congenital glaucoma. *Transl Vis Sci Technol*. 2019;8(5):22.
- 127. Huang AS, Camp A, Xu BY, Penteado RC, Weinreb RN. Aqueous Angiography: Aqueous Humor Outflow Imaging in Live Human Subjects. *Ophthalmology*. 2017;124(8):1249-1251.
- 128. Huang AS, Penteado RC, Saha SK, et al. Fluorescein aqueous angiography in live normal human eyes. *J Glaucoma*. 2018;27(11):957-964.
- 129. Akagi T, Uji A, Huang AS, et al. Conjunctival and intrascleral vasculatures assessed using anterior segment optical coherence tomography angiography in normal eyes. *Am J Ophthalmol*. 2018;196:1-9.
- 130. Alario AF, Pirie CG, Pizzirani S. Anterior segment fluorescein angiography of the normal feline eye using a dSLR camera adaptor. *Vet Ophthalmol*. 2013;16(3):204-213.
- 131. Zhou XX, Liu AH, Lin S, Wu JG. A simultaneous iris angiography technique in pigmented rabbits. *Ophthal Res.* 2012;47(2):109-112.

- 132. Huang AS, Saraswathy S, Dastiridou A, et al. Aqueous angiography with fluorescein and indocyanine green in bovine eyes. *Transl Vis Sci Technol*. 2016;5(6):5.
- 133. Wakaiki S, Maehara S, Abe R, et al. Indocyanine green angiography for examining the normal ocular fundus in dogs. *J Vet Med Sci.* 2007;69(5):465-470.
- 134. Bellhorn R. Fluorescein fundus photography in veterinary ophthalmology. *J Am Anim Hosp Assoc*. 1973;9:227-233.
- 135. Engel E, Schraml R, Maisch T, et al. Light-induced decomposition of indocyanine green. *Invest Ophthalmol Vis Sci.* 2008;49(5):1777-1783.
- 136. Snyder K, Oikaw K, S. G, et al. Dynamic imaging of distal aqueous humor outflow pathways in feline congenital glaucoma (FCG). In: *American College of Veterinary Ophthalmologists 49th Annual Conference, Minneapolis MN, September 26-29, 2018.*; 2018.
- 137. Nieuwenhuizen J, Watson PG, Jager MJ, Emmanouilidis-van der Spek K, Keunen JEE. The value of combining anterior segment fluorescein angiography with indocyanine green angiography in scleral inflammation. *Ophthalmology*. 2003;110(8):1653-1666. doi:10.1016/S0161-6420(03)00487-1
- 138. Watson PG, Bovey E. Anterior segment fluorescein angiography in the diagnosis of scleral inflammation. *Ophthalmology*. 1985;92:1-11. doi:10.1037//0003-066X.46.5.506
- 139. Willerslev A, Li XQ, Munch IC, Larsen M. Relation between fluorescein angiographic and spectral-domain optical coherence tomography findings of blood flow turbulence at arteriovenous crossings in the retina. *Retin Cases Br Rep.* 2019;13(1):61-66.
- 140. McLellan GJ, Snyder KC, Oikaw K, Kiland JA, Gehrke S, Huang AS. Imaging distal aqueous outflow pathways in a spontaneous model of primary congenital glaucoma (PCG). *Invest Ophthalmol Vis Sci.* 2018;59:5908.
- 141. Huang AS, Saraswathy S, Dastiridou A, et al. Aqueous angiography—mediated guidance of trabecular bypass improves angiographic outflow in human enucleated eyes. *Invest Ophthalmol Vis Sci.* 2016;57(11):4558-4565.
- 142. Saraswathy S, Tan JCH, Yu F, et al. Aqueous Angiography: Real-Time and Physiologic Aqueous Humor Outflow Imaging. *PLoS One*. 2016;11(1):e0147176. doi:10.1371/journal.pone.0147176
- 143. Telle MR, Snyder KC, Teixeira LBC, et al. Development and validation of new methods to visualize conventional aqueous outflow pathways in canine glaucoma. In: *American College of Veterinary Ophthalmologists 49th Annual Conference, Minneapolis MN, September 26-29, 20182.*; 2018.
- 144. Roy S, Boldea R, Perez D, Curchod M, Mermoud A. Visualisation du systeme d'ecoulement de l'humeur aqueuse chez le lapin avec la fluoresceine et le vert d'indocyanine. *Klin Monbl Augenheilkd*. 2000;216(5):305-308.
- 145. Huang AS, Penteado RC, Papoyan V, Voskanyan L, Weinreb RN. Aqueous angiographic outflow improvement after trabecular microbypass in glaucoma patients. *Ophthalmol*

- Glaucoma. 2019;2(1):11-21.
- 146. Hann CR, Bentley MD, Vercnocke A, Ritman EL, Fautsch MP. Imaging the human aqueous humor outflow pathway in human eyes by three dimensional micro-computed tomography (3D micro-CT). *Exp Eye Res.* 2011;92(2):104-111. doi:10.1038/jid.2014.371
- 147. Bahler CK, Hann CR, Fjield T, Haffner D, Heitzmann H, Fautsch MP. Second-generation trabecular meshwork bypass stent (iStent inject) increases outflow facility in cultured human anterior segments. *Am J Ophthalmol*. 2012;153(6):1206-1213. http://dx.doi.org/10.1016/j.ajo.2011.12.017.
- 148. Leszczyński B, Sojka-Leszczyńska P, Wojtysiak D, Wróbel A, Pędrys R. Visualization of porcine eye anatomy by X-ray microtomography. *Exp Eye Res.* 2018;167:51-55.
- 149. Johnstone M, Martin E, Jamil A. Pulsatile flow into the aqueous veins: Manifestations in normal and glaucomatous eyes. *Exp Eye Res*. 2011;92(5):318-327.
- 150. Phillips C, Tsukahara S, Hosaka O, Adams W. Ocular pulsation correlates with ocular tension: the choriod as piston for an aqueous pump? *Ophthal Res.* 1992;24:338-343.
- 151. Thomassen TL, Perkins ES, Dobree JH. Aqueous veins in glaucomatous eyes. *Br J Ophthalmol*. 1950;34(4):221-227.
- 152. Meijer DKF, Weert B, Vermeer GA. Pharmacokinetics of biliary excretion in man. VI. Indocyanine green. *Eur J Clin Pharmacol*. 1988;35:295-303.
- 153. Ott P, Keidin S, Johnsen AH, Bass L. Hepatic removal of two fractions of indocyanine green after bolus injection in anesthetized pigs. *Am J Physiol*. 1994;266(6):1108-1122.
- 154. Tofflemire KL, Wang C, Jens JK, Ellinwood NM, Whitley RD, Ben-shlomo G. Evaluation of three hand-held tonometers in normal canine eyes. *Vet J.* 2017;224:7-10.
- 155. Camras LJ, Stamer WD, Epstein D, Gonzalez P, Yuan F. Differential effects of trabecular meshwork stiffness on outflow facility in normal human and porcine eyes. *Invest Ophthalmol Vis Sci.* 2012;53(9):5242-5250.
- 156. Gelatt KN, Henderson JD, Steffen GR. Fluorescein angiography of the normal and diseased ocular fundi of the laboratory dog. *J Am Anim Hosp Assoc*. 1976;169(9):980-984.
- 157. Jabs DA, Nussenblatt RB, Rosenbaum JT, Group S of UN (SUN) W. Standardization of uveitis nomenclature for reporting clinical data. Results of the First International Workshohp. *Am J Ophthalmol*. 2005;140(3):509-516.
- 158. van Buskirk E, Brett J. The canine eye: In vitro dissolution of the barriers to aqueous outflow. *Invest Ophthalmol Vis Sci.* 1978;17(3):258-263.
- 159. Flower RW, Hochheimer BF. A clinical technique and apparatus for simultaneous angiography of the separate retinal and choroidal circulation. *Invest Ophthalmol Vis Sci.* 1973;12(4):248-261.
- 160. Yuzawa M, Kawamura A, Matsui M. Clinical evaluation of indocyanine green video angiography in the diagnosis of choroidal neovascular membrane associated with agerelated macular degeneration. *Eur J Ophthalmol*. 1992;1(3):115-121.

- 161. Azoulay T, Dulaurent T, Isard P, Poulain N, Goulle F. Chirurgie de la cataracte bilatérale immédiatement séquentielle chez le chien : une étude rétrospective de 128 cas (256 yeux). *J Fr Ophtalmol*. 2013;26(8):645-651.
- 162. Maarek JI, Holschneider DP, Harimoto J. Fluorescence of indocyanine green in blood: intensity dependence on concentration and stabilization with sodium polyaspartate. *J Photoc Photobio B*. 2001;65:157-164.
- 163. Li P, Shen TT, Johnstone M, Wang RK. Pulsatile motion of the trabecular meshwork in healthy human subjects quantified by phase- sensitive optical coherence tomography. *Biomed Opt Express*. 2013;4(10):2051-2065.
- 164. Ascher K. The Aqueous Veins. Vol. 1. Springfield: Charles C. Thomas.; 1961.
- 165. Ascher K. The Aqueous Veins: I. Physiologic importance of the visible elimination of intraocular fluid. *Am J Ophthalmol*. 1942;25(10):1174-1209.
- 166. Wang B, Kagemann L, Schuman JS, et al. Gold nanorods as a contrast agent for Doppler optical coherence tomography. *PLoS One*. 2014;9(3):e90690. doi: 10.1371/journal.pone.0090690.
- 167. Francis AW, Kagemann L, Wollstein G, et al. Morphometric analysis of aqueous humor outflow structures with spectral-domain optical coherence tomography. *Invest Ophthalmol Vis Sci.* 2012;53(9):5198-5207.
- 168. Gelatt K, Gwin R, Peiffer Jr R, Gum G. Tonography in the normal and glaucomatous beagle. *Am J Vet Res.* 1977;38(4):515-520.
- 169. Gong H, Freddo TF. The washout phenomenon in aqueous outflow why does it matter? *Exp Eye Res*. 2009;88(4):729-737.
- 170. Kaufman P, True-Gabelt B, Erickson-Lamy K. Time-dependence of perfusion outflow facility in the cynomolgus mokey. *Curr Eye Res.* 1988;7(7):721-726.
- 171. Erickson K, Kaufman P. Comparative effects of three ocular perfusates on outflow facility in the cynomolgus monkey. *Curr Eye Res.* 1981;1(4):211-216.
- 172. Trusko B, Thorne J, Jabs D, et al. The standardization of uveitis nomenclature (SUN) project: Development of a clinical evidence base utilitzing informatics tools and techniques. *Methods Inf Med.* 2013;52(3):259-265. doi:10.3414/ME12-01-0063
- 173. Cantor E, Méndez F, Rivera C, Castillo A, Martínez-Blanco A. Blood pressure, ocular perfusion pressure and open-angle glaucoma in patients with systemic hypertension. *Clin Ophthalmol*. 2018;12:1511-1517.
- 174. Peiffer, Jr RL, Gum GG, Crimson RC, Gelatt KN. Aqueous humor outflow in beagles with inherited glaucoma: constant pressure perfusion. *Am J Vet Res.* 1980;41(11):1808-1813.
- 175. Gelatt KN, Gwin RM, Peiffer RL, Gum GG. Tonography in the normal and glaucomatous beagle. *Am J Vet Res.* 1977;38(4):515-520.
- 176. Toris CB, Gabelt BT, Kaufman PL. Update on the mechanism of action of topical

prostaglandins for intraocular pressure reduction. <code>Surv Ophthal</code>. 2008;53(Suppl 1):107-120. http://dx.doi.org/10.1016/j.survophthal.2008.08.010.